A MULTI-DIMENSIONAL CODE-DIVISION-MULTIPLEXED OFDMA MODEM USING CYCLIC ROTATED ORTHOGONAL COMPLETE COMPLEMENTARY CODES

by

Alexander Merensky

Submitted in partial fulfilment of the requirements for the degree

Master of Engineering (Electronic Engineering)

in the

Faculty of Engineering, Built Environment and Information Technology

Department of Electrical, Electronic and Computer Engineering

UNIVERSITY OF PRETORIA

August 2011

SUMMARY

A MULTI-DIMENSIONAL CODE-DIVISION-MULTIPLEXED OFDMA MODEM USING CYCLIC ROTATED ORTHOGONAL COMPLETE COMPLEMENTARY CODES

by

Alexander Merensky

Supervisor: Prof L.P. Linde
Co-supervisor: J.H. van Wyk
Department of Electrical, Electronic and Computer Engineering
University of Pretoria
Master of Engineering (Electronic Engineering)

One of the main objectives in the design of next-generation digital communication systems is to make use of the limited radio spectrum in order to achieve higher data rates, power efficiency and high user-capacity in harsh channel conditions. This need for a high performing and spectrum efficient modulation technique that can support numerous bit rates and services has risen in the last decade due to the rapid growth and increasing demand in wireless services. However, the primary goal of future generation communication systems is not only the development of new technologies that can achieve faster data rates and throughput, but also the integration of existing technologies into a standard platform, thereby designing improved reconfigurable and adaptable systems that promote and encourage interest for future developments.

This research focused on the design, integration and evaluation of a newly developed multiple access scheme based on a combination of multi-carrier techniques and a multi-dimensional spread spectrum modem that makes use of rotated mutually orthogonal complete complementary codes. This multi-dimensional code-division multiple access (MD-CDMA) modem, with recent designs of perfectly orthogonal complete complementary codes, produces an innovative modulation technique, which is further improved upon by exploiting the rotational properties of the spreading codes to increase the throughput, bandwidth efficiency, and capacity. The system integrates existing techniques into a design that is adaptable and reconfigurable to changing channel conditions and quality of service re-

quirements. The inherent benefits of both multi-carrier modulation and spread spectrum techniques are combined to produce a spectrally efficient and flexible multiple-access communications system that supports high data rates.

The main purpose of this work was to introduce the different elements of the analysed system and to advance the study of the novel communication technique by providing simulation results of the integrated system operating in different channel conditions. The system has shown to possess several key benefits, most notably the high spectral efficiency - double that of the theoretical efficiency when using BPSK modulation, i.e. 2 bits/s/Hz. Additionally, the system offers multiple access interference (MAI)-free operation, resulting in co-channel interference reduction and capacity increase. The flexible code-division-multiplexed multi-carrier system allows for numerous design alternatives, which offer different spreading techniques that can lead to diversity improvements and more reliable transmission. A periodic fast Fourier transform cross-correlation receiver has been devised to optimally de-spread the cyclic rotated complete complementary (CRCC) codes, which lowered the receiver complexity and reduced arithmetic complexity. Other benefits, such as low complex channel estimation and synchronisation, rate adaption, and resistance to the near-far problem, can be attributed to the system.

Keywords: *Cyclic rotated complete complementary (CRCC) codes, Code-division multiple access (CDMA), Multiple access, Multi-dimensional modem, Multi-carrier modulation, Orthogonal frequency-division multiplexing (OFDM), Spread spectrum.*

OPSOMMING

'N MULTIDIMENSIONELE KODEGEDEELDE-MULTITOEGANG OFDMA-MODEM WAT SIKLIES GEROTEERDE ORTOGONALE VOLLEDIG KOMPLEMENTÊRE KODES GEBRUIK

deur

Alexander Merensky

Studieleier: Prof L.P. Linde
Mede-studieleier: J.H. van Wyk
Departement van Elektriese, Elektroniese en Rekenaaringenieurswese
Universiteit van Pretoria
Magister in Ingenieurswese (Elektroniese Ingenieurswese)

Een van die hoofdoelwitte van die ontwerp van volgende generasie syferkommunikasiestelsels is om die beperkte radiospektrum te benut om hoër snelhede, drywingsdoeltreffendheid en hoë gebruikerskapasiteit in strawwe kanaaltoestande te behaal. Hierdie behoefte aan 'n modulasietegniek wat hoë werksverrigting bied en spektrumdoeltreffend is en dus talle bissnelhede en dienste kan lewer, het oor die afgelope dekade ontstaan vanweë die snelle groei van en toenemende vraag na koordlose radio-kommunikasiedienste. Die primêre doelwit van volgende generasie kommunikasiestelsels is egter nie net die ontwikkeling van nuwe tegnologieë wat vinniger snelhede en deurvoering kan behaal nie; dit behels ook die integrasie van bestaande tegnologieë op 'n standaardplatform wat kan lei tot die ontwerp van verbeterde, herkonfigureerbare en aanpasbare stelsels wat belangstelling in toekomstige ontwikkelings bevorder en aanwakker.

Die navorsing het gefokus op die ontwerp, integrasie en evaluering van 'n pas ontwikkelde multitoegangskema gebaseer op 'n kombinasie van multidraertegnieke en 'n multidimensionele sprei-spektrum modem, wat gebruik maak van geroteerde wedersyds ortogonale volledig komplementêre kodes. Hierdie multidimensionele kodegedeelde-multitoegang modem, met onlangs ontwerpte volkome ortogonale volledig komplementêre kodes, lewer 'n innoverende modulasietegniek op, wat verder verbeter word deur die roterende eienskappe van die spreidingskodes te ontgin, om die datadeursettempo, bandwydte-effektiwiteit en kapasiteit van die stelsel te verhoog. Die stelsel voeg bestaande tegnieke saam in 'n ontwerp wat

volgens veranderende kanaaltoestande en diensgehaltevereistes aangepas en herkonfigureer kan word. Die inherente voordele van sowel multidraermodulasie- en sprei-spektrum tegnieke is gekombineer om 'n spektraal doeltreffende en buigsame multitoegangkommunikasiestelsel daar te stel wat hoë datasnelhede ondersteun.

Die hoofdoelwit van hierdie werk was om die verskillende elemente van die stelsel wat ontleed is, bekend te stel en bestudering van dié kommunikasietegniek te bevorder deur middel van simulasieresultate van die geïntegreerde stelsel wat in verskillende kanaaltoestande bedryf word. Dit blyk dat die stelsel verskeie sleutelvoordele het, vernaamlik die hoë spektrale doeltreffendheid - twee keer soveel as die teoretiese doeltreffendheid wat met BPSK-modulasie verkry word, naamlik 2 bits/s/Hz. Die stelsel kan ook bedryf word sonder veelvuldigetoegangsteuring (MAI), wat ko-kanaalsteuring verminder en groter kapasiteit bied. Die buigsame kodegedeelde-multipleks multidraerstelsel bied talle ontwerpskeuses met verskillende spreidingstegnieke, wat veelsydigheid kan verbeter en data-oordrag meer betroubaar kan maak. 'n Periodiese vinnige Fouriertransformasie-kruiskorrelasie-ontvanger is ontwikkel om die siklies geroteerde volledig komplementêre (CRCC) kodes optimaal te ontsprei, waardeur die ontvangerkompleksiteit en rekenkundige intensiteit aansienlik verminder word. Ander voordele, soos laekompleksiteit kanaalestimasie en -sinkronisasie, snelheidsaanpassing en weerstand teen die naby-ver-probleem, kan aan die stelsel toegeskryf word.

Sleutelwoorde: *Multidimensionele modem, ortogonale frekwensiegedeelde-multitoegang (OFDMA), kodegedeelde-multitoegang (CDMA), multidraermodulasie, siklies geroteerde volledig komplementêre kodes (CRCCC).*

ACKNOWLEDGMENTS

I am extremely thankful to my supervisor, Prof L.P. Linde, whose guidance and support has aided me throughout the course of my studies and enabled me to develop an understanding of the research. A special thanks also goes out to Jacque van Wyk whose encouragement, support and invaluable assistance has not gone unnoticed.

I would also like to acknowledge the financial support from the industry partners Telkom, Unisys, Tellumat, EMC and Alvarion; and the Technology and Human Resources for Industry Program (THRIP) managed by the National Research Foundation (NRF), financed by the Department of Trade and Industry (DTI).

Lastly, I offer my regards and blessings to all of those who supported me during the completion of this research.

Mein besonderer Dank geht an meine Familie, die mir das Studium ermöglicht haben, und mir in jeder Lage eifrig beiseite standen und mich immer sehr tatkräftig unterstützt haben. Ich danke euch, für eure stete Unterstützung in jeder Hinsicht.

Alexander Merensky

TABLE OF CONTENTS

LIST OF ABBREVIATIONS

AWGN	Additive White Gaussian Noise
BER	Bit Error Rate
BPSK	Binary Phase Shift Keying
CDMA	Code Division Multiple Access
CRCC	Cyclic Rotated Complete Complementary Codes
CSI	Channel State Information
DFT	Discrete Fourier Transform
DSSS	Direct-Sequence Spread Spectrum
FDD	Frequency Division Duplexing
FDMA	Frequency Division Multiple Access
FEC	Forward Error Correction
FFT	Fast Fourier Transform
FWGN	Filtered White Gaussian Noise
GPRS	General Packet Radio Service
GSM	Global System for Mobile Communication
HSDPA	High Speed Downlink Packet Access
HSUPA	High Speed Uplink Packet Access
ICI	Inter-Carrier Interference
IDFT	Inverse Discrete Fourier Transform
IEEE	Institute of Electrical and Electronics Engineers
IFFT	Inverse Fast Fourier Transform
ISI	Inter-Symbol Interference
ITU	International Telecommunication Union
MA	Multiple Access
MAI	Multiple Access Interference
MC-CDMA	Multi-Carrier Code Division Multiple Access
MC-DS-CDMA	Multi-carrier Direct Spread CDMA
MI	Multipath Interference
MIMO	Multiple Input Multiple Output
MUI	Multi-User Interference
MLSE	Maximum Likelihood sequence estimation
MMSE	Minimum Mean Square Error

MRC	Maximal Ratio Combining
OFDM	Orthogonal Frequency-Division Multiplexing
OFDMA	Orthogonal Frequency-Division Multiple Access
OVSF	Orthogonal Variable Spreading Factor
PAPR	Peak-to-Average Power Ratio
P/S	Parallel-to-Serial
PDP	Power Delay Profile
PDF	Probability Density Function
PG	Processing Gain
PN	Pseudo Noise
PSD	Power Spectral Density
PSK	Phase Shift Keying
QoS	Quality of service
QPSK	Quadrature Phase Shift Keying
RUF	Root-of-Unity Filtered
RMS	Root Mean Square
S/P	Serial-to-Parallel
SDMA	Spatial Division Multiple Access
SER	Symbol Error Rate
SNR	Signal-to-Noise Ratio
SS	Spread Spectrum
STBC	Space-Time Block Code
TDD	Time Division Duplexing
TDMA	Time Division Multiple Access
TDL	Tapped Delay Line
UMTS	Universal Mobile Telephony System
WCDMA	Wideband Code Division Multiple Access
ZCC	Zero Cross Correlation
2D	Two Dimensional
4D	Four Dimensional
2G	2nd Generation
3G	3rd Generation
4G	4th Generation

CHAPTER 1

INTRODUCTION

A digital communications system involves the transmission of information in a digital format from a source that generates the information, to one or multiple destinations across a channel. Today, digital communication systems are constantly used to carry information through a variety of communication media, such as wireline telephone channels, fibre optic channels, microwave radio, and satellite channels. Sophisticated, high-speed and versatile digital communication systems provides a high information capacity, compatibility with digital data services, high data security, as well as quality communications and quick system availability. Developers are commonly faced with bandwidth, power and noise constraints and additionally need to share the RF spectrum.

A typical digital information transmission system consists of three basic parts, namely the transmitter, the channel, and the receiver. These main building blocks are further broken up into those shown in Figure 1.1, which are made up of digital parts consisting of the digital source, source encoder-decoder, channel encoder-decoder and digital modulator-demodulator; additionally, analogue parts consist of an analogue source, transmitter and receiver antenna systems, channel models and noise models. In the communications system, data (images, voice, text, etc.) is sent across a channel which undergoes multipath propagation, noise interference, fading and other channel impairments. However, a digital communication system is made up of several key building blocks which, combined, produce a communications device capable of transmitting and receiving data reliably, even under such harsh channel conditions.

This research investigates the combination of a multi-dimensional spread spectrum system and multi-carrier technology with the use of cyclic rotated complete complementary codes. The multiple access scheme combines the inherent benefits of both multi-carrier modulation and spread spectrum techniques. The focus of this study lies in the design, integration and evaluation of this novel combination. This introductory chapter provides a brief history

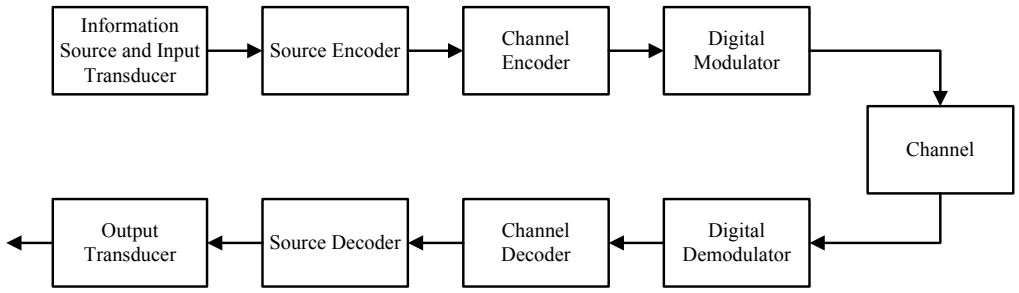

Figure 1.1: *Functional block diagram of a typical digital information transmission system.*

and overview of telecommunications and some background information on various technologies existing in the field. This is followed by an illustration of the fundamentals of spread spectrum and multi-carrier technologies currently available. The chapter ends with a motivation, the contributions and a short layout of the dissertation.

1.1 SHORT HISTORY OF CELLULAR TECHNOLOGY

The first telecommunications standard which was based on analogue technology with FM modulation, was introduced in the 1980s. The first 1G commercial cellular network was launched in Japan by Nippon Telegraph and Telephone (NTT) in 1979. This was then later followed by the launch of the total access communication system (TACS), Nordic Mobile Telephony (NMT) in Europe and the advanced mobile phone system (AMPS) in North America. This first generation of wireless telephone technology (1G) was replaced by the second generation (2G) digital telecommunication, which encoded the voice into a digital signal during a call [1].

Second generation (2G) cellular networks were launched in Finland on the global system for mobile communication (GSM) standard in 1991 using digital modulation and time division multiple access (TDMA) in combination with frequency-division multiple access (FDMA). Other digital mobile standards, such as IS-95 or cdmaOne made use of code-division multiple access (CDMA), whereas IS-54/IS-136, personal digital cellular (PDC) and GSM made use of TDMA. Further improvements on the 2G standard produced an upgraded 2.5G and 2.75G standard, referred to as the general packet radio service (GPRS) and the enhanced data rates for GSM/Global Evolution (EDGE) standard, respectively.

The technology that is currently available today is the third generation cellular standard.

A third generation or 3G system was designed for multimedia communication, higher data rates, and new flexible communication capabilities. The 3G standard is a generation of standards that fulfill the international mobile telecommunications-2000 (IMT-2000) specifications set by the International Telecommunication Union (ITU). The universally accepted 3G standards include the universal mobile telecommunication system (UMTS), also referred to as wideband code-division multiple access (W-CDMA), which was commercially released in Japan in 2001 and is now used in countries previously employing GSM 2G standards, and the CDMA2000 standard sharing infrastructure with the IS-95 (cdmaOne) standard, making use of multi-carrier CDMA (MC-CDMA) technology [1].

An evolution and improvement of the 3G mobile communications technology, namely high-speed downlink packet access (HSDPA), also referred to as 3.5G, began to be implemented in the mid 2000s. High-speed packet access (HSPA) is a combination of the high speed downlink packet access (HSDPA) and high speed uplink packet access (HSUPA), allowing systems based on universal mobile telecommunications system (UMTS) or W-CDMA protocols to have higher data transfer speeds and capacities. Downlink speeds of 14.4 Mbit/s are currently supported by HSDPA. Evolved HSPA, known as HSPA+, was released at the end of 2008, which provides even greater speeds of up to 42 Mbit/s and 84 Mbit/s with the Release 9 of the 3GPP standards. It introduced MIMO (Multiple-Input, Multiple-Output) capabilities and higher order modulation [2].

The industry has begun looking for further improved 4th generation technologies, due to the fact that 3G networks would not be able to deal with the future growth of bandwidth intensive data and multimedia services. The ITU-R specified the international mobile telecommunications advanced (IMT-Advanced) requirements for 4G standards in 2008, by setting the peak speed requirements for 4G service at 100 Mbit/s for high mobility communication and 1 Gbit/s for low mobility/stationary communication [3].

Technologies such as mobile WiMAX and the first long term evolution (LTE) standards were introduced in 2006 and 2009 respectively, but did not fulfill the ITU-R requirements and were branded as pre-4G (3.9G) technologies. However, in 2010, according to [4], evolved versions or predecessors of IMT-Advanced, such as LTE and WiMAX, could be considered as 4G, provided they show substantial improvements in performance and capabilities with respect to the initial 3G systems.

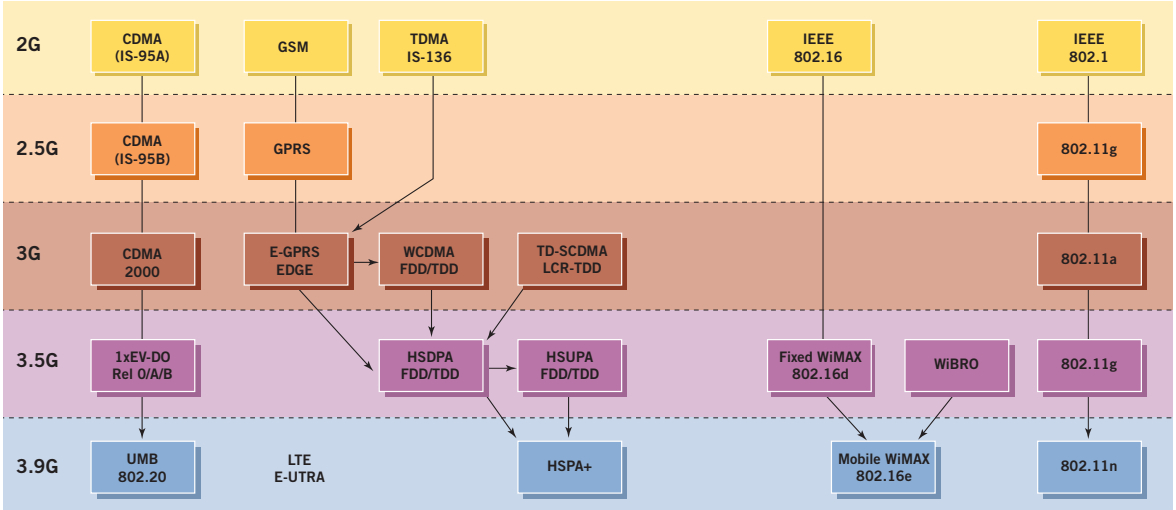

Figure 1.2: *Evolution of wireless communications technologies [5].*

Newer technologies such as LTE-Advanced, standardised by the 3GPP and 802.16m, standardised by the IEEE (i.e. WiMAX Release 2) are current true 4G candidates which have been submitted to the ITU. These proposed technologies aim to reach the requirements set out by the ITU, but are still far from being implemented. A detailed specification of the IMT-Advanced technologies is expected to be provided by a new ITU-R recommendation in 2012 [4].

Current 3G systems use W-CDMA or TDMA to accommodate multiple users. Future 4G systems are likely to employ improved multiple-access schemes and move away from traditional spread spectrum radio technology (3G and IS-95) to orthogonal frequency-division multiple access (OFDMA) [1]. WiMAX, for example, uses orthogonal frequency-division multiplexing (OFDM) in both the downlink as OFDMA and the uplink as OFDM/TDM. 3G LTE uses OFDMA in the downlink, but SC-FDMA in the uplink to avoid the high peak to average ratio (PAR) of OFDM, thus decreasing mobile battery power usage [5].

The evolution of the wireless communications standards towards 4G and their respective technologies are illustrated in Figure 1.2. Similarly, the wireless standards of the IEEE, dealing with wireless local area networks (WLAN) and metropolitan area networks (MAN), evolved throughout the years and are created and maintained by the IEEE LAN/MAN standards committee (IEEE 802). The IEEE Mobile WirelessMAN (WiMAX) standard was originally defined by the 802.16 standard and provides high throughput broadband connections over long distances for mobile users, whereas the 802.11 standard focused on high

throughput for low mobility in WLANs. Since the release, several updated and supplementary standards were added, including the 802.11a/b/g and 802.11n released in 2009 [6]. For the WiMAX standard, current versions are the IEEE 802.16-2009 amended by IEEE 802.16j-2009, and the recently approved 802.16m-2011 standard [7].

1.2 THEORETICAL FOUNDATION AND LITERATURE

1.2.1 Radio-channel access schemes

The radio spectrum is a scarce resource and it needs to be efficiently exploited. Hence, wireless systems use various techniques to allow multiple users to access the same spectrum simultaneously, thereby increasing efficiency and capacity. There are primarily four multiple access schemes which are known as FDMA, TDMA, CDMA and SDMA.

First generation (1G) wireless standards made use of FDMA and TDMA. FDMA consumed more bandwidth, due to a guard band which was needed to avoid inter-carrier interference (ICI); TDMA was similarly inefficient in handling high data rates, as it required a guard period to reduce the multipath effects. Therefore, in second generation systems a combination of FDMA and TDMA was used and another access technique, namely CDMA, was introduced to increase the system capacity. Improved CDMA techniques are currently still being used in primary third generation technologies [8].

1.2.1.1 FDMA

In an FDMA system, the available spectrum is divided into several frequency bands to create different data streams. These data streams can then be allocated to different users or nodes [8]. A guard band needs to be inserted between adjacent spectra in order to minimise interference from adjacent channels, as seen in Figure 1.3. FDMA was predominantly used in analogue 1G systems and some elements can still be found in currently implemented digital systems. The low transmit power and the unnecessary or low complexity equalisation methods required are the main advantages of FDMA. FDMA is often paired with frequency-division duplexing (FDD) where the uplink and downlink are separated by using different frequency bands. This technique is used in, for example, GSM, IS-95 and WCDMA/UMTS FDD mode [9]. OFDM is an efficient frequency-division multiplexing scheme in which sub-carrier frequencies are chosen to be orthogonal to each other. This eliminates the inter-

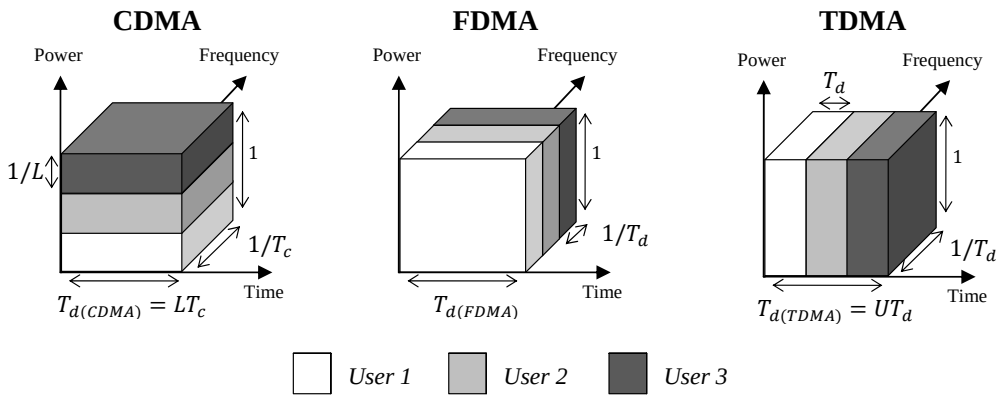

Figure 1.3: *Principles of the various multiple access schemes adopted from [10].*

ference from adjacent channels, making the inter-carrier guard bands redundant and reducing the receiver and transmitter design complexity.

1.2.1.2 TDMA

In a TDMA system, the entire bandwidth is divided into different time slots. These numerous time slots are periodically allocated to the same user, who can use the same frequency channel only for a short period at a time. This time division allows each user to gain access to the system, but only a certain number of users can be allocated within the available bandwidth. Therefore, another channel may be utilised and a combination of time and frequency-division multiple access (FDMA/TDMA) can be used. This is the case in second generation digital cellular systems such as GSM and IS-136 [8]. In GSM networks for example, multiple groups of users are assigned to different frequency channels, which are again split up into several time slots to accommodate each user.

1.2.1.3 CDMA

Code-division multiple access is another popular access scheme which is based on spread spectrum techniques. CDMA is currently used in various 3G cellular standards, such as IS-95 (cdmaOne), W-CDMA/UMTS, HSPA, and IS-2000 known as CDMA2000. In a CDMA system, users transmit at the same time and on the same frequency using a wider bandwidth than TDMA systems. The signals of different users are multiplexed over the same physical channel and are separated by special codes that are applied to transform each user's signal

into a spread-spectrum-coded version of the user's data stream. This spread signal has a much higher bandwidth than the original data and carries the information of several users over a single communication channel. Different users are distinguished by different spreading codes that have low cross-correlation properties. Thus, when correlating the received spread-spectrum signal with the spreading code originally used, only the desired signal of a specific user can be retrieved and the other unwanted signals remain spread over the large bandwidth [8]. CDMA allows the same frequency channel to be used by multiple users, where the wanted user's signal can only be extracted with the correct spreading code exclusively known by the receiver.

1.2.1.4 SDMA

A space-division multiple access (SDMA) system makes use of the spatial dimension for multiplexing of different data streams to offer superior performance in radio multiple access communication systems. Multiple data streams are transmitted over different, non-overlapping parallel spatial transmission channels and can be performed by equipping multiple antennas at both the transmitter and receiver front end. Access to a communication channel is achieved by providing a connection between the network bandwidth division and the spatial location of a user. Space-division multiplexing can make use of various techniques such as beamforming or sectorisation. Sectorisation divides a cell into smaller subcells that provide a fixed coverage area in which the frequency can be reused. Beamforming is known as antenna array signal processing in which intelligent antennas can form narrow spot beams in a desired direction to increase the system capacity [8]. SDMA is a common multiple antenna schematic architecture or a multiple-input and multiple-output (MIMO) scheme used in cellular wireless systems. An SDMA architecture can be implemented in all of the above mentioned communication schemes.

1.2.1.5 OFDMA

The latest third generation systems and multiple access schemes considered for fourth generation cellular systems make use of a combination of frequency domain and time domain multiple access techniques together with OFDM. This combination is also known as orthogonal frequency-division multiple access. Resources can be divided in the time and frequency space, and slots can be assigned along OFDM symbol and sub-carrier indices. OFDM is known as a modulation scheme and not a multiple access scheme, but existing

multiple access schemes can be combined with OFDM in various ways to achieve multiple access. Current 4G contenders such as LTE-Advanced and WiMAX (802.16m) make use of OFDMA.

1.2.2 Spread spectrum techniques

In a spread spectrum system, the transmitted signal is spread in the frequency domain, which results in a much wider bandwidth than is required to transmit the information. This spreading operation is accomplished by multiplying the original binary data sequence with a spreading code that has a much larger bandwidth than the original signal [8]. At the receiver, the wideband signal is despread again to the original narrowband signal using the same set of codes. Spread spectrum techniques have the advantages of secure communications, low probability of interception, increased resistance to interference and jamming, multipath and diversity reception, and the possibility of multiple access [9]. Direct-sequence spread spectrum (DSSS), frequency-hopping spread spectrum (FHSS), time-hopping spread spectrum (THSS), and chirp spread spectrum (CSS) are the main forms of the spread spectrum concept. In direct-sequence spread spectrum systems, the information message is modulated with a pseudo-random spreading sequence or code to spread the signal over a much larger bandwidth. However, in frequency-hopping the data is not spread over a continuous bandwidth, but rather is hopped according to a frequency hopping pattern over a number of channels having the same bandwidth [9]. Some IEEE 802.11 wireless ethernet standards make use of either FHSS or DSSS.

The two primary multiple access spread spectrum techniques are direct sequence code-division multiple access (DS-CDMA) and frequency-hopping code-division multiple access (FH-CDMA). Other methods to modulate CDMA signals are time-hopping CDMA (TH-CDMA) and multi-carrier CDMA techniques (MC-CDMA). Various hybrid combinations of the above mentioned schemes are also possible. These multiple access schemes are all based on DSSS. In DS-CDMA, a special coding or spreading scheme is employed, where each transmitter is assigned a unique code to allow multiple users to be multiplexed over a common channel and share a band of frequencies. This multiple access scheme is based on direct-sequence spread spectrum and is the most widely used type of CDMA. The codes used for spreading require good cross- and autocorrelation properties, since they determine the robustness in harsh channel conditions and the division amongst the different users. In Figure 1.4, the basic concept of direct sequence code-division multiple access is shown.

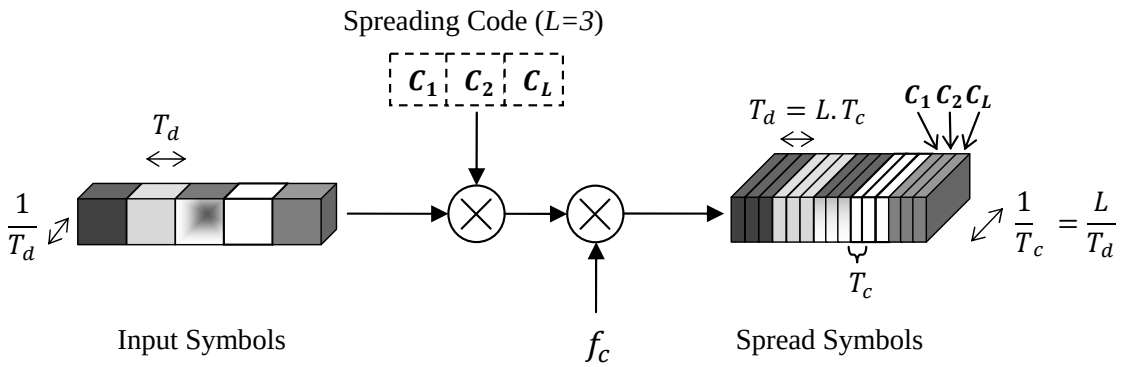

Figure 1.4: *Basic principle behind DS-CDMA.*

Spread spectrum techniques are deployed in many mobile communication systems, such as the IS-95 (cdmaOne) standard and third-generation CDMA standards (W-CDMA/UMTS, CDMA-2000).

1.2.3 Multi-carrier transmission

In multi-carrier transmission, a serial high data rate stream is converted into numerous parallel low rate sub-streams which are then modulated on to different sub-carriers [11]. A high immunity against multipath dispersion can be provided, since the symbol rate on each sub-carrier is far less than the initial serial data rate, making the useful symbol duration on each carrier much larger than the channel time dispersion. This reduces the effects of delay spread or inter-symbol interference (ISI), which in turn reduces the signal processing complexity by equalisation in the frequency domain [9]. An example of a multi-carrier system with four sub-carriers is depicted in Figure 1.5.

This basic principle of transmitting data simultaneously through a band-limited channel without inter-carrier/channel interference (ICI) and without interference between consecutive transmitted symbols (ISI) in the time domain, received wide interest for high data rate broadcast applications [9]. With the addition of digital signal processing techniques making use of the Fourier transform, an efficient digital realisation of multi-carrier transmission, termed OFDM, was developed.

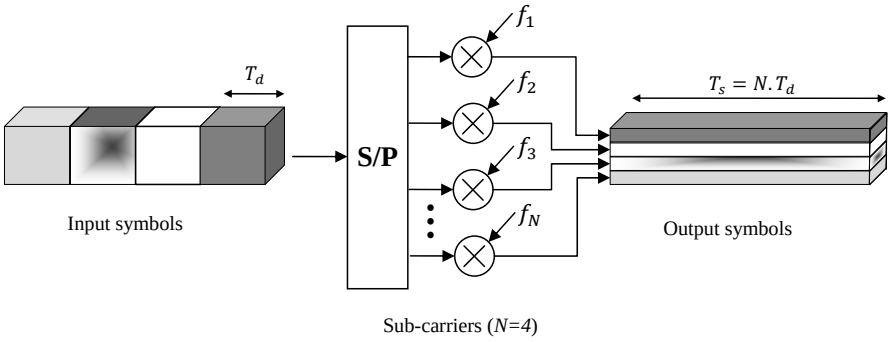

Figure 1.5: *Multi-carrier modulation.*

1.2.3.1 OFDM

Orthogonal frequency-division multiplexing is a form of a digital multi-carrier transmission which is suited to frequency selective channels and a high data rate. In OFDM, a frequency-selective wideband channel is transformed into a group of non-selective narrowband channels, making it robust against delay spreads by maintaining orthogonality in the frequency domain. Through the use of cyclic redundancy at the transmitter, the complexity is reduced to only simple fast Fourier transform (FFT) processes and a tap scalar equalisation at the receiver [11]. Thus, OFDM splits a signal into multiple smaller sub-signals that are then transmitted simultaneously at different frequencies to the receiver. Multi-carrier schemes that employ FDMA/TDMA are referred to as OFDMA, which can be seen as a multi-user or multiple access version of OFDM.

1.2.4 Multi-carrier spread spectrum

The combination of multi-carrier modulation and spread spectrum techniques has received significant attention by many researchers, resulting in the development of a multiple access scheme known as multi-carrier spread spectrum (MC-SS). The combination has shown to offer spectral efficiency, robustness in harsh channel conditions, simple detection techniques, narrowband interference rejection capability, and flexibility. The two different approaches to combining multi-carrier modulation and spread spectrum are called MC-CDMA (or OFDM-CDMA) and MC-DS-CDMA [9].

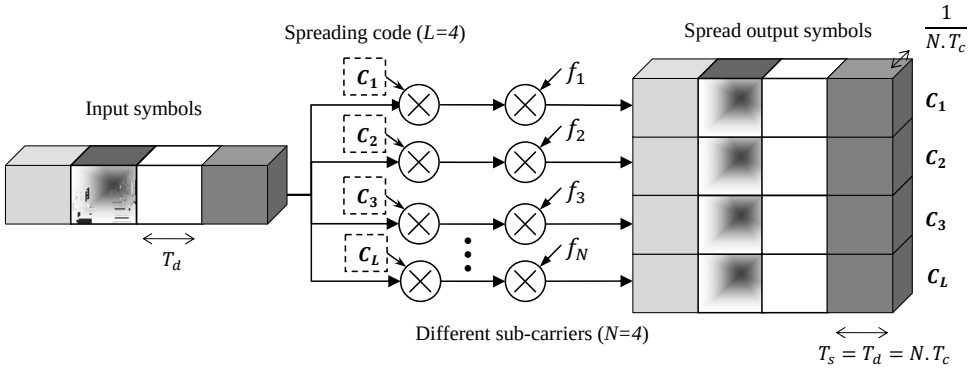

Figure 1.6: *The general concept of a single user MC-CDMA system with frequency diversity.*

1.2.4.1 MC-CDMA

Multi-carrier code-division multiple access (MC-CDMA), also known as OFDM-CDMA, is a multiple access scheme that allows the system to support multiple users at the same time. In MC-CDMA, each user symbol is spread in the frequency domain and each data symbol is transmitted simultaneously over numerous narrowband sub-carriers. By using different orthogonal spreading codes for each user, multiple access can be achieved by transmitting all users simultaneously over the same set of sub-carriers. At the receiver, the separation of the user signals is carried out in the code domain. Multi-carrier modulation is used to reduce the spread symbol rate, which reduces the ISI in the sub-carriers [9]. In a MC-CDMA system, the chips of a spread data symbol are mapped onto different parallel carriers to achieve frequency diversity, as seen in Figure 1.6.

1.2.4.2 MC-DS-CDMA

In multi-carrier direct spread CDMA systems (MC-DS-CDMA), similar to MC-CDMA, the users share the same bandwidth at the same time and are separated by different user codes. The difference between the two schemes lies in the allocation of the spread data chips to the carriers and OFDM symbols. In MC-DS-CDMA, the spread data symbols are mapped in the time direction over several multi-carrier symbols and not in the frequency domain as in MC-CDMA. The high data rate symbols are converted to parallel low rate sub-streams and are then separately spread with the specific user code in the time direction which corresponds to direct sequence spreading on each channel. Here, the same spreading codes can be applied

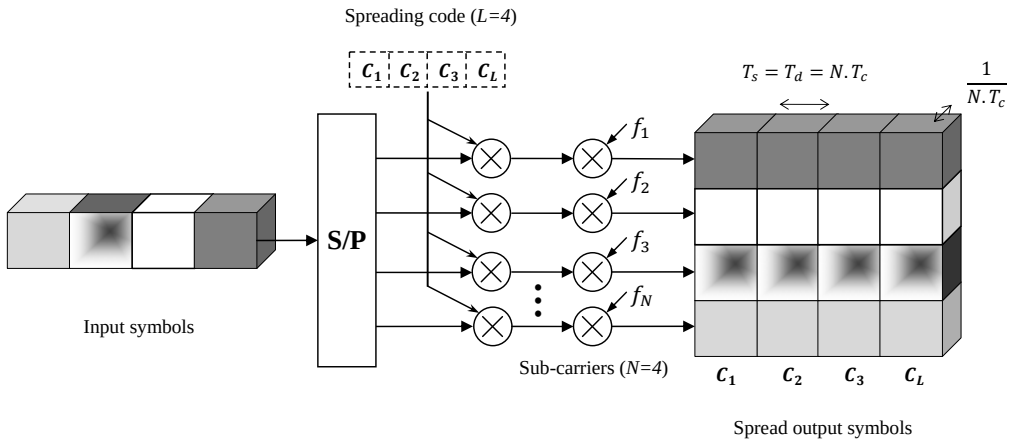

Figure 1.7: *The general concept of a single user MC-DS-CDMA system with time diversity.*

to the different sub-channels [9]. In Figure 1.7, the basic signal generation of the MC-DS-CDMA technique is illustrated.

1.2.4.3 Hybrid multi-carrier schemes

The above mentioned combinations have received significant attention as they capitalise on the benefit of both multi-carrier and spread spectrum techniques. New concepts of alternative hybrid multiple access solutions, such as OFDMA, OFDMA with code-division multiplexing (CDM), distributed DFT-spread OFDM or interleaved FDMA (IFDMA) and localised IFDMA, form some of the currently available techniques [9]. Other hybrid combinations, in which the information is spread onto the various sub-carriers of the OFDM type system in different ways, are possible. As an example, the extension of OFDMA with code-division multiplexing combines both the multiple access multi-carrier OFDMA system with spread spectrum code-division technology [12]. This is sometimes referred to as spread spectrum multi-carrier multiple access (SS-MC-MA) [13], [14].

Spectral efficiency, throughput and flexibility are considered as one of the most crucial criteria for the choice of candidates in future generation high speed wireless multimedia communications systems, and multi-carrier modulation and multi-carrier spread spectrum techniques have shown their potential to fulfill these criteria.

1.3 MOTIVATION AND OBJECTIVES

The need for a modulation technique that can reliably transmit at high data rates and with high bandwidth efficiency has risen in the last decades, due to the enormous growth of wireless services (local-area networks, cellular telephones, to name but a few). OFDM has been applied extensively in many high speed wireline and wireless communication standards, such as in ADSL, VDSL, WiMAX, WLAN radio interfaces (IEEE 802.11a,b,g,n) and in many other mobile broadband solutions, due to its efficient usage of the available frequency bandwidth and robustness to frequency selective fading environments. However, it is limited by its spectral efficiency and with the growing demand of digital audio/video broadcasting, the availability of spectrum becomes a serious problem [15]. Meanwhile, CDMA has proven its spectral efficiency through flexible frequency reuse and multiple access techniques [15], [16].

The combination of multiple access techniques like CDMA and OFDM, demonstrated increased spectral efficiency, flexibility in radio resource allocation and improved anti-multipath and anti-interference features [16]. Thus, these combined systems have received significant attention, as they capitalise on the benefits of both schemes and combine high bandwidth efficiency and high data rates with robustness against multipath distortion.

An important factor in the overall performance of a CDMA multi-carrier type modulation scheme is the perfect autocorrelation and zero cross-correlation property of the spreading codes. Due to non-ideal spreading codes used in current standardised CDMA systems, such as those used in existing 2-3G systems, problems of self-interference are evident [17], [18]. Existing problems such as slow transmission rate, low capacity, and complex system implementation in current systems are caused by the imperfect spreading codes implemented [19]. For example, according to [20], the Walsh-Hadamard sequences in the IS-95 (cdmaOne) standard and the OVSF codes in W-CDMA (UMTS) standards made it impossible to ensure symmetric data throughput at the very beginning of the system design because of their imperfect correlation characteristics in asynchronous and synchronous transmission modes. Hence, there is clearly a need for a design of a combined system that addresses these shortcomings.

This study consists of a body of original academic research on an innovative modulation technique that combines the architecture of a multi-dimensional spread spectrum modem with recent designs of perfectly orthogonal complete complementary codes. The rotational

or shift properties of the spreading codes are further exploited in a novel way to improve spectral efficiency and spreading code usage. Additionally, a low complexity periodic cross-correlation method at the receiver has been implemented to optimally de-correlate these cyclic rotated spreading codes. The entire system architecture allows for a high processing gain (PG) for interference suppression without limiting the amount of users. The system is extended by making use of multiple carrier frequencies (OFDMA) and can thus spread the information in frequency and/or in time, leading to a gain in diversity. Traditional CDMA-based systems (i.e. IS-95, cdma2000, and W-CDMA), and even multi-carrier adaptations, have a spreading efficiency of $1/L$ information bits per chip per link (where L is the sequence length) [17], [21], whereas the novel multi-layered modulation technique proposed here can transmit at double the theoretical spectral efficiency (2 bits/s/Hz) of the digital modulation method used when implementing unspreaded binary phase shift keying (BPSK). This eliminates any loss in efficiency caused by spreading, resulting in greater data throughput.

1.3.1 Main objectives of the research

Multi-carrier and spread spectrum systems, with their higher transmission rates, flexibility, and frequency usage efficiency, appear to be the most prominent and suitable candidates for future mobile communication systems [9]. By combining OFDM and a modified multi-dimensional CDMA modulation technique in a novel manner with the use of perfect orthogonal complete complementary codes and a cyclic rotation scheme, a unique digital broadcasting scheme, which supports high data rates and greater spectral efficiency, can be developed.

The benefits of both OFDM and a CDMA type modulation scheme are merged and further improved by the multi-dimensionality and spreading of cyclically rotated mutually orthogonal complete complementary codes. This novel combination forms an attractive modulation technique for next generation communication systems that require high data rates, high spectral efficiency, diversity and robustness in harsh channel conditions.

The goal of the research lies in the performance evaluation of the combination of the above mentioned techniques in one system. Different spreading techniques need to be considered for various designs and the implementation and manipulation of the cyclic rotated complete complementary codes needs to be investigated. The way in which the spreading codes can be utilised to achieve an optimal system capable of being as spectrally efficient as possible,

while still achieving a high throughput, needs to be studied.

The benefits of this newly proposed system and the system's performance, such as its bit error rate, spectral efficiency and throughput in various channel conditions needs to be addressed and evaluated. Thus, this research has the main purpose of advancing the study of the novel modulation technique and to make an original contribution to prior knowledge on multi-carrier spread spectrum multiple access systems.

1.4 CONTRIBUTIONS OF THIS DISSERTATION

The interest in spread spectrum and multi-carrier transmission schemes is ever growing, and this research contributes and provides insight into a novel multi-dimensional multi-carrier spread spectrum technique of which a comprehensive system design and implementation was still lacking.

The work presents the design of a communications system that incorporates various novel and existing techniques into one system. The system was simulated and tested in various channel conditions to assess its performance. A range of design parameters were considered and evaluated, such as the type of spreading (time and frequency), the multi-dimensionality of the modem, the specific spreading codes and their rotational properties and finally the multi-carrier/user adaptation. The entire system and its benefits was examined in various channel conditions. It is to be noted that this combination of various techniques is new and has not been addressed in previous research literature.

It will be shown that the system possesses several advantages over currently available 2G and 3G mobile cellular systems. It can, firstly, achieve a much higher bandwidth efficiency than conventional CDMA systems. Secondly, the system offers multiple access interference (MAI)-free operation in both synchronous and asynchronous channels, due to the chosen spreading codes and multi-carrier implementation. This attributes to co-channel interference reduction and capacity increase and in addition, the system shows an improved throughput. Thirdly, the flexible design shows other advantages, such as simple rate adaption, resistance to the near-far problem, low complex channel estimation and synchronisation.

This research also raises some interesting and underexplored issues and creates opportunity for future study and further research. Successive incremental and progressive results will be

provided to ensure constructive progress in this field of communications.

1.4.1 Publications

Some of the work presented and discussed in this research provided new results, ideas and contributions in fields related to telecommunications. The following lists some of the publications that form part of the contributions to the study:

- "*A Multi-levelled OFDM-CDMA Modem Using Complete Complementary Codes*", was presented at the SATNAC'11 proceedings in East London, South Africa in September 2011. The paper investigates the design and concept of a novel multiple access scheme based on a combination of a multi-levelled modem and multi-carrier techniques with the use of complete complementary codes.

- "*A Multi-Dimensional Code-Division Multiplexed OFDMA Modem Using Cyclic Rotated Orthogonal Complete Complementary Codes*", was submitted to the South African Institute of Electrical Engineer (SAIEE) Research Journal in 2011 (accepted and published in 2012). The paper presents a novel spread spectrum multi-carrier multiple access technique that combines a multi-dimensional modem with cyclic rotated orthogonal complete complementary codes. The system makes use of a multi-dimensional CDMA type modem combined with OFDMA techniques to produce a novel high throughput, flexible and spectrally efficient modulation technique.

1.5 STRUCTURE OF THIS DISSERTATION

This research is devoted to demonstrate and highlight the importance of this combination of multi-carrier and spread spectrum technology for future wireless communications. Chapter 1 covered the fundamentals and background of spread spectrum and multi-carrier technologies currently available.

In Chapter 2, the dissertation describes the basic multi-dimensional CDMA type modem which is used for spreading of the data.

The spreading codes or sequences of the system, which are vital to the performance of the entire system, are studied in Chapter 3. The creation of cyclic rotated complete complementary

codes (CRCC) and their properties are further analysed.

Chapter 4 deals with the design of the multi-dimensional code-division OFDMA system, where the combination of various spread spectrum, multi-carrier and multiple access techniques are detailed. The key building blocks of the communication system are described and a system model is given. This chapter combines the concepts of the multi-dimensional CDMA type modem (Chapter 2) with cyclic rotated orthogonal complete complementary spreading codes (Chapter 3) and OFDMA techniques.

Chapter 5 initially focuses on the channel models used to test and evaluate the error performance of the system. These channel models are vital in describing and realistically simulating additive white Gaussian noise (AWGN) and multipath fading effects typically encountered in wireless systems. This section is then followed by error performance results of the system in various authentic channel configurations. Numerous simulation parameters are given and bit error rate of different system setups are shown. Some of the benefits and similarities compared to other multi-carrier spread spectrum systems are presented, ending with a summary of the properties and advantages of the investigated system.

Finally, Chapter 6 concludes the results drawn from the study and identifies future research possibilities.

CHAPTER 2

MULTI-DIMENSIONAL WCDMA MODEM

The novel modulation technique proposed in this research makes use of a multi-dimensional WCDMA type modem building block to improve spreading code usage, throughput and overall performance of the system. This building block will be studied in this chapter.

The multi-dimensional modulation alternative to M-QAM WCDMA was analysed by [22–26]. It was shown that the 4-dimensional modem building block (without the newly implemented cyclic rotated complete complementary codes) has data throughput rates equivalent to that of a 16-ary quadrature amplitude modulated (16-QAM) WCDMA modulation scheme, but with the bit error rate (BER) performance equivalent to that of BPSK/QPSK in both AWGN and fading multipath channel scenarios, given identical spreading sequence lengths and spreading bandwidths. The system has four times the data rate of a conventional BPSK DSSS system with the same BER performance for a single user in an AWGN channel [22], [27].

The multi-dimensional code-division multiple access platform, consisting of multiple 4-dimensional (4D) transmitters and receivers, is described in this chapter.

2.1 FOUR DIMENSIONAL WCDMA MODEM BUILDING BLOCK

The 4D transmitter spreads four parallel data streams with complex spreading sequences and modulates them onto quadrature carriers. In the mathematical model, the input vectors are transmitted in both the real and imaginary planes on both quadrature carriers. Multiple dimensions of the modem can be created by placing multiple 4D transmitters in parallel. Section 2.1.1 examines the 4D mathematical modem in detail and in Section 2.1.2, the simplified transmitter and receiver models are discussed.

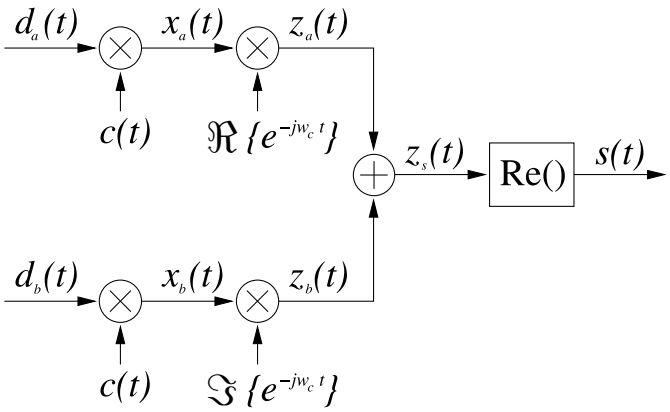

Figure 2.1: *Mathematical 4D transmitter structure from [26].*

2.1.1 Analysis of a 4-dimensional modem

2.1.1.1 Transmitter

A modulator is split up in such a way that the real and imaginary components of $e^{-jw_c t}$ are multiplied onto the real and imaginary branches, as seen in Figure 2.1 [26].

Two complex input signals are divided into real and imaginary parts, $d_a(t) = d_1(t) + jd_2(t)$ and $d_b(t) = d_3(t) + jd_4(t)$, which are multiplied with a complex spreading sequence $c(t) = c_r(t) + jc_i(t)$ to produce

$$x_a(t) = [d_1(t)c_r(t) - d_2(t)c_i(t)] + j[d_2(t)c_r(t) + d_1(t)c_i(t)] \tag{2.1}$$

$$x_b(t) = [d_3(t)c_r(t) - d_4(t)c_i(t)] + j[d_4(t)c_r(t) + d_3(t)c_i(t)]. \tag{2.2}$$

After the two signals $x_a(t)$ and $x_b(t)$ are modulated, z_a and z_b are obtained as follows

$$\begin{aligned} z_a(t) &= x_a(t)\cos(w_c t) \\ &= [d_1(t)c_r(t) - d_2(t)c_i(t)]\cos(w_c t) + j[d_2(t)c_r(t) + d_1(t)c_i(t)]\cos(w_c t) \end{aligned} \tag{2.3}$$

$$\begin{aligned} z_b(t) &= -x_b(t)\sin(w_c t) \\ &= -[d_3(t)c_r(t) - d_4(t)c_i(t)]\sin(w_c t) - j[d_4(t)c_r(t) + d_3(t)c_i(t)]\sin(w_c t). \end{aligned} \tag{2.4}$$

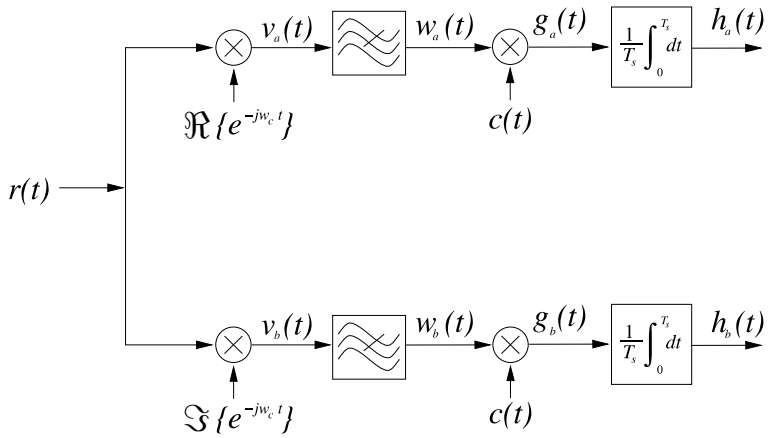

Figure 2.2: *Mathematical 4D receiver structure from [26].*

Finally the transmitted signal $s(t)$ results in

$$\begin{aligned} s(t) &= \Re\{z_a(t) + z_b(t)\} \\ &= [d_1(t)c_r(t) - d_2(t)c_i(t)]\cos(w_c t) - [d_3(t)c_r(t) - d_4(t)c_i(t)]\sin(w_c t). \end{aligned} \tag{2.5}$$

2.1.1.2 Receiver

The transmitted four dimensional signal $s(t)$, now redefined as the received signal $r(t)$, is demodulated by a receiver, depicted in Figure 2.2 [26]. After demodulation of the signal, assuming an ideal channel,

$$\begin{aligned} v_a(t) &= r(t)\,\Re\left\{e^{-jw_c t}\right\} \\ &= [d_1(t)c_r(t) - d_2(t)c_i(t)]\cos^2(w_c t) - [d_3(t)c_r(t) - d_4(t)c_i(t)]\sin(w_c t)\cos(w_c t) \end{aligned} \tag{2.6}$$

$$\begin{aligned} v_b(t) &= r(t)\,\Im\left\{e^{-jw_c t}\right\} \\ &= [d_1(t)c_r(t) - d_2(t)c_i(t)]\cos(w_c t)\sin(w_c t) - [d_3(t)c_r(t) - d_4(t)c_i(t)]\sin^2(w_c t), \end{aligned} \tag{2.7}$$

are low-pass filtered to produce

$$w_a(t) = \frac{1}{2}[d_1(t)c_r(t) - d_2(t)c_i(t)] \tag{2.8}$$

$$w_a(t) = \frac{1}{2}[-d_3(t)c_r(t) + d_4(t)c_i(t)]. \tag{2.9}$$

The signals $h_a(t)$ and $h_b(t)$ are produced with the dot product of signals $w(t)$ and the spreading sequence

$$\begin{aligned} h_a(t) &= w_a(t) \cdot c(t) \\ &= \frac{1}{2T_s} \int_0^{T_s} \left[d_1(t)c_r(t) - d_2(t)c_i(t)\right]\left[c_r(t) + jc_i(t)\right]\, dt \\ &= \frac{1}{2T_s} \int_0^{T_s} \left\{\left[d_1(t)c_r^2(t) - jd_2(t)c_i^2(t)\right] - c_r(t)c_i(t)\left[d_2(t) - jd_1(t)\right]\right\}\, dt \end{aligned} \tag{2.10}$$

$$\begin{aligned} h_b(t) &= w_b(t) \cdot c(t) \\ &= \frac{1}{2T_s} \int_0^{T_s} \left[-d_3(t)c_r(t) + d_4(t)c_i(t)\right]\left[c_r(t) + jc_i(t)\right]\, dt \\ &= \frac{1}{2T_s} \int_0^{T_s} \left\{\left[-d_3(t)c_r^2(t) + jd_4(t)c_i^2(t)\right] + c_r(t)c_i(t)\left[d_4(t) - jd_3(t)\right]\right\}\, dt. \end{aligned} \tag{2.11}$$

Now if the spreading sequence has orthogonal complex components and

$$\int_0^{T_s} c_r(t)c_i(t)dt = 0, \tag{2.12}$$

then the above equations can be simplified to

$$\begin{aligned} h_a(t) &= \frac{1}{2T_s}\left[d_1(t)c_r^2(t) - jd_2(t)c_i^2(t)\right] dt \\ &= k_r d_1(t) - jk_i d_2(t) \end{aligned} \tag{2.13}$$

$$\begin{aligned} h_b(t) &= \frac{1}{2T_s}\left[-d_3(t)c_r^2(t) + jd_4(t)c_i^2(t)\right] dt \\ &= -k_r d_3(t) - jk_i d_4(t), \end{aligned} \tag{2.14}$$

where k_r and k_i are the real and imaginary auto dot products of the complex spreading sequence $c(t) = c_r(t) + jc_i(t)$, respectively. Finally, the original transmitted signals $d_a(t)$ and $d_b(t)$ can be recovered from the above two equations [26].

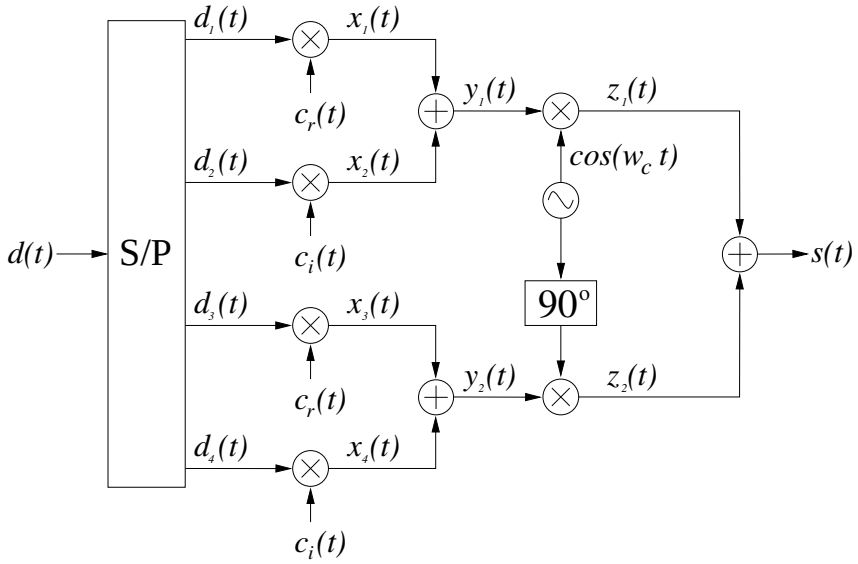

Figure 2.3: *A 4D (WCDMA) modem transmitter building block [22].*

2.1.2 Simplified description of a 4D modem transmitter

The simplified 4D transmitter, which is based on the mathematical model, is essentially a QPSK modulator of which the inphase and quadrature branches are extended by a 2D spread spectrum module. The simplified/actual 4D modem transmitter building block can be seen in Figure 2.3.

The input sequence is split up into four parallel data streams $d_1(t)$ to $d_4(t)$. The upper two streams are spread using orthogonal complete complementary codes to produce the inphase component and likewise, the lower two streams are spread to produce the quadrature component. The inphase and quadrature components are then modulated onto quadrature carriers and summed to produce the transmitted signal

$$\begin{aligned} s(t) = &[d_1(t)c_r(t) + d_2(t)c_i(t)]\cos(\omega_c t) \\ &+ [d_3(t)c_r(t) + d_4(t)c_i(t)]\sin(\omega_c t), \end{aligned} \tag{2.15}$$

$$\mathbf{s} = (d_1\mathbf{c}_r + d_2\mathbf{c}_i) + j.(d_3\mathbf{c}_r + d_4\mathbf{c}_i) \tag{2.16}$$

Due to the orthogonal properties of the carrier signals, the modulating signals can be independently detected. This allows the quadrature and inphase components to optionally use the same set of codes and thus save spreading sequences of the available code family.

The building block depicted in Figure 2.3 can be extended to more dimensions by adding more 4D blocks in parallel, each using additional spreading sequences from the family of spreading codes used. This can be achieved while still maintaining the respective BER performance of one original building block, provided that a perfectly orthogonal set of complex spreading sequences (CSS) is employed, with the emphasis being placed on the zero cross-correlation property amongst the members of the CSS family [23].

In [22], [23] it was shown that the data throughput rate of one basic 4D building block is twice that of a QPSK DSSS modulation system, yielding a spectral efficiency of $4/L$ bits/s/Hz, i.e. equal to that of M=16-QAM, but with the BER performance of BPSK/QPSK, assuming equal spreading sequence lengths, bandwidths and without the addition of rotating CRCC codes (explained in Chapter 3).

2.1.3 Simplified description of a 4D modem receiver

A typical low complexity matched filter correlation-type receiver for a 4D modem is shown in Figure 2.4. Following a similar approach to Section 2.1.1.2, the signals after carrier synchronisation are

$$\begin{aligned} v_1(t) = &[d_1(t)c_r(t) + d_2(t)c_i(t)]\cos^2(w_c t) \\ &+ [d_3(t)c_r(t) + d_4(t)c_i(t)]\sin(w_c t)\cos(w_c t) \end{aligned} \tag{2.17}$$

$$\begin{aligned} v_2(t) = &[d_1(t)c_r(t) + d_2(t)c_i(t)]\cos(w_c t)\sin(w_c t) \\ &+ [d_3(t)c_r(t) + d_4(t)c_i(t)]\sin^2(w_c t). \end{aligned} \tag{2.18}$$

After low-pass filtering v_1 and v_2, the signals obtained are

$$w_1(t) = \frac{1}{2}[d_1(t)c_r(t) + d_2(t)c_i(t)] \tag{2.19}$$

$$w_2(t) = \frac{1}{2}[d_3(t)c_r(t) + d_4(t)c_i(t)]. \tag{2.20}$$

Then, after despreading with the respective spreading codes, the outputs are integrated-and-dumped (I&D) to yield $g_m(t),\ m = 1,2,3,4$, which are then optimally sampled to produce

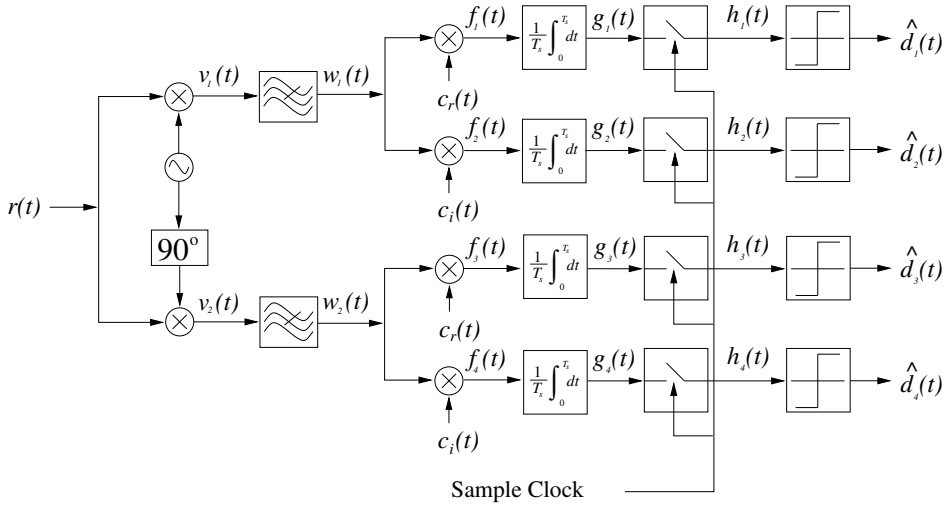

Figure 2.4: *A 4D (WCDMA) modem correlation-type receiver building block [22].*

the decision variables

$$h_1(t) = k_r d_1(t) \tag{2.21}$$

$$h_2(t) = k_i d_2(t) \tag{2.22}$$

$$h_3(t) = k_r d_3(t) \tag{2.23}$$

$$h_4(t) = k_i d_4(t). \tag{2.24}$$

The symbol estimates $\hat{d}_1(t), \hat{d}_2(t), \hat{d}_3(t)$ and $\hat{d}_4(t)$ are obtained through decision elements (assuming perfectly orthogonal spreading codes) [26]. The use of a unique family of orthogonal spreading codes contributes to a significantly simplified multiple-user interference (MUI)-free or (MAI)-free receiver structure. The performance of the 4D system mainly depends on the cross-correlation characteristics between the real and imaginary components of the spreading codes used.

2.1.4 Spreading sequences for the 4D modem

In any CDMA type modem, the performance greatly depends on the autocorrelation and zero cross-correlation properties of the spreading codes used. In the developed 4D system of [25], the complex spreading sequences are filtered by a constant envelope root-of-unity-filtering (RUF) technique to provide the spreading sequences with a near Nyquist bandwidth and constant complex envelope, which is an attractive characteristic resulting in more effi-

cient use of power amplifiers in communication systems [28], [29]. The spreading sequences were derived from the zero cross-correlation (ZCC) sequences proposed in [30] and the applied root-of-unity-filtering technique presented in [31]. The presented spreading sequences require a synchronous, or at least quasi-synchronous communication scenario in both the down- and up-links of the wireless system [23]. In [26], two classes of complex spreading sequences (constant envelope generalised chirp-like (CE-GCL) and ZCC sequences) were analysed by evaluating and comparing their time, spectral and correlation characteristics.

The above mentioned spreading codes were used for the 4D modem only and different spreading codes with ideal or perfect auto and cross-correlation properties will be used for the novel multi-dimensional code-division-multiplexed OFDMA modem design, which combines the 4D system in this chapter with perfect spreading sequences (see Chapter 3) and OFDMA techniques. Orthogonal complete complementary spreading codes that are well suited for CDMA are analysed in Chapter 3 of this research, and implemented in the design of the novel system in Chapter 4.

2.2 MODEM THEORETICAL PERFORMANCE ANALYSIS

By placing multiple 4D transmitters in parallel, multiple dimensions of the modem can be created. It was shown by [23], that the uncoded BER performance of a multi-dimensional modem configuration remains BPSK/QPSK-like, with increasing dimensions M_D, due to the orthogonality among the spreading sequences.

By defining M_L as the number of symbol levels per dimension M_D, and assuming both the spreading bandwidth and the spreading length L are fixed, the total number of symbols M and the corresponding number of bits per symbol K can be given by

$$M = (M_L)^{M_D} = 2^K \qquad \text{(symbols)}. \tag{2.25}$$

The multi-dimensional modem signal constellation is an M_D-dimensional hypercube centered on the origin of the signal space spanned by an orthonormal base similar to (2.15) [23]. With $M_D = 4$ and $M_L = 2$, $M = 2^{M_D} = 16$ symbols are situated on the vertices of an $M_D = 4$-dimensional hypercube, where the number of bits per symbol equals $K = M_D = 4$ [23]. Only one bit of information is carried by each dimension of the signal space, when the modulator performs binary ($M_L = 2$) modulation per dimension. The signal

constellation exhibits a natural Gray mapping of bits onto symbols, due to the fact that the nearest neighbour symbols differ only in one bit position.

When analysing the bit error rate (BER) in AWGN, it is known that the correlation ρ_r amongst all adjacent pairs of symbols in a M_D-dimensional hypercube signal space is given by [11]:

$$\rho_r = \frac{M_D - 2}{M_D}. \tag{2.26}$$

The Euclidean distance between the nearest-neighbour symbols can be found using (2.26) to give

$$d = \sqrt{2E_s(1-\rho_r)} = \sqrt{\frac{4E_s}{M_D}}. \tag{2.27}$$

Now, since the symbol energy equals $E_s = M_D E_b$, with E_b being the energy per bit, d simplifies to

$$d = \sqrt{4E_b}, \tag{2.28}$$

and the symbol error rate (SER) of the modem scheme in AWGN is approximated, according to [11], [23] by

$$\begin{aligned} P_{M_D} &= \left[1-(1-P_2)^{M_D}\right] \\ &= 1-\left(1-M_D P_2 + \frac{M_D\,(M_D-1)\,P_2^2}{2!} - \ldots + P_2^{M_D}\right) \\ &\approx M_D P_2 \qquad \text{if} \quad M_D \geq 4 \quad \text{and} \quad P_2 \ll 1, \end{aligned} \tag{2.29}$$

where P_2 denotes the pair-wise symbol error between adjacent or nearest-neighbour symbols at distance d [23], given by

$$P_2 = Q\left[\sqrt{\frac{d^2}{2N_0}}\right], \tag{2.30}$$

with d defined in (2.27). The one-sided noise power spectral density is denoted by N_0, and

$Q(.)$ is the well-known Gauss tail probability [23], defined as

$$Q(x) = \frac{1}{\sqrt{2\pi}} \int_x^{\infty} \exp^{-\frac{y^2}{2}} \, dy. \tag{2.31}$$

According to [23], if $M_D \geq 4$ and $P_2 \ll 1$, equation (2.29) simplifies to

$$P_{M_D} \approx M_D P_2 = M_D Q\left[\sqrt{\frac{4E_s}{2M_D N_0}}\right] = M_D Q\left[\sqrt{\frac{2E_b}{N_0}}\right]. \tag{2.32}$$

When considering the Gray bit-encoding of the nearest-neighbour symbols, the bit error rate in AWGN is well approximated by

$$P_b \approx \frac{1}{M_D} P_{M_D} = P_2 = Q\left[\sqrt{\frac{2E_b}{N_0}}\right]. \tag{2.33}$$

It was shown in [23] that (2.33) is independent of the number of dimensions M_D, which implies that the BER of the multi-dimensional modulation scheme remains QPSK-like when $M_D \to \infty$. The only requirement is that a set of orthogonal spreading sequences are employed.

This means the overall data throughput rate and the spectral efficiency (for a fixed spreading bandwidth) can be doubled, compared to a QPSK system, for every doubling of the number of dimensions ($M_D = 4$) [22], [23]. To increase the dimension of the modem, multiple $M_D =$ 4-dimensional building blocks need to be added in parallel, using new distinct orthogonal spreading sequences for each new added dimension. The only limitation to this is the amount of spreading codes available from a given code family set.

Consequently, the multi-dimensional modem, which is made up of multiple $M_D = 4$-dimensional building blocks, can achieve data throughput rates that linearly increase (double) with the addition of each new set of $M_D = 4$-dimensions.

2.2.1 Error rate performance in AWGN

The theoretical BER performance in AWGN of the system is verified by the simulated performance results depicted in Figure 2.5. The modem used for the simulation made use of a uniquely extended family of root-of-unity-filtered constant-envelope generalised chirp-like complex spreading sequences (CE-GCL-CSS), exhibiting zero periodic cross-correlation

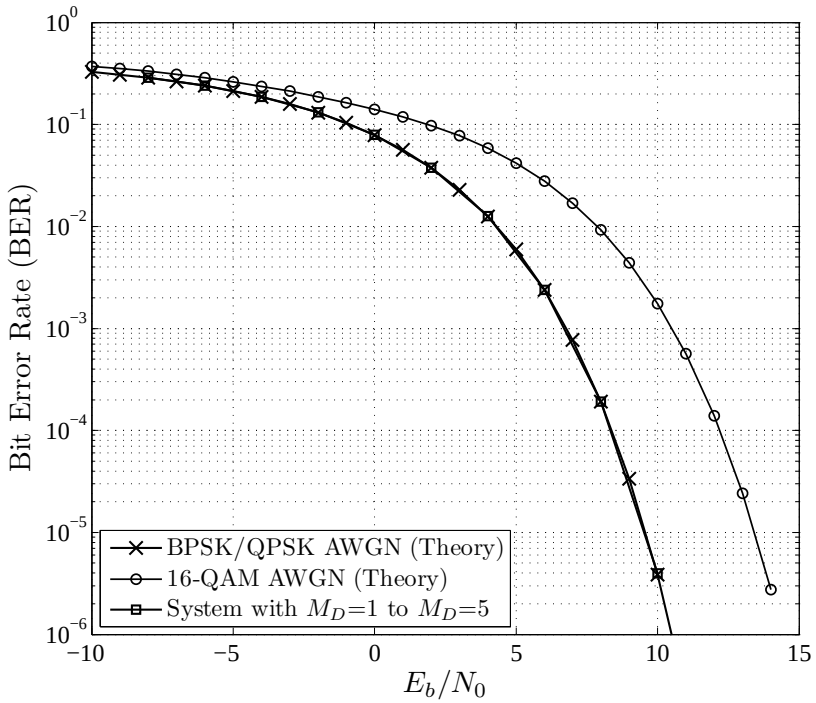

Figure 2.5: *Simulated uncoded BER performance in AWGN for a 4 to 20-dimensional system, compared to QPSK and 16-QAM WCDMA.*

values for all relative time shifts (orthogonal) [23]. The results depict the BER performance for $M_D = 4$ to $M_D = 20$-dimensional WCDMA modulators in AWGN. The $M_D = 20$-dimensional case made use of 5 $M_D = 4$-dimensional building blocks in parallel.

It is given by [23], that the system facilitates data throughput rates of up to 2 to 10 times a normal 2D-QPSK WCDMA type modem, and 1 to 5 times a 16-QAM WCDMA modem, respectively, given identical spreading sequence lengths and Nyquist filtered spreading bandwidth. This is achieved by the multi-dimensional modem while maintaining the BER performance of QPSK, which is a huge advantage compared to single and multi-carrier M-QAM CDMA modulation schemes. Other advantages of the modulation scheme (such as its power and spectral efficiency) can be found in [22–26], [32].

This multi-dimensional building block forms the foundation of the proposed novel modulation technique. The inherent beneficial properties of the multi-dimensional building block are adapted and combined with orthogonal complete complementary spreading codes to further improve the system when combined with multi-carrier techniques (i.e. OFDM). The spreading codes used in the novel system and the unique cyclic rotation scheme are both

presented in the following chapter. Thereafter, in Chapter 4, the combined system model of the multi-carrier CDMA type spread spectrum modulation scheme with cyclic rotated orthogonal complete complementary codes is presented.

CHAPTER 3

SPREADING CODES

An important factor in the performance of any CDMA type system is the ideal orthogonality, auto and cross-correlation property of the spreading code used, since this determine the amount of users that can be accommodated in the system, the robustness in harsh channel conditions, and the division amongst the different users. CDMA type systems rely on the orthogonal properties of the spreading codes to separate users or channels in a communications system, whereas traditional FDMA and TDMA systems require different frequency bands and different time slots to offer separation among different channels or users [33]. Therefore, the properties of the spreading codes largely determine the performance of the communications system.

If the correlation functions are not ideal, every user or additional data stream can be viewed as another source of noise. Therefore, low cross-correlation values between spreading codes allow the receiver to separate user signals, whereas low autocorrelation sidelobe values aid in filtering out multiple received signals which are delayed due to multipath propagation [34].

If a CDMA system is not MAI-free and multipath interference (MI)-free, due to non-ideal cross-correlation and autocorrelation properties respectively, then the capacity of the overall system can merely achieve approximately one-third to a half of its processing gain (PG), which is currently seen in available CDMA based 2G to 3G wireless systems [20], [35]. The design or selection of the spreading codes is very important at an early stage of a CDMA system design. Shortcomings in the system architecture due to the use of unsuitable codes are unrectifiable and examples thereof have been found in numerous 2G to 3G standards, where non-optimal code design was carried through to successive standards [9], [36].

This chapter expands on the properties and generation of the spreading codes, which were used in the design of the multi-dimensional spread spectrum multi-carrier system.

3.1 DIFFERENT TYPES OF SPREADING CODES

Spreading codes or spreading sequences, as they are also known, can be distinguished with respect to their orthogonality, implementation complexity, correlation, and autocorrelation properties. The best known and most commonly used set of CDMA codes are briefly described in the following sections.

3.1.1 Pseudo noise (PN) sequences

Pseudo noise sequences have properties similar to random sequences which are generated by sampling a white noise process. They are typically deterministically generated by using linear feedback shift registers [21]. PN sequences are periodic and have a noise-like behaviour, but are not orthogonal. Each additional user adds interference to the others. This interference increases linearly with each additional user [19]. The following are some of the well known PN sequences:

3.1.1.1 Maximum length sequences

Maximum length shift register sequences, also known as m-sequences, are often used PN sequences that have a small code set, good autocorrelation but bad cross-correlation properties. These have been used in many applications, including the IS-95 standard. A sequence of length $n = 2^m - 1$ bits is generated by m length shift registers with linear feedback and has a period of length n. Each period contains 2^{m-1} ones and $2^{m-1} - 1$ zeros, thus making it a near balanced sequence [9].

3.1.1.2 Gold sequences

Gold codes are types of binary sequences that have better cross-correlation properties than m-sequences and are used in DSSS systems such as UMTS. A set of Gold codes can be derived from a pair of preferred m-sequences to produce $2^m - 1$ sequences, each one with a period of $2^m - 1$. Gold sequences can be used in asynchronous communication, because they have favourable but non-ideal cross-correlation properties [9], [37].

3.1.1.3 Kasami sequences

Kasami sequences are obtained by decimating m-sequences and performing modulus-2 additions on cyclically shifted sequences. Small and large set Kasami codes can be generated [19]. Kasami binary sequences have good, but non-zero cross-correlation values that reach the Welch lower bound.

3.1.2 Orthogonal codes

Orthogonal codes provide zero cross-correlation amongst users, if the codes are used in synchronous channels. Orthogonal codes will lose their orthogonality if they are used in asynchronous transmission channels, such as in the uplink channels in a mobile cellular environment [21]. Therefore, the CDMA system requires accurate synchronisation of the codes to prevent the users from interfering with each other. Some of the commonly used orthogonal spreading are the following.

3.1.2.1 Walsh-Hadamard codes

Walsh-Hadamard codes are generated by recursively constructing Hadamard matrices. They have a fixed spreading factor and are not very efficient due to their power density being concentrated in a small number of discrete frequencies [21]. The rows of a generated Hadamard matrix correspond to a Walsh-Hadamard sequence. A maximum of L orthogonal spreading codes for K users can be generated as seen in (3.1) [9].

$$\mathbf{C}_L = \begin{bmatrix} \mathbf{C}_{L/2} & \mathbf{C}_{L/2} \\ \mathbf{C}_{L/2} & -\mathbf{C}_{L/2} \end{bmatrix}, \qquad \forall L = 2^m, \qquad m \geq 1, \quad \mathbf{C}_1 = 1. \tag{3.1}$$

Walsh-Hadamard codes form the basis for orthogonal codes with different spreading factors (OVSF), and are mainly used in cdma2000 and IS-95 systems.

3.1.2.2 Orthogonal variable spreading factor (OVSF) codes

Orthogonal variable spreading factor codes are useful in scenarios where signals require different spreading factors to share the same frequency channel and where multiple rate service is needed [21]. OVSF codes are constructed using a binary tree structure, which shows the construction of Hadamard matrices and better visualises the different code lengths and orthogonality between them [9]. OVSF codes can be found in WCDMA and time division synchronous CDMA (TD-SCDMA) systems.

Some of the main CDMA spreading codes were given above, but there are other codes and sequences available. For example, the Zadoff-Chu codes have an ideal periodic autocorrelation function and a low constant magnitude periodic cross-correlation function [9]. They are a special case of generalised chirp-like sequences and enable a low peak-to-average power ratio (PAPR) when implemented. Then, there are less widely used codes including Kronecker sequences, Gordon Mills Welch (GMW) sequences, cross-correlation level (CCL) codes, Bent sequences, multi-band wavelet packet spreading codes, and No codes [33].

3.2 LIMITATIONS OF TRADITIONAL CDMA CODES

The performance of a CDMA system is directly related to the performance of the CDMA codes it uses. Many problems in CDMA systems stem from the spreading sequences or codes used. Unfortunately, CDMA technology has not drastically changed nor improved, and the core CDMA technologies have been repeatedly used in 2G and 3G systems.

Spreading sequences were not designed for wireless cellular concepts and were proposed much earlier with other design applications in mind. Specifically, they were designed based on their autocorrelation functions for radar applications and were proposed much earlier by researchers working in information theory [33]. These spreading codes were not created with the knowledge of the degrading effects of wireless channels and those codes which were used in the first CDMA systems, such as cdma2000, IS-95, and W-CDMA were developed before the CDMA cellular concept was proposed [33]. Thus, systems were designed around inherent flaws of the codes and interference-limited performance was unavoidable.

The codes/sequences mentioned above, namely Kasami codes, Gold codes, m-sequences, Walsh-Hadamard sequences, and OVSF codes, all have limitations and are not ideally suited

for future wireless systems. Regrettably, they are still used by both 2G and 3G mobile systems for CDMA purposes. Some of the main inherent limitations of traditional orthogonal CDMA spreading codes currently used by 2G to 3G mobile cellular systems are listed below [33]:

- A huge problem in these aforementioned spreading codes are their non-ideal correlation properties, which predominantly leads to multi-user interference effects. Bad aperiodic correlation properties makes them unsuitable for high speed applications in bursty traffic channels.

- Another limitation is the problem of supporting variable data rates and the ability to change their spreading factor/rate at any required time. For example, in WCDMA, OVSF codes are not able to provide exact rate matches for particular rate demands. Rate matching can only be addressed in multiples of two, which can waste a great deal of precious bandwidth. Solutions to this require complex rate matching algorithms which can adjust the data rates to the spreading rates. Additionally, code assignment blocking (CAB) problems can occur in which the use of a code for a particular spreading factor will block all its parent codes and all its child codes.

- A poor aperiodic cross-correlation function resulting from their use in asynchronous CDMA transmission causes multiple interference problems in the system, and orthogonal spreading codes that are used in asynchronous transmission channels lose their orthogonality.

- Traditional CDMA systems are sensitive to time-selective fading caused by time-variations and Doppler effects in the mobile channel. This in turn produces multiple access interference.

As pointed out, existing spreading codes are not suitable for future wireless CDMA technologies. The complexity of the receiver must grow significantly in order to improve the performance of the system and deal with many of the inherent impairing problems traditional codes introduce. Ideal interference-free CDMA systems will not be realisable using traditional spreading codes as applied to existing 2G to 3G systems. However, perfect orthogonal complementary codes proposed by [35], [20] and [36], have shown that an interference-free CDMA system can be developed. These ideal orthogonal complete complementary codes

show perfect correlation properties, allowing a simple correlator to solve MAI and MI problems in CDMA systems that support high speed bursty traffic [33].

3.3 ORTHOGONAL COMPLETE COMPLEMENTARY CODES

The proposed system presented in this study is based on orthogonal complete complementary codes, which can achieve interference-free performance, suppress MAI/MUI effects and improve system capacity due to their inherent ideal auto- and cross-correlation properties.

The main difference between traditional CDMA and complete complementary codes is that the orthogonality of complete complementary codes is based on a set of element codes called a flock, instead of a single code [21]. These codes have a zero autocorrelation for all shifts except the zero shift and zero cross-correlation function for all possible shifts [17].

The family size or number of flocks is equal to the number of element codes in one flock and can be defined as $M = \sqrt{L}$. The processing gain of the codes can then be defined by $L.\sqrt{L}$, where L is the length of every element code sequence [17], [21].

The autocorrelation of the code can be expressed as follows [38]:

$$\phi_{xx}(k) = \sum_{n=-\frac{L}{2}}^{\frac{L}{2}-1} \sum_{i=1}^{\sqrt{L}} a_{n,i}^{(x)} a_{n+k,i}^{(x)} = \begin{cases} L\sqrt{L}, & k = 0 \\ 0, & k \neq 0, \end{cases} \tag{3.2}$$

where ϕ_{xx} is the autocorrelation function (3.2) of set x. The cross-correlation function (3.3) of sets x and y is given by

$$\phi_{xy}(k) = \sum_{n=-\frac{L}{2}}^{\frac{L}{2}-1} \sum_{i=1}^{\sqrt{L}} a_{n,i}^{(x)} a_{n+k,i}^{(y)} = 0, \qquad \forall k \tag{3.3}$$

where k is the number of shifts between the sequences, and n is the nth element of each code sequence [38].

3.3.1 Complete complementary code generation

There are various ways to construct complete complementary codes. In [20], [36] an algebraic method is used to generate super complementary code sets, called the real environment adapted linearisation (REAL) approach. The REAL approach generates interference-free CDMA code sets with perfect auto- and cross-correlation properties. This approach however, requires a great computational load [19]. Super complementary codes support more users in the same code set under a fixed PG value [33], [36]. For the purposes of this system design the practical advantage of supporting more users is not required. Below, a more practical approach to generating the codes is presented according to the algorithm outlined in [18].

A matrix approach is taken in generating the code sets using a $\sqrt{L}$-dimensional orthogonal matrix, where L is the length of the element code generated [36]. Define an $N \times N$ dimensional orthogonal matrix $\mathbf{A}$,

$$\mathbf{A} = \begin{pmatrix} \mathbf{A}_1 \\ \mathbf{A}_2 \\ \vdots \\ \mathbf{A}_N \end{pmatrix} = \begin{pmatrix} a_{11} & a_{12} & \cdots & a_{1N} \\ a_{21} & a_{22} & \cdots & a_{2N} \\ \vdots & \vdots & \vdots & \vdots \\ a_{N1} & a_{N2} & \cdots & a_{NN} \end{pmatrix}, \tag{3.4}$$

consisting of a_{ik} for $i = 1,2,...,N$ and $k = 1,2,...3$ complex elements, such that the absolute values are $|a_{ik}| = 1$ and the inner product of any two different rows in the matrix should be zero, or

$$\sum_{i=1}^{N} a_{ik} a_{mi}^{*} = 0, \qquad \text{where } k \neq m. \tag{3.5}$$

From this it can be shown that the autocorrelation function of the sequence or matrix $\mathbf{A}$ is zero for all N-multiple shifts, except the zero shift [33].

Then let $\mathbf{B}$ be another $N \times N$ orthogonal matrix

$$\mathbf{B} = \begin{pmatrix} \mathbf{B}_1 \\ \mathbf{B}_2 \\ \vdots \\ \mathbf{B}_N \end{pmatrix} = \begin{pmatrix} b_{11} & b_{12} & \cdots & b_{1N} \\ b_{21} & b_{22} & \cdots & b_{2N} \\ \vdots & \vdots & \vdots & \vdots \\ b_{N1} & b_{N2} & \cdots & b_{NN} \end{pmatrix}, \tag{3.6}$$

from which N sequences of length N^2 can be constructed as follows:

$$\begin{aligned} \mathbf{E}_1 &= (b_{11}\mathbf{A}_1, b_{12}\mathbf{A}_2, \ldots, b_{1N}\mathbf{A}_N) \\ \mathbf{E}_2 &= (b_{21}\mathbf{A}_1, b_{22}\mathbf{A}_2, \ldots, b_{2N}\mathbf{A}_N) \\ &\vdots \\ \mathbf{E}_N &= (b_{N1}\mathbf{A}_1, b_{N2}\mathbf{A}_2, \ldots, b_{NN}\mathbf{A}_N), \end{aligned} \tag{3.7}$$

where $\mathbf{A}_i$ is the ith row of the $\mathbf{A}$ matrix [19]. Each $\mathbf{E}_i$ $(1 \leq i \leq N)$ has an autocorrelation of zero for any shift except the zero shift and the cross-correlation of any two sequences is zero for all shifts. These N sequences $\mathbf{E}_i$ $(i = 1, 2, \ldots, N)$, can be rewritten as

$$\begin{aligned} \mathbf{E}_1 &= (e_{11}, e_{12}, \ldots, e_{1N^2}) \\ \mathbf{E}_2 &= (e_{21}, e_{22}, \ldots, e_{2N^2}) \\ &\vdots \\ \mathbf{E}_N &= (e_{N1}, e_{N2}, \ldots, e_{NN^2}). \end{aligned} \tag{3.8}$$

Again let $\mathbf{D}$ be another $N \times N$ dimensional orthogonal matrix

$$\mathbf{D} = \begin{pmatrix} \mathbf{D}_1 \\ \mathbf{D}_2 \\ \vdots \\ \mathbf{D}_N \end{pmatrix} = \begin{pmatrix} d_{11} & d_{12} & \cdots & d_{1N} \\ d_{21} & d_{22} & \cdots & d_{2N} \\ \vdots & \vdots & \vdots & \vdots \\ d_{N1} & d_{N2} & \cdots & d_{NN} \end{pmatrix}, \tag{3.9}$$

from which a complete complementary code set $\mathbf{C} = (\mathbf{C}_1, \mathbf{C}_2, \ldots, \mathbf{C}_N)$ can be constructed by

$$\begin{aligned} \mathbf{C}_{ik} =& (e_{i1}d_{k1}, \ldots, e_{iN}d_{kN}, e_{i(N+1)}d_{k1}, \ldots, e_{i(2N)}d_{kN}, \ldots, \\ & e_{i(N^2-N+1)}d_{k1}, \ldots, e_{i(N^2)}d_{kN}) \qquad (3.10) \\ =& (c_{ik1}, c_{ik2}, \ldots, c_{ikN^2}), \qquad \text{for } i, k = 1, 2, ..., N, \qquad (3.11) \end{aligned}$$

which gives N flocks of complete complementary codes, each flock consisting of N element codes

$$\begin{aligned} \mathbf{C}_1 &= \{\mathbf{C}_{11}, \mathbf{C}_{12}, \ldots, \mathbf{C}_{1N}\} \\ \mathbf{C}_2 &= \{\mathbf{C}_{21}, \mathbf{C}_{22}, \ldots, \mathbf{C}_{2N}\} \\ &\vdots \\ \mathbf{C}_N &= \{\mathbf{C}_{N1}, \mathbf{C}_{N2}, \ldots, \mathbf{C}_{NN}\}, \end{aligned} \tag{3.12}$$

where $\mathbf{C}_{ik}$ $(i,k = 1,2,\ldots,N)$ denotes the basic elementary code sequence of a set [36].

To improve the practical application of the spreading codes, the complete complementary codes can be extended to super complementary codes according to a unique code design approach, called the real environment adaptation linearisation (REAL) approach [20], [33], [35], [36].

Both complete complementary codes and super complementary codes are ideally orthogonal complementary codes. There is no difference in terms of their orthogonality properties, as they are both perfectly orthogonal [33]. However, super complementary codes can support more users than complete complementary codes, assuming similar PG values. Therefore, they add value in practical applications and the benefits are negligible in this study, in which smaller family sizes can be used.

3.4 ANALYSIS OF ORTHOGONAL COMPLETE COMPLEMENTARY CODES

As mentioned earlier, orthogonal complete complementary codes can retain their perfect cross-correlation properties for both synchronous and asynchronous transmission. This means zero cross-correlation functions for any relative shifts, resulting in the desirable MAI-free operation. Additionally, these codes ensure ISI free operation and show immunity against MI due to their perfect autocorrelation function [33]. In the following sections the notion of ideal or perfect orthogonality of the codes is explained.

3.4.1 Perfect/Ideal correlation properties

3.4.1.1 Periodic cross-correlation functions

If spreading codes are ideally orthogonal, then both the even and the odd periodic cross-correlations of any two codes in the set are zero for any possible relative chip shifts.

If **A** and **B** are two codes from a perfectly orthogonal set of spreading codes and they can be described by $\mathbf{A} = (\mathbf{A}_1, \mathbf{A}_2, \ldots, \mathbf{A}_M)$ and $\mathbf{B} = (\mathbf{B}_1, \mathbf{B}_2, \ldots, \mathbf{B}_M)$, then they are said to be complementary codes containing M element codes. Each element code is made up of N chips, rewritten as $\mathbf{A}_m = (a_{m1}, a_{m2}, \ldots, a_{mN})$ and $\mathbf{B}_m = (b_{m1}, b_{m2}, \ldots, b_{mN})$, where $m = 1, 2, \ldots, M$ [33].

Now if **A** and **B** are two codes from an ideally orthogonal set, they have to satisfy the even (positive sign) and the odd (negative sign) periodic cross-correlation functions in (3.13).

$$R_{\mathbf{A},\mathbf{B}}(\tau) = \sum_{m=1}^{M} \left[\sum_{i=1}^{\tau} a_{mi} b_{m(N-\tau+i)} \pm \sum_{i=\tau+1}^{N} a_{mi} b_{m(i-\tau)} \right] = 0, \qquad \forall \tau, \tag{3.13}$$

where τ is the relative delay between the two codes **A** and **B** [33]. Equation (3.13) is in a general form applicable to any code, when $M = 1$, implying that non-complementary codes, such as those listed in Section 3.1, are considered. Otherwise, when using the equation with $M > 1$, it refers to complementary codes that have a flock of M element codes. The complementary codes given in Section 3.3, have perfect cross-correlation functions and can therefore be defined as ideally or perfectly orthogonal codes [33].

3.4.1.2 Periodic autocorrelation functions

The cross-correlation function defines the ideal orthogonality of the set of codes, whereas the autocorrelation function determines the detection efficiency. This important even and odd periodic autocorrelation function for an ideal spreading code, can be defined as follows [33]:

$$R_{\mathbf{A},\mathbf{A}}(\tau) = \begin{cases} \sum_{m=1}^{M} \left[\sum_{i=1}^{\tau} a_{mi} a_{m(N-\tau+i)} \pm \sum_{i=\tau+1}^{N} a_{mi} a_{m(i-\tau)} \right] = NM, & \tau = 0 \\ \sum_{m=1}^{M} \left[\sum_{i=1}^{\tau} a_{mi} a_{m(N-\tau+i)} \pm \sum_{i=\tau+1}^{N} a_{mi} a_{m(i-\tau)} \right] = 0, & \text{elsewhere,} \end{cases} \tag{3.14}$$

where τ is the relative chip delay between the incoming code received and the local correlator. Similar to the previous cross-correlation function, if $M = 1$, the correlation requirements imply a simple unitary code set, or else it would refer to a complementary code set. The positive and negative sign produces the even or odd periodic autocorrelation functions respectively, as seen in (3.14) [33].

If the set size of a specific code is K, then $\frac{K!}{2!(K-2)!} = \binom{K}{2}$ equations need to be specified to verify the ideally orthogonal conditions as given by the cross-correlation function in (3.13) and K equations need to specify the ideal autocorrelation function in (3.14) [33].

3.4.2 Periodic and aperiodic correlations

As mentioned before, the correlation properties are of great importance in any CDMA type system and determine the overall performance of a CDMA system. There are two types of correlation functions often referred to, namely the periodic and aperiodic correlation functions. It was proven by [33], that if a code under consideration is an ideally orthogonal code set and thus has perfect periodic correlation properties, the code set will also have perfect aperiodic correlation properties and vice versa. The perfect correlation property requirement for a code set was defined in the previous Section 3.4.1. In other words, it was shown that perfect aperiodic correlation properties of a code set is a sufficient condition to achieve perfect periodic correlation properties of the same code set. This result greatly reduces the complexity of the code analysis, as the aperiodic correlation functions have a less complex form than the periodic correlation functions. This aids in the application of the codes in a practical system and allows for side benefits when applying a novel cyclic rotation scheme (see Section 3.4.3.1 and 4.1.2.1).

3.4.2.1 Aperiodic correlation functions

Similar to the periodic correlation functions of (3.13) and (3.14), two code sets with flock size and element code length M and N, respectively, can be defined by

$$\mathbf{X} = \begin{pmatrix} x_{1,1} & x_{1,2} & \dots & x_{1,N} \\ x_{2,1} & x_{2,2} & \dots & x_{2,N} \\ & & \vdots & \\ x_{M,1} & x_{M,2} & \dots & x_{M,N} \end{pmatrix}, \qquad \mathbf{Y} = \begin{pmatrix} y_{1,1} & y_{1,2} & \dots & y_{1,N} \\ y_{2,1} & y_{2,2} & \dots & y_{2,N} \\ & & \vdots & \\ y_{M,1} & y_{M,2} & \dots & y_{M,N} \end{pmatrix}. \tag{3.15}$$

With these code sets in mind, the less complex aperiodic autocorrelation function can be written as

$$R_{\mathbf{X},\mathbf{X}}(i) = \sum_{m=1}^{M} \sum_{n=1}^{N-i} x_{m,n} x_{m,n+i}, \tag{3.16}$$

and the aperiodic cross-correlation function with an offset chip shift being i chips, is given by

$$R_{\mathbf{X},\mathbf{Y}}(i) = \sum_{m=1}^{M} \sum_{n=1}^{N-i} x_{m,n} y_{m,n+i}. \tag{3.17}$$

These aperiodic functions cover one element code length, whereas the periodic functions (Section 3.4.1) consider consecutive bits which may have different signs, leading to different correlation values being generated [33].

3.4.3 Correlation properties

To illustrate the ideal correlation properties of an orthogonal complete complementary code set, the correlation properties of an example code set with a processing gain of $PG = L \times M = 16 \times 4 = 64$, are shown in Figure 3.1 and Figure 3.2. The code set has a flock and set size of $M = 4$ and an element code length of $L = 16$.

In Figure 3.1 it can be seen that the autocorrelation of each element code is not ideal and has many non-zero side lobes. However, the sum of the separate autocorrelations yield an ideal autocorrelation value $R_A(\tau)$ with a large peak equal to the processing gain and zero side lobes. In the figure, $R_{A0,A0}(\tau)$ is the autocorrelation of element code A_0, $R_{A1,A1}(\tau)$ is the autocorrelation of element code A_1, and so forth for $M = 4$ element codes in each flock and then summing up to obtain $R_A(\tau)$.

Similarly, in Figure 3.2 the same characteristics can be seen in which the separate correlations of the element codes of flock A and B add up to produce a zero cross-correlation with zero side lobe values for all chip shifts. These desirable characteristics can be found in other orthogonal complementary codes, some of them listed in Appendix A. These features of the codes have previously not been found in traditional CDMA codes such as Walsh-Hadamard sequences, OVSF codes, etc. (as listed in Section 3.1).

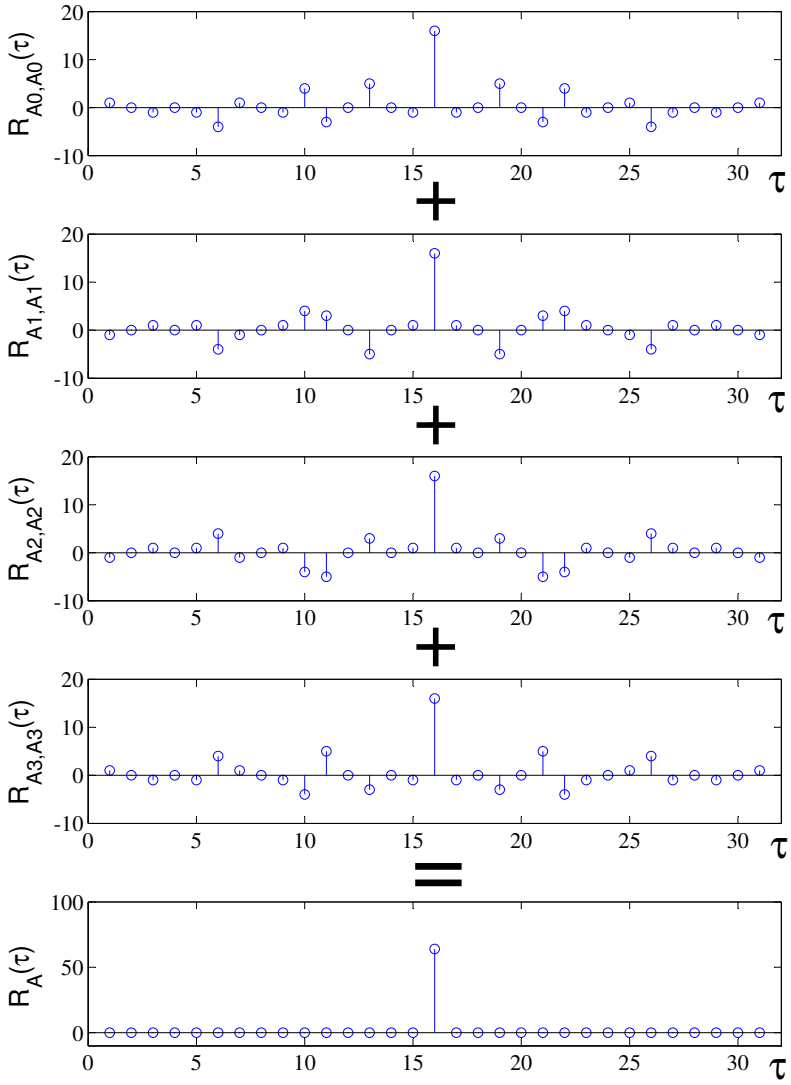

Figure 3.1: *Autocorrelation properties of an orthogonal complete complementary code, with four element codes of length 16 and a processing gain of 64, where $R_A(\tau)$ is the sum of $R_{A0,A0}(\tau)$, $R_{A1,A1}(\tau)$, $R_{A2,A2}(\tau)$, and $R_{A3,A3}(\tau)$, producing an ideal autocorrelation function with a peak and no side lobes.*

Orthogonality among the complementary codes is established after all non-zero side lobes of the cross-correlation and autocorrelation are cancelled at the summation unit of the receiver [33]. When considering a code set with a flock size of $M = 4$, which is equal to the set size $K = 4$ (number of element codes in a flock), then there are $\binom{K}{2} = \binom{4}{2} = 6$ cross-correlations, and $K = 4$ autocorrelations that need to be performed to specify and confirm these ideally orthogonal and perfect correlation properties. This example of a complete complementary spreading code is presented in Appendix A.

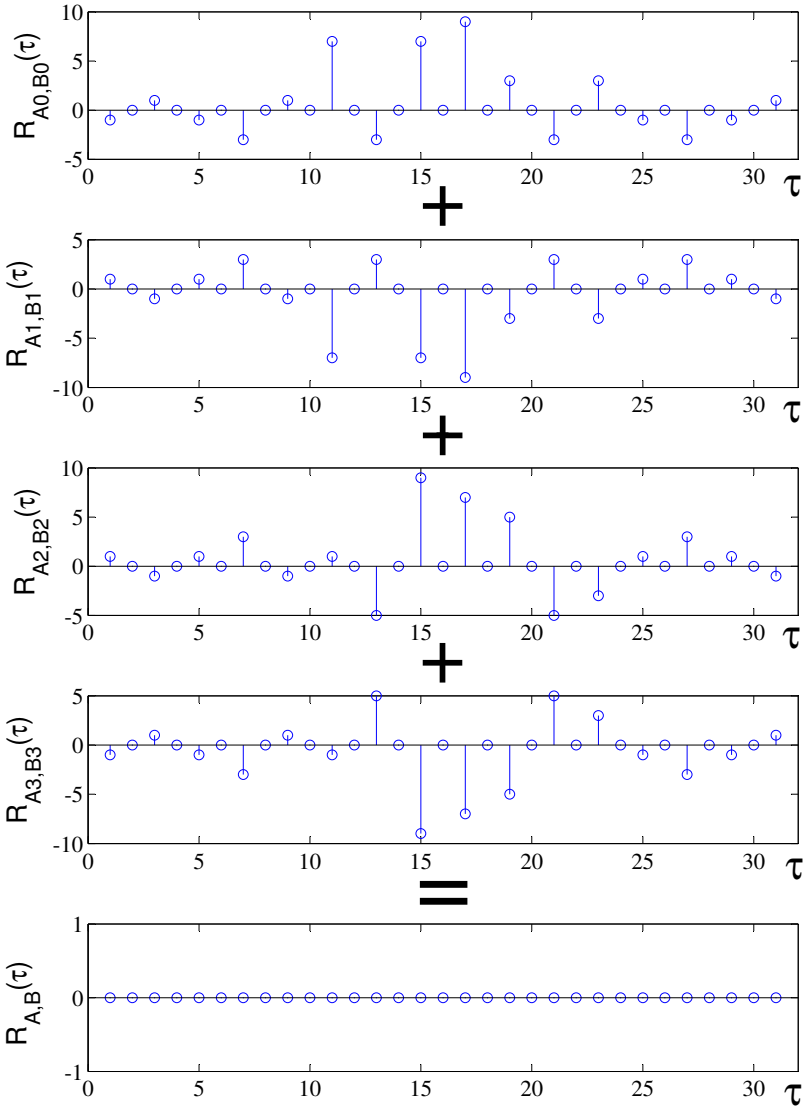

Figure 3.2: *Cross-correlation function of an orthogonal complete complementary code, where $R_{A,B}(\tau)$ is the sum of all cross-correlation values of the individual code elements of flock A and flock B, resulting in a zero cross-correlation function with no side lobes.*

3.4.3.1 Periodic correlation functions

Similar to the aperiodic correlation functions, the periodic out-of-phase autocorrelation functions are zero and a large peak is visible in the first chip position, as seen in Figure 3.3(a), where $R^p_A(\tau)$ is the sum of $R^p_{A0,A0}(\tau)$, $R^p_{A1,A1}(\tau)$, $R^p_{A2,A2}(\tau)$, and $R^p_{A3,A3}(\tau)$. The summed periodic cross-correlation values are given in Figure 3.3(b), where $R^p_{A,C}(\tau)$ is the sum of all cross-correlation values of the individual code elements of flock A and flock C. The cross-

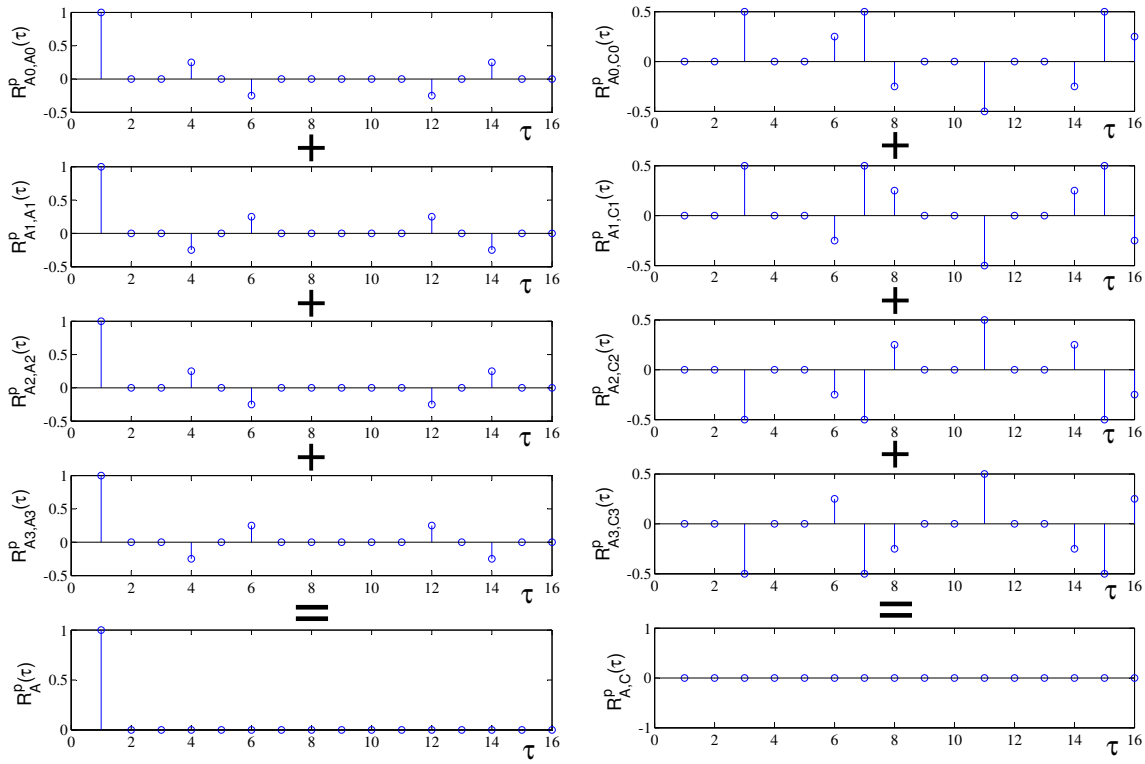

(a) Periodic autocorrelation (b) Periodic cross-correlation

Figure 3.3: *Periodic correlation properties of an orthogonal complete complementary code, with four element codes of length 16 and a processing gain of 64. No side lobes in the summed autocorrelation (a) and zero cross-correlation values seen in (b).*

correlation values are all zero for all possible time shifts, again showing that the codes are ideal, as formulated in Section 3.4.1. It can be seen that the autocorrelation peak is located at chip index one. This property is used in the modem design to identify shifted sequences, which would produce a peak at the chip index equaling the number of cyclic shifts the sequence has undergone.

Generally, a direct evaluation of the correlation or convolution summation requires $O(N^2)$ operations for an output sequence with a length N. However, by making use of fast convolution algorithms and using transforms, the arithmetic complexity can be reduced to $O(N \log N)$. The implemented novel system described in the following chapter makes use of fast convolution algorithms and fast Fourier transforms to achieve much better performance with less complexity. In convolution, one signal is mirrored prior to calculating the overlap, and in cross-correlation, two different signals are shifted and multiplied without reversing or mirroring one sequence. Seeing that the convolution of two signals is similar to their cross-

correlations, these methods can be adapted at the receiver to perform the correlation with less complexity and with simple FFT operations. This unique reception strategy is further explained in Chapter 4, in which the cyclic rotated code design is described in more detail.

By using the FFT and the circular convolution theorem, the correlation of two finite length sequences can be found by taking the FFT of one sequence and the complex conjugate FFT of another, point-wise multiplying them, and then performing an inverse FFT of the result. Thus, the cross-correlation of sequences $\mathbf{x}$ and periodically extended $\mathbf{y_N}$, can be given by

$$\mathscr{F}^{-1}\left\{\mathbf{X}^* \cdot \mathbf{Y}\right\}_n = \sum_{l=0}^{N-1} x_l^* \cdot (y_N)_{n+l} \stackrel{\text{def}}{=} (\mathbf{x} \star \mathbf{y_N})_n. \tag{3.18}$$

This can also be rewritten using the FFT operators ($\mathscr{F}$) as

$$R_{A,B}^p = \mathscr{F}^{-1}\left(\mathscr{F}(\mathbf{A}) \cdot \overline{\mathscr{F}(\mathbf{B})}\right), \tag{3.19}$$

where $\mathbf{A}$ and $\mathbf{B}$ are the different element codes previously used and $\mathscr{F}^{-1}$ is the inverse fast Fourier transform. With the use of the FFT method, the periodic correlation functions can be determined much faster and with far less arithmetic complexity.

The concept of cyclically convolving two sequences using fast Fourier transforms built the foundation for many asymptotically fast multiplication algorithms for large integers. For instance, the well known Schönhage-Strassen algorithm depends fundamentally on the convolution theorem [39]. Most optimised multiplication algorithms make use of this theorem and have proven the benefits and complexity reduction of using fast Fourier transforms when needing to multiply large numbers or computing complex convolutions. Thus, the convolution theorem or FFT methods provide an efficient and far less complex algorithm to compute the cyclic convolution or cross-correlation of two sequences. This greatly helps in the design and efficiency of a performance improved communications system such as the one proposed in this research.

CHAPTER 4

SYSTEM MODEL

This chapter introduces the system design of the proposed multi-dimensional code-division-multiplexed OFDMA modem, which makes use of cyclic rotated orthogonal complete complementary codes. First, the basics of the spread spectrum system are explained, followed by the description of the multiple access and carrier implementation. Then, the flexibility in the design and the adaptability to existing technologies such as OFDMA will be presented.

The novel multi-layered modulation technique makes use of a multi-dimensional modem to improve spreading code usage, throughput and overall performance of the system. The term *multi-layered* modulation specifically refers to the use of practically all available diversity means to modulate and spread in all possible dimensions, excluding the spatial domain, which is not addressed in this research. The modem is implemented with cyclic rotated super-orthogonal complete complementary codes (CRCC) to offer MAI-free operation, only possible due to the perfect autocorrelation and zero cross-correlation properties of the codes. Hence, *super-orthogonality* refers to the perfect periodic and a-periodic even and odd auto and cross-correlation properties of the family of CC codes utilised. The use of CRCC codes and a multi-dimensional modulation scheme enables the 4D block to reach double the theoretical spectral efficiency when using BPSK. Although it is a spread spectrum system, there is no loss in spectrum efficiency and high throughput can be achieved.

4.1 SYSTEM DESCRIPTION

4.1.1 Cyclic rotation scheme for spreading codes

Conventional complete complementary codes support only a limited number of users. Therefore, a cyclic rotation technique is used to extend the original code family size, allowing codes to be reused, increase system capacity, and spectral efficiency without losing performance. The rotations make up the spectral efficiency lost by the conventional CDMA

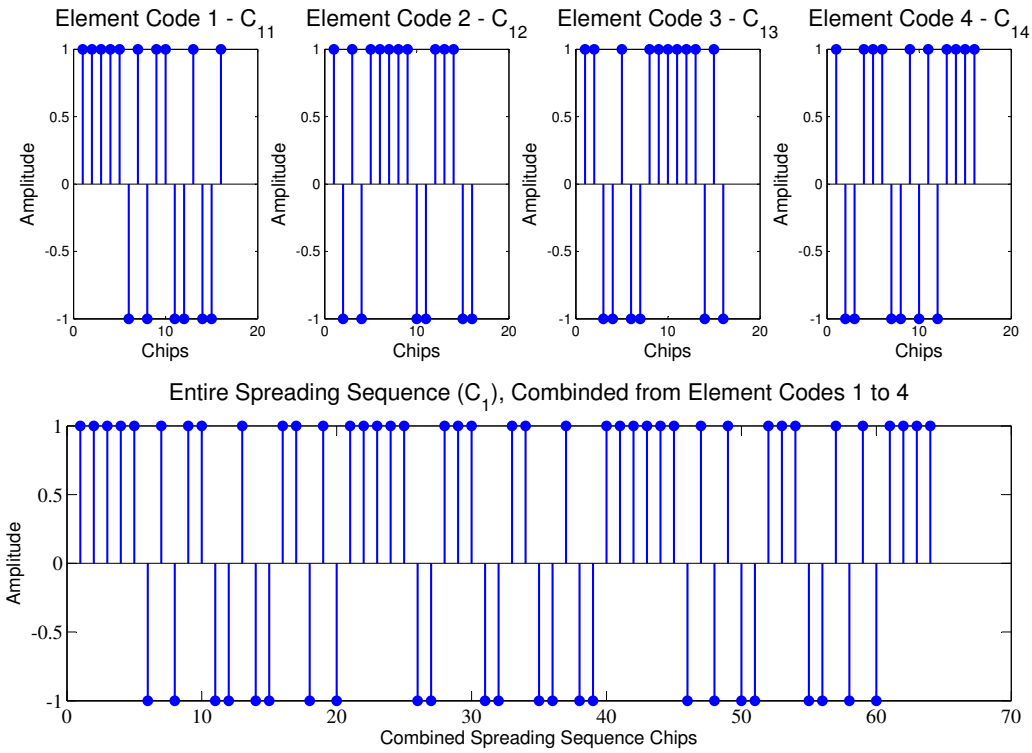

Figure 4.1: *One spreading sequence C_1, combined from 4 element codes from flock 1 ($PG = 64$, $M = 4$ and $L = 16$).*

spreading process. The periodic property of the code makes it possible to transmit more data simultaneously by carrying data in each rotation of the code, thus improving the throughput significantly. The de-spreading or reception of the rotated spreading codes can be performed by a simplified periodic cross-correlation receiver structure making use of fast Fourier transform algorithms (as explained in Section 3.4.3.1). Only the periodic cross-correlation of the original non-rotated sequence needs to be taken when using the FFT or the circular convolution theorem method to identify each rotated information bit.

For example, a complete complementary code set with $M = 4$ flocks and an elementary code length of $L = 16$, can be defined as

$$\mathbf{C}_1 = \{\mathbf{C}_{11}, \mathbf{C}_{12}, \mathbf{C}_{13}, \mathbf{C}_{14}\} \tag{4.1}$$

$$\mathbf{C}_2 = \{\mathbf{C}_{21}, \mathbf{C}_{22}, \mathbf{C}_{23}, \mathbf{C}_{24}\} \tag{4.2}$$

$$\mathbf{C}_3 = \{\mathbf{C}_{31}, \mathbf{C}_{32}, \mathbf{C}_{33}, \mathbf{C}_{34}\} \tag{4.3}$$

$$\mathbf{C}_4 = \{\mathbf{C}_{41}, \mathbf{C}_{42}, \mathbf{C}_{43}, \mathbf{C}_{44}\}, \tag{4.4}$$

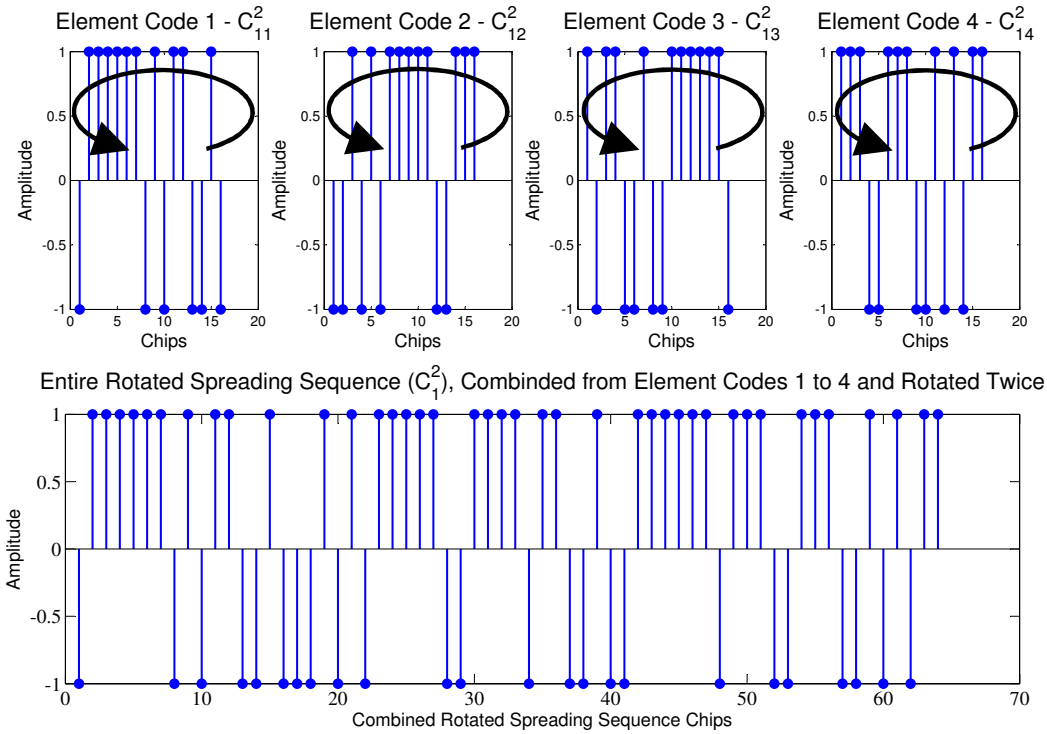

Figure 4.2: *Cyclic rotated spreading code $C^{r=2}_{n=1}$, combined from 4 element codes from flock 1 each rotated by 2 chip shifts ($PG = 64$, $M = 4$ and $L = 16$).*

where $\mathbf{C}_{ik}$ $(i,k = 1,2,3,4)$ is the basic elementary code sequence of a set or flock.

From this, a combined un-rotated spreading sequence for flock 1 can be created by combining all the elementary codes of the first flock $\mathbf{C}_{11}$, $\mathbf{C}_{12}$, $\mathbf{C}_{13}$, and $\mathbf{C}_{14}$. This resulting spreading sequence of the first flock $\mathbf{C}_1$ can be seen in Figure 4.1. The spreading sequence given by (4.1) (or seen in Figure 4.1) can then be cyclically rotated $L = 16$ times, creating a new set of sequences defined as $\mathbf{C}^r_n$, where r defines the rotational index or number of cyclic chip shifts of the code and n still refers to the specific flock number. The orthogonality and perfect correlation properties of the codes are not destroyed by the cyclic shifting operation, so the newly defined cyclic rotated codes of the first flock ($n = 1$) can be given by

$$\mathbf{C}^{r=1}_1 = \{\mathbf{C}^1_{11}, \mathbf{C}^1_{12}, \mathbf{C}^1_{13}, \mathbf{C}^1_{14}\} \tag{4.5}$$

$$\mathbf{C}^{r=2}_1 = \{\mathbf{C}^2_{11}, \mathbf{C}^2_{12}, \mathbf{C}^2_{13}, \mathbf{C}^2_{14}\} \tag{4.6}$$

$$\cdots$$

$$\mathbf{C}^{r=L}_1 = \{\mathbf{C}^L_{11}, \mathbf{C}^L_{12}, \mathbf{C}^L_{13}, \mathbf{C}^L_{14}\}, \tag{4.7}$$

Table 4.1: *Spreading code properties and relations.*

Matrix dimension	Element code length	Flock, set size	Processing gain
N	$N^2 = L$	$N = M$	N^3

where L equals the elementary code length (16 in this example). Thus, 16 rotations can be applied to the first flock before cyclically repeating the sequence.

In Figure 4.2, an example spreading sequence of the first flock with a 2 chip shift cyclic rotation is depicted. Each separate elementary code needs to be rotated 2 times ($r = 2$) before combining the $M = 4$ elementary codes together to form an entire LM length spreading sequence $\mathbf{C}_1^2$.

This rotation technique produces L spreading codes from one flock and allows additional data bits to be transmitted with each rotation of the code. The cyclic rotated complete complementary codes improve the throughput and negate the loss in spectral efficiency resulting from the spreading of the data. The periodic correlation properties are still maintained when applying the cyclic rotation. The rotation of the codes in the proposed system allows $4 \times r$ additional bits to be transmitted simultaneously for r-rotations of the code in one multi-dimensional building block (or $2M \times r$ for the entire system); this process will be further explained in the following section.

4.1.2 Multi-layered multi-dimensional spread spectrum system design

The multi-layered building block described in Chapter 2 and the spreading codes described in Chapter 3, form the foundation of the proposed modulation technique. The signal of the novel system is generated using a combination of CDMA and OFDMA techniques. Multiple transmitter blocks are combined and parallelised by the CRCC codes to form a high throughput modulation technique which is spectrally efficient and capable of exploiting the diversity in the radio channel to improve performance. The usage of the CRCC codes enables the data from multiple combined multi-dimensional building blocks to be transmitted simultaneously over one channel, since the codes allow the data to be differentiated again at the receiver, as in CDMA techniques. A collection of these combined blocks can then be spread onto different sub-carrier frequencies using OFDMA principles.

The input information sequence of the Uth user is first converted into $2ML$ parallel data sequences $d^U_{m,r}$ for $m = 1,\ldots,2M$ and $r = 1,\ldots,L$, where M defines the flock or set size and L the length of every element code sequence.

The whole set of code sequences in one flock is used to spread a symbol, thus, the processing gain is large and is sometimes referred to as the congregate processing gain [38]. Every information symbol or bit $d^U_{m,r}$ is spread with the corresponding spreading sequence $\mathbf{C}^r_n[l]$, $n = 1,\ldots,M$ as seen in (4.8), where the length of $\mathbf{C}^r_n[l]$ is LM ($l = 1\ldots LM$). Then, through the novel rotation of the CRCC codes, the entire process is repeated L times, where $r = 1,\ldots,L$ refers to the rotational index. Leaving out the time index, the transmitted signal $\mathbf{S}^U$ can be described by

$$\begin{aligned}\mathbf{S}^U = &\sum_{r=1}^{L}\sum_{i=0}^{\frac{M}{2}-1}\sum_{l=1}^{LM}\left[\left(d^U_{4i+1,r}\mathbf{C}^r_{2i+1}[l] + d^U_{4i+2,r}\mathbf{C}^r_{2i+2}[l]\right)\right.\\ &\left.+j\left(d^U_{4i+3,r}\mathbf{C}^r_{2i+1}[l] + d^U_{4i+4,r}\mathbf{C}^r_{2i+2}[l]\right)\right] \qquad (4.8)\\ = &\sum_{r=1}^{L}\sum_{i=1}^{\frac{M}{2}}\left(\mathbf{Z}^U_{i,r}\right). \qquad (4.9)\end{aligned}$$

For binary input symbols (BPSK) a total of $2LM$ symbols are spread and summed together, which enables parallel transmission, thereby improving spectral efficiency. This shows that a large number of data symbols can be processed in one instance. The spectral efficiency is not equal to $1/PG$ as in traditional CDMA systems, but instead is equal to the theoretical unspread spectral efficiency of the modulation method, except when using BPSK, in which case an improved spectral efficiency of 2 bits/s/Hz can be achieved for one user's building block if the set size equals the flock size (i.e. equal to unspread QPSK). This is only possible, because of the multi-dimensionality of the system and the use of the created CRCC codes. The multi-dimensional transmitter reduces the spreading code usage and adds an imaginary dimension to the input bits.

The simplified transmitter structure of the proposed system is portrayed in Figure 4.3. It describes the implementation of the Uth user's transmitter and the generated signal $\mathbf{S}^U$. Multiple access is then achieved by assigning the users to different sub-carriers, as in OFDMA, to provide multi-user and frequency diversity. The proposed system uses CDMA not to distinguish between users, which the OFDMA technique can do, but rather to improve the multi-dimensional modem design and spectral efficiency when spreading the data, and to

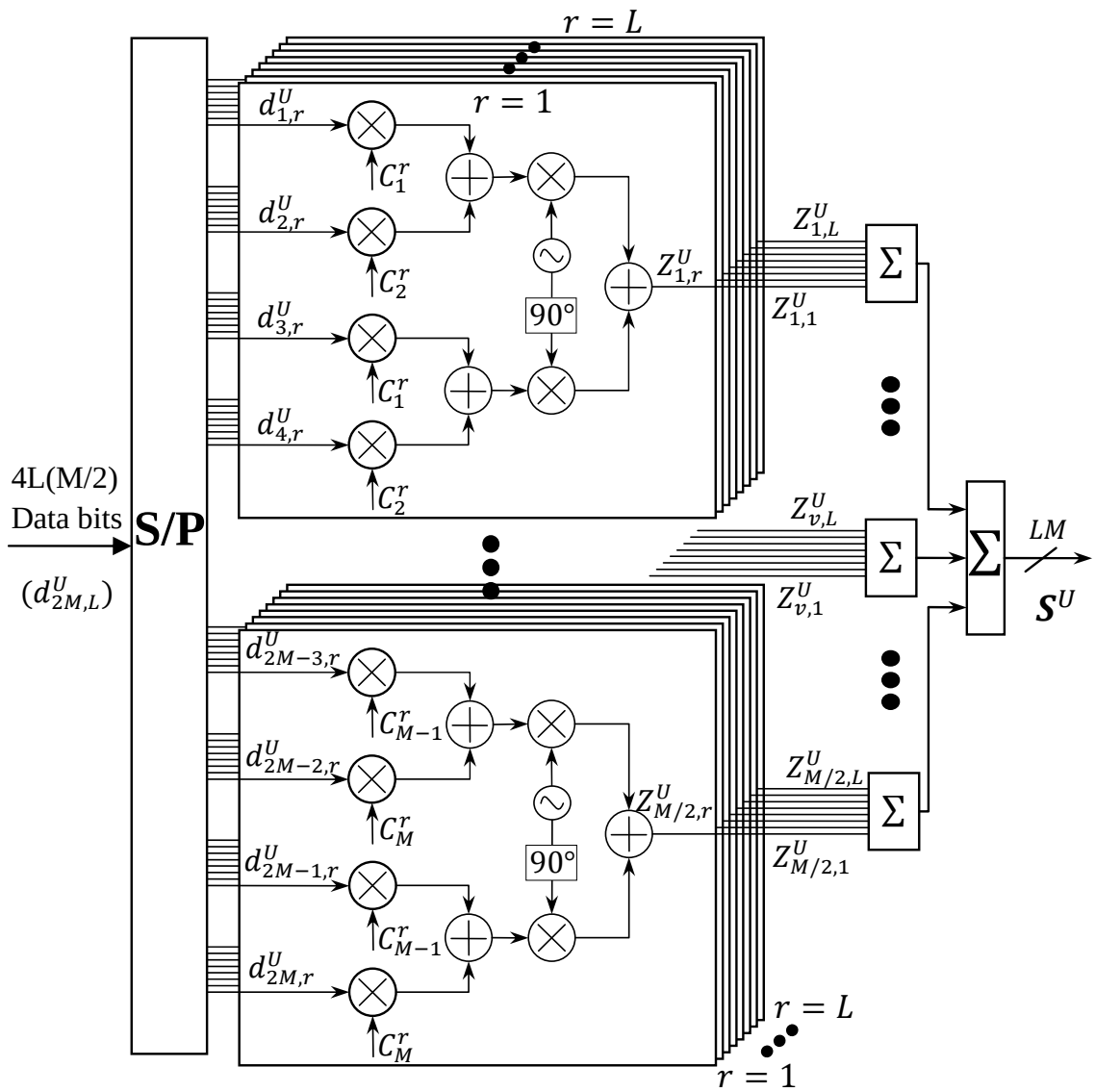

Figure 4.3: *The multi-dimensional spread spectrum code-division-multiplexed type structure of the transmitter.*

improve the throughput. Other advantages of this technique of combining code-division multiplexing and multi-carrier schemes will be presented in sections to follow.

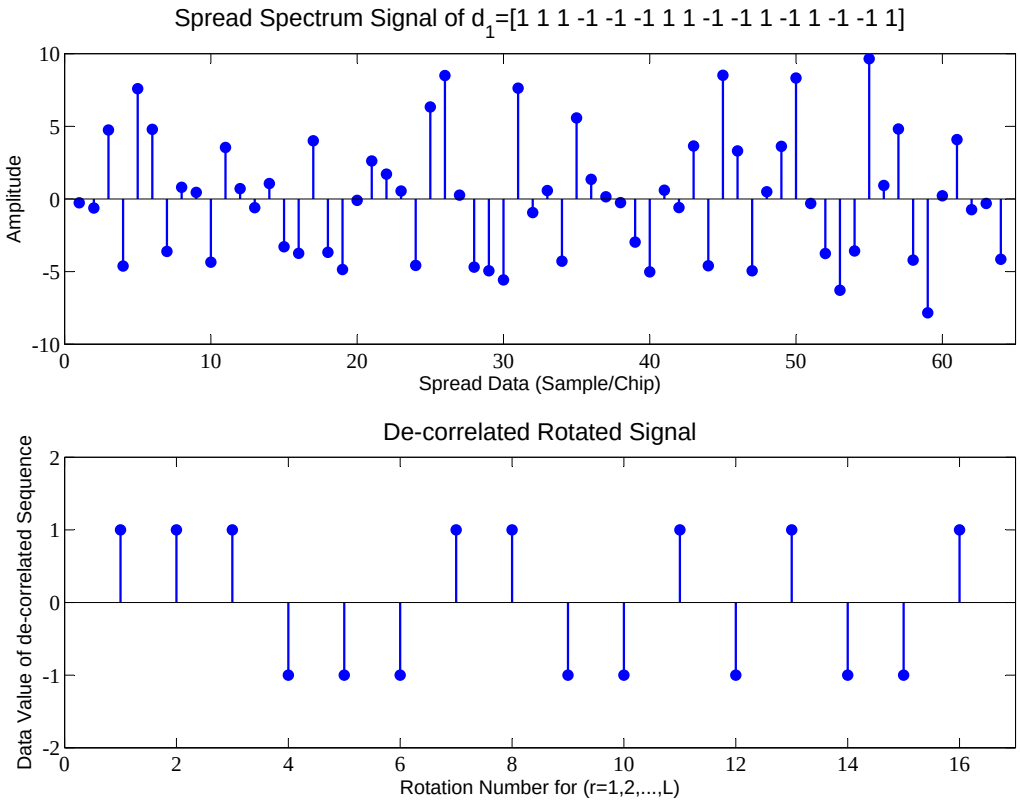

Figure 4.4: *Example of one data stream input which is rotated 16 times with flock 1. The input data in this example is binary [1 1 1 -1 -1 -1 1 1 -1 -1 1 -1 1 -1 -1 1], which is spread with one flock and all its rotations ($PG = 64$, $M = 4$ and $L = 16$).*

4.1.2.1 Example usage of the CRCC codes

As previously explained, the rotation of one spreading sequence of one flock can transmit L data symbols simultaneously. For example, a code family with a processing gain of $PG = 64$, a flock size of $M = 4$ and an elementary code sequence length of $L = 16$, can transmit or combine 16 data symbols using only one flock (or code sequence $\mathbf{C}_n$). Each data symbol would be positioned in one rotational position of the de-correlated sequence when using the FFT algorithm explained in Section 3.4.3.1. When considering the first branch of the multi-dimensional modem in Figure 4.3, and taking an example input symbol/bit vector d_1, r for $r = 1, 2, ..., 16$, as

$$d_{1,r} = [1\ 1\ 1\ \text{-1}\ \text{-1}\ \text{-1}\ 1\ 1\ \text{-1}\ \text{-1}\ 1\ \text{-1}\ 1\ \text{-1}\ \text{-1}\ 1] \text{ for } r = 1, 2, .., 16, \tag{4.10}$$

then the de-correlated data would show each data bit from the input vector in its corresponding rotational shift position of the received de-correlated sequence. The creation of the

spread spectrum signal $\mathbf{S}$ for the first branch only, with input bits $d_{1,r}$ given in (4.10), spread with the spreading sequence $\mathbf{C}_n^r$, can be expressed as

$$\mathbf{S}_{example} = \sum_{r=1}^{L} \sum_{l=1}^{LM} \left(d_{1,r} \cdot \mathbf{C}_1^r[l] \right). \tag{4.11}$$

To de-correlate the spread spectrum signal, one fast Fourier periodic cross-correlation function needs to be calculated with the un-rotated original spreading sequence $\mathbf{C}_n^{r=1}$ to yield a length L vector. This vector holds each rotated data bit at its specific rotational index. For example, rotated data bit $d_{1,4}$ would be positioned at rotational index 4 of that received vector. This method of making use of a fast Fourier transform algorithm, which is based on the convolution theorem, decreases the receiver complexity and shows a huge speed improvement in the de-correlation of the received signal. When de-correlating the transmitted signal using the same example codes previously used, the algorithm for de-correlating the length 64 transmitted signal and all of its rotations can be given by

$$\begin{aligned}
\mathbf{R} &= \mathscr{F}^{-1}\left(\mathscr{F}(\mathbf{S}) \cdot \overline{\mathscr{F}(\mathbf{C}_1^{r=1})} \right) \\
&= \mathscr{F}^{-1}\Big(\mathscr{F}\big(\mathbf{S}[1 \to 16]\big) \cdot \overline{\mathscr{F}\big(\mathbf{C}_{11}^1\big)} + \mathscr{F}\big(\mathbf{S}[17 \to 32]\big) \cdot \overline{\mathscr{F}\big(\mathbf{C}_{12}^1\big)} + \\
&\qquad \mathscr{F}\big(\mathbf{S}[33 \to 48]\big) \cdot \overline{\mathscr{F}\big(\mathbf{C}_{13}^1\big)} + \mathscr{F}\big(\mathbf{S}[49 \to 64]\big) \cdot \overline{\mathscr{F}\big(\mathbf{C}_{14}^1\big)} \Big),
\end{aligned} \tag{4.12}$$

where $S[.]$ refers to a sub-set range of values of the transmitted vector. The spread spectrum signal and the de-correlated received vector can be seen in Figure 4.4. In the received vector, each rotation shows the peak autocorrelation value or originally transmitted data bit. The rest of the values are zero, since the cross-correlation of any two sequences is zero for all shifts and the autocorrelation is also zero except for the zero-shift.

4.1.2.2 Multi-user assignment

In the spread spectrum transmitter, as described in the previous sections, the information bits are separated by multiple branches and their respective assigned spreading codes. Thus, each branch can be distinctly separated by code-division, as is the case in a CDMA type spread spectrum system. The system has various design alternatives in which the user assignment is not fixed. For example, different users can be assigned to different data input branches and thus each user has his own data input stream. Alternatively, an entire 4D building block can be used for one user. However, to improve throughput, and with the use of

OFDMA techniques, an entire transmitter as seen in Figure 4.3, was chosen to define one user block. Thus, each user utilises the same building block structure, but is separated by assigning the transmitted spread spectrum signal $\mathbf{S}^U$ to different frequencies using OFDMA techniques. Thereby, each user can obtain the highest spectral efficiency and throughput by using all spreading codes and all dimensions of the modem. Multiple users are now spread across different frequencies using OFDMA techniques, which will be explained in more detail in the following sections. When using OFDMA, users can even be spread in the time and frequency, making the system able to adapt to different system requirements depending on the characteristics of the channel in which the system is operating. The OFDMA transmission scheme can still be adhered to and the spread spectrum code-division transmitter block simply acts as the input or spreading unit for one user before transmitting the entire data using OFDMA techniques. OFDMA is used for the user separation and the spread spectrum code-division type building block to separate data symbols belonging to the same user. This improves the throughput dramatically without the loss of spectral efficiency and additionally achieves diversity gains.

For performance reasons, and due to the fact that generally the code family size is small and always restricts the number of active users in a CDMA type system, the proposed modem assigns the transmitter of Figure 4.3 to one user. Thus, the different data streams are separated by codes and the users are separated by placement on different frequency/time sub-carriers in an OFDMA system.

Multi-user detection strategies apply to the different data branches and not to users themselves, since they are distinctly separated by different sub-carrier assignments in an OFDMA frame. But, as the codes have perfect correlation properties and are orthogonal, multi-user, or in this case, input data branch detection and separation techniques are unnecessary due to the fact that the transmitted signalling structure is MAI-free and the transmissions from the different branches are already pre-decorrelated as the spreading shows isotropic MAI-free properties [40].

In the following section OFDM and OFDMA concepts are explained. This is followed by the multi-user implementation of the system and how multiple access was be achieved by using orthogonal frequencies and different sub-carrier allocation strategies.

4.2 INTRODUCTION TO MULTI-CARRIER MODULATION (OFDM)

The fact that orthogonal frequency-division multiplexing provides multipath delay spread tolerance and is immune to frequency selective fading channels, makes it an attractive wireless communications technology which has become a popular technique in various high-speed wireless data transmission systems [41], [42].

OFDM has been implemented in many wireline communication standards, such as in ADSL and VDSL broadband access via POTS copper wiring, as well as in digital video broadcasting (DVB). It has also been readily deployed in many wireless communications standards such as the mobile worldwide interoperability for microwave access (WiMAX), which is based on the IEEE 802.16 standard, the wireless LAN (WLAN) radio interfaces (IEEE 802.11a,g,n), in many mobile broadband solutions and in the IEEE 802.20 mobile wireless MAN standard, also known as MBWA [43].

OFDM is a form of multi-carrier transmission which is suited to frequency selective channels and high data rates. In OFDM, a frequency-selective wideband channel is transformed into a group of non-selective narrowband channels, making it robust against delay spreads by maintaining orthogonality in the frequency domain. Through the use of cyclic redundancy at the transmitter, the complexity is reduced to only simple fast Fourier transform processes and a tap scalar equalisation at the receiver [11]. Thus, OFDM splits a signal into multiple narrowband sub-signals that are then transmitted simultaneously at different frequencies to the receiver.

The sensitivity to time variations in the channel caused by Doppler, carrier frequency offsets and phase noise, are some of the primary drawbacks of OFDM. In OFDM the sensitivity to frequency synchronisation, which originates from close sub-carrier spacing, is a problem. If the sub-carriers are not perfectly orthogonal at $f = k/T_B$ $k = 0, 1, ..., N-1$, then the sub-carriers interfere with one another. This is termed ICI and successively causes ISI [44].

4.2.1 Principles of OFDM modulation

A main appeal in orthogonal frequency-division multiplexing is the support for high data rate links without the complex conventional equalisation techniques. In OFDM, data or N symbols are transmitted in blocks instead of being transmitted serially, which makes the block periods N times longer than the symbol period. This extended block period is longer than the channel's impulse response. ISI is additionally avoided by inserting a guard interval between blocks in which a cyclic prefix is transmitted [11]. The guard band interval is designed to be greater than the channel's maximum propagation delay (coherence time). This guard band prevents the OFDM blocks from getting corrupted by allowing the channel to be absorbed by the guard interval [11].

In general, OFDM signals without the guard band interval can be expressed as

$$s(t) = \sum_{n} \left[\sum_{k=0}^{N-1} I_{n,k} e^{j2\pi f_k t} \right] g(t - nT_B), \tag{4.13}$$

where $g(t)$ is a typical rectangular pulse shape and T_B is the block period given as

$$g(t) = \begin{cases} 1, & 0 \leq t < T_B \\ 0, & \text{otherwise.} \end{cases} \tag{4.14}$$

During the nth block, N data symbols of the form $\left\{I_{n,k}\right\}_{k=0}^{N-1}$ are transmitted. The sub-carriers $\left\{e^{j2\pi f_k t}\right\}_{k=0}^{N-1}$ have a center frequency of $f = k/T_B$ and are spaced by $1/T_B$ Hz. This spacing makes the sub-carriers orthogonal over the block interval. That is,

$$\int_0^{T_B} \cos(2\pi f_k t + \phi_k) \cos(2\pi f_j t + \phi_j)\, dt = 0, \tag{4.15}$$

where $f_k - f_j = n/T$, $n = 1, 2, ..., N-1$, independent from the phases ϕ_k and ϕ_j [11]. It can also be expressed as

$$\frac{1}{T_B} \int_0^{T_B} (e^{j2\pi f_k t})^* (e^{j2\pi f_j t})\, dt = 0, \tag{4.16}$$

when $f_k \neq f_j$. These mathematical expressions define a unique type of multi-carrier modulation in which the sub-carriers of the corresponding sub-channels are mutually orthogonal [11]. This produces orthogonal, i.e., non-interfering, tightly packed sub-carriers, which greatly improves spectral efficiency.

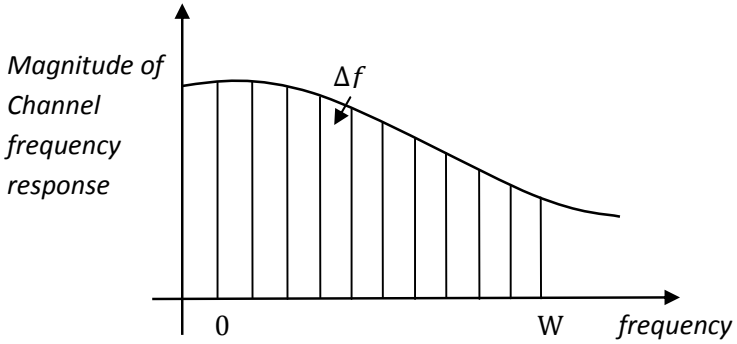

Figure 4.5: *Sub-division of the channel bandwidth into narrowband sub-channels with a width of Δf [11].*

In single carrier modulation the entire bandwidth is occupied by a symbol as opposed to multi-carrier modulation, which divides the available bandwidth into narrow width $\Delta f = W/N$ bins or frequency bands [11]. This allows the multi-carrier signal to transmit the N data symbols simultaneously over multiple sub-carriers, each with a different center frequency $(f_c + k/T_B)\ Hz$, $k = 0, 1, ..., N-1$. If the Δf is chosen small enough, the channel frequency response is essentially constant across all the sub-bands, hence making the ISI negligible [11]. The sub-carrier spacing makes the frequency bins frequency-nonselective by converting the wideband frequency-selective channels into N neighbouring narrowband frequency-nonselective bins. A subdivision of the channel bandwidth W is illustrated in Figure 4.5.

The removal of ISI in the channel and the fact that a signal in each sub-band can be independently coded and modulated at a synchronous symbol rate of $1/\Delta f$, adds to the main advantages of OFDM. Another huge benefit which adds to the appeal of OFDM is the ability that the modulation and demodulation can be done via a simple discrete-time domain inverse fast Fourier transform (IFFT) and a fast Fourier transform, respectively. When taking the zeroth ($n = 0$) OFDM block from (4.13), it yields

$$s(t) = \sum_{k=0}^{N-1} I_{0,k} e^{j2\pi f_k t}, \qquad 0 \leq t < T_B, \tag{4.17}$$

and the frequency-domain representation is [45]

$$S(f) = \mathscr{F}\{s(t)\}(f) = T_B e^{-j2\pi f T_b/2} \sum_{k=0}^{N-1} I_{0,k} \text{sinc}\left[\left(f - \frac{k}{T_B}\right) T_B\right], \tag{4.18}$$

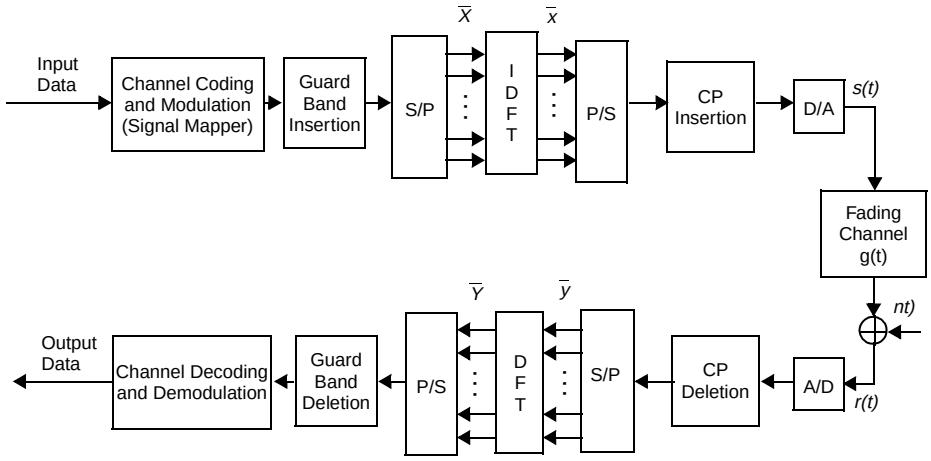

Figure 4.6: *A digital implementation of a baseband OFDM system from [46].*

where

$$\text{sinc}(x) = \begin{cases} 1, & x = 0, \\ \frac{sin\pi x}{\pi x}, & \text{otherwise.} \end{cases} \tag{4.19}$$

Sampling the zeroth OFDM block (4.17) at N equally spaced timed intervals, the inverse discrete Fourier transform (IDFT) of the symbol vector $I_0 = [I_{0,0}, I_{0,1}, ..., I_{0,N-1}]$ is found below in (4.20) [42]:

$$y[n] \equiv s(t)|_{t=nT_B/N} = \sum_{k=0}^{N-1} I_{0,k} e^{j2\pi kn/N}, \qquad n = 0, 1, ..., N-1. \tag{4.20}$$

The transmitted signal $s(t)$ generated at the transmitter with the IDFT, is sent through a digital-to-analogue (D/A) converter. In (4.21) the frequency-domain symbols $\{I_{0,k}\}_{k=0}^{N-1}$ are given, which is the discrete Fourier transform (DFT) performed on the previously given time-domain samples [44]

$$I_{0,k} = \frac{1}{N} \sum_{n=0}^{N-1} y[n] e^{-j2\pi kn/N}, \qquad k = 0, 1, ..., N-1. \tag{4.21}$$

At the receiver, the signal is passed through an analogue-to-digital (A/D) converter followed by a discrete Fourier transform. The IDFT and DFT are performed using the FFT algorithm, which simplifies the modulation/demodulation.

A block diagram of a digital implementation of an OFDM system is given in Figure 4.6. By referring to Figure 4.6, the system can be described in matrix format. Let $\mathbf{X} = [X_k]^T$

and $\mathbf{Y} = [Y_k]^T$ $(k = 0, ..., N-1)$, denote the input data for the IDFT blocks at the transmitter and the output data of the DFT block at the receiver, respectively. Let $\mathbf{g} = [g_n]^T$ define the sampled channel impulse response and $\mathbf{n} = [n_n]^T$ $(n = 0, ..., N-1)$ the sampled additive white Gaussian noise. The input matrix can be defined as the diagonals of $\mathbf{X}$, $\underline{\mathbf{X}} = diag(\mathbf{X})$. The respective DFT-matrix can be defined as

$$\underline{\mathbf{F}} = \begin{bmatrix} W_N^{00} & \cdots & W_N^{0(N-1)} \\ & \ddots & \\ W_N^{(N-1)0} & \cdots & W_N^{(N-1)(N-1)} \end{bmatrix}, \tag{4.22}$$

where $W_N^{i,k} = (1/\sqrt{N})^{-j2\pi(ik/N)}$. Similarly $\mathbf{H} = DFT_N(\mathbf{g}) = \underline{\mathbf{F}}\mathbf{g}$ and $\mathbf{N} = \underline{\mathbf{F}}\mathbf{n}$. Now, if the interference is assumed to be eliminated, one can derive:

$$\mathbf{Y} = DFT_N(IDFT_N(\mathbf{X}) \otimes \mathbf{g} + \mathbf{n}) = \underline{\mathbf{X}}\underline{\mathbf{F}}\mathbf{g} + \mathbf{N} = \underline{\mathbf{X}}\mathbf{H} + \mathbf{N}. \tag{4.23}$$

From (4.23), an OFDM system can be seen as the transmission of data over a set of parallel channels. As a result, the fading channel of the OFDM system can be viewed as a 2D lattice in a time-frequency plane which is sampled at specified pilot positions, and the channel characteristics between pilots can be estimated by interpolation (see for example [11], [46], [47]).

4.2.2 Basics of multiple-access OFDM (OFDMA)

In OFDM, all sub-carriers are used for transmitting data of a single user in a multiplexed fashion. Therefore, OFDM on its own is not regarded as a multiple-access technique, but when combined with existing multiple-access techniques such as FDMA, TDMA or CDMA, OFDM can be converted into a multi-user system. As seen in Figure 4.7, sub-carriers can be assigned to different users by using different multiple-access schemes, in which OFDM carriers are assigned to users in the time, frequency or code domain. Therefore, OFDMA can be regarded as a multiple-access extension of OFDM.

OFDMA is closely related to OFDM and similarly employs multiple closely spaced sub-carriers. However, in OFDMA sub-carriers are divided into groups of sub-carriers also called sub-channels, which can then be allocated to numerous users to achieve multiple-access. Today, OFDMA can be found in the latest technologies such as in the downlink of the 3GPP

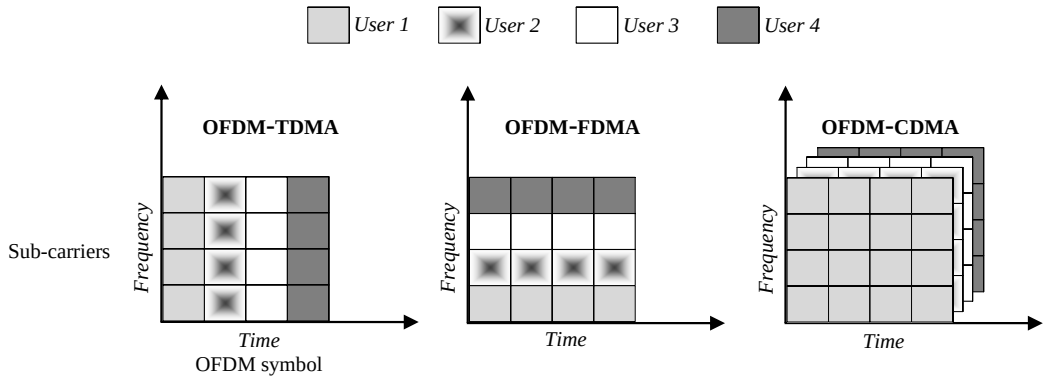

Figure 4.7: *Multiple-access techniques that can be used in OFDM systems to map users to different sub-carriers using the time, frequency or code domain.*

LTE standard and the IEEE 802.16 Wireless MAN (WiMAX) standard.

CDMA technology on its own has become less popular and future wireless systems will run on non-CDMA based platforms such as OFDMA. OFDMA has overtaken CDMA as a multiple access technology and future trends show the shift from CDMA (3G) technology to OFDM multiple access techniques, which are already found in all candidates for 4G systems [1], [2]. However, benefits can still be obtained by using code-division prior to OFDMA, resulting in improved throughput, spectral efficiency and diversity.

In the proposed system multiple access and user separation is achieved by OFDMA and code-division multiplexing (CDM) is introduced to achieve additional diversity gains. This system allows the signals of different users to be orthogonal in the frequency and code space, which provides additional isolation between users and in turn provides MAI suppression. The multiple access implementation or OFDMA part of the system has multiple design alternatives and some are considered in the following section.

4.3 MULTIPLE ACCESS/CARRIER IMPLEMENTATION

The usage of the CRCC codes enables the data from multiple combined multi-dimensional building blocks to be transmitted simultaneously with a high throughput over one channel, since the rotated spreading codes allow the data to be differentiated again at the receiver, as is the case with CDMA techniques. A collection of these combined blocks can then be spread onto different sub-carrier frequencies using OFDMA principles. This scheme is a type of

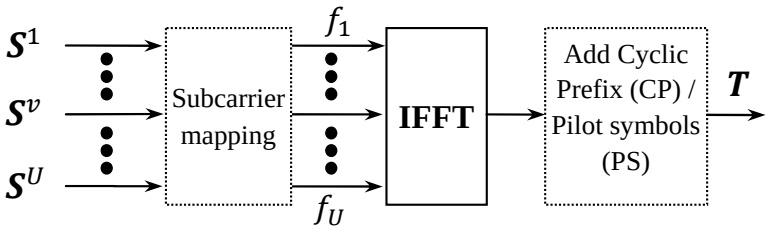

Figure 4.8: *Multi-carrier transmission via IFFT/FFT for multiple access.*

multi-carrier spread spectrum system with multiple-access, which capitalises on the benefits of both spread spectrum (CDMA) and OFDM techniques.

The generated signal of the Uth user is fed through an inverse fast Fourier transform (IFFT) to produce a multi-user system by assigning subsets of sub-carriers to individual users. The multiple access implementation of the system can be seen as an OFDMA modulation technique. The use of the simple IFFT/FFT operations in the generation of the signal results in a low complexity transmitter and receiver structure.

A simplified block diagram of the multiple access implementation is shown in Figure 4.8. It depicts how the signal $\mathbf{S}^U$ from Figure 4.3 is transmitted further via OFDM or multi-carrier techniques to produce a multi-user or multiple access system. Multiple access is achieved by assigning different OFDM sub-channels to different users by making use of various sub-carrier allocation strategies. For example, a group of adjacent sub-carriers or sub-bands can be assigned to each user in both frequency and time, or users can be assigned to interleaved or randomly chosen sub-carriers.

To support different types of physical channel conditions, IEEE 802.16 OFDMA systems define several ways to allocate sub-channels, three for downlink: FUSC (fully utilised subchannelisation), PUSC (partially utilised subchannelisation) and AMC (adaptive modulation and coding), and two for uplink: PUSC and AMC [48]. In FUSC and PUSC, a sub-channel consists of sub-carriers distributed over the entire spectrum, providing frequency diversity, while the AMC sub-channel consists of adjacent sub-carriers and provides for multi-user diversity [49], [50].

In the design of the novel modulation technique, the above mentioned allocation strategies of the IEEE standards can be directly implemented. The multi-carrier aspect can be designed in many ways to adapt to the requirements of the system and channel conditions. After the

sub-carriers and sub-channels are assigned and sent through the IFFT, a guard interval or cyclic prefix can be inserted into the signal to eliminate ISI from the previous symbols. The cyclic prefix allows for simple frequency domain processing, such as channel estimation and equalisation, due to the circular convolutional properties of the repeated end-part of the symbols when taking its discrete Fourier transform. Pilot symbols can additionally be inserted to aid in the measurement of the channel conditions and can also be used to avoid time and frequency synchronisation problems, which can cause ISI and ICI, respectively. The pilot and guard sub-carriers placement parameters can be found in the various sub-carrier usage strategies as defined in the IEEE standards [48].

The implemented multiple access scheme allows different users to transmit over different portions of the broadband spectrum. When a broadband signal experiences frequency selective fading, different users perceive different channel qualities (multi-user diversity). For example, a deep faded channel for one user can still be favourable to another user. The use of the OFDMA technique allows for efficient use of the spectrum with simple FFT processing and it produces a better performing system in fading environments.

4.3.1 Different spreading domains

The proposed system has many design alternatives in which the spreading can be carried out in the time, the frequency or in both directions. Spreading in both the frequency and time direction is sometimes referred to as two dimensional spreading, in which the frequency and time diversity is exploited [33]. When considering spreading in both the time and frequency domain, the spreading factors or processing gains of both dimensions are multiplied.

Time and frequency spreading can be adaptively exploited depending on the channel characteristics. When using a larger time domain spreading factor and a smaller frequency domain spreading factor, the orthogonality of the codes is relatively sensitive to time variations in the channel, but less susceptible to frequency-selective fading effects. Then again, when using a smaller time domain spreading factor and a large frequency domain spreading factor, the orthogonality of the codes will be more sensitive to the frequency-selectivity of the channel than to time-selective fading [33]. Thus, the system can be designed to exploit the features of the different spreading alternatives to be able to react to different channel conditions and make the codes more resilient against time-/frequency selective fading.

4.4 COMBINED SYSTEM MODEL

A spread spectrum multi-dimensional code-division-multiplexed system described in Section 4.1.2, combined with multiple access techniques such as OFDMA (Section 4.3), results in the proposed multi-layered code-division-multiplexed OFDMA type system seen in Figure 4.9. Similar types of systems without CRCC codes and multiple dimensions have been proposed that combine OFDM and CDMA in a similar fashion by extending OFDMA with code-division multiplexing [12].

As mentioned, different types of spreading techniques in different dimensions can be used, however, in this case each user is assigned to a subset of sub-carriers according to an FDMA scheme, time spreading is not considered in this context. This achieves the highest throughput and spectral efficiency without the bandwidth efficiency loss when spreading in multiple dimensions. The system downlink transmitter of the multiple access scheme proposed is illustrated in Figure 4.9, which applies OFDMA for user separation and code-division multiplexing on the data belonging to each individual user. This exploits the frequency diversity by spreading over L sub-carriers. Additionally, ISI and ICI can be avoided, resulting in less complex detection techniques. Similarly, each sub-carrier is assigned to one user, making the channel estimation far less complex. It can be seen that the joint system makes use of the frequency space, optionally the time and code space, to achieve flexible resource allocation and diversity.

Similarly to multi-carrier CDMA systems, the proposed system takes advantage of the combination of spread spectrum techniques and multi-carrier modulation. As seen in Figure 4.9, one user assigns LM data symbols to one sub-system or LM sub-carriers, which are only used by that particular user. In the FDMA scheme, U users are transmitted over a total of $N_c = U \times LM$ sub-carriers.

4.4.1 Frequency sub-carrier allocation schemes

In Figure 4.9, the spread symbols are transmitted on adjacent sub-carriers. This limits the frequency diversity of each symbol. Hence, to take full advantage of the frequency diversity of the entire available bandwidth, the sub-carrier assignment in the frequency domain can be interleaved [12].

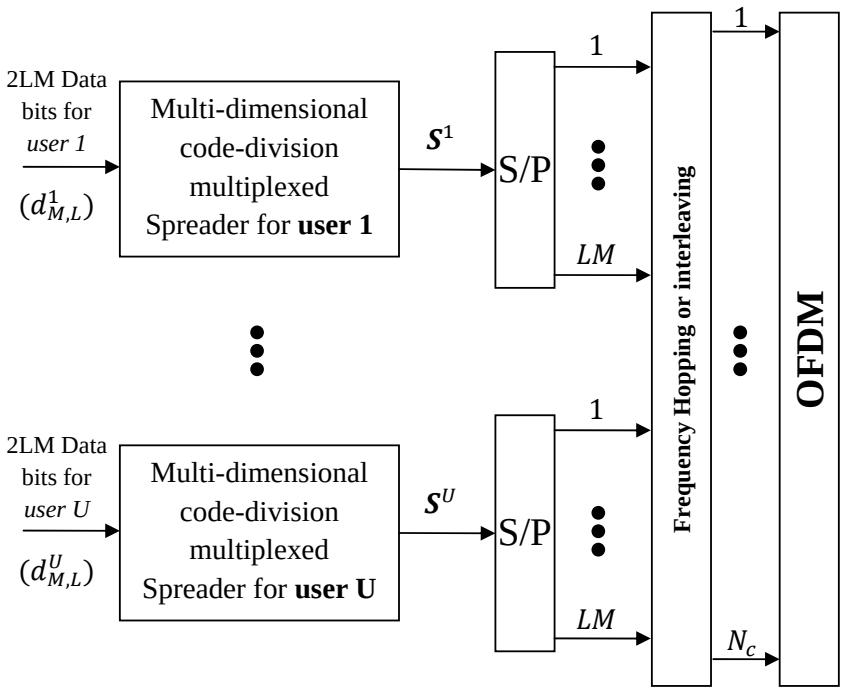

Figure 4.9: *Downlink configuration of the code-division-multiplexed OFDMA transmitter.*

Various frequency allocation schemes can be used in the system, such as standard block interleaving and adjacent sub-carrier allocation. In standard block interleaving, the spread symbols are distributed across the entire bandwidth in order to maximise the frequency separation between the chips, thereby increasing the frequency diversity available at the receiver. In the adjacent sub-carrier scheme, the user's spread data symbols are grouped together and spread onto neighbouring sub-carriers. This does not optimally exploit the frequency diversity [12]. Frequency diversity is therefore only achieved on the reduced number of sub-carriers that are assigned to that user, however, this scheme has been found to be more resistant to user frequency offsets [51]. Additionally, guard sub-carriers between different users can be implemented to absorb the ICI with a minimum spectrum efficiency loss but for an important performance gain. With adjacent sub-carriers, a less complex channel estimation scheme needs to be performed on adjacent sub-carriers and interpolation techniques on a reduced number of pilot symbols can achieve similar performance, resulting in lower spectrum and power efficiency losses when compared to the block interleaved technique [52].

A different allocation scheme, which combines the adjacent sub-carrier scheme with a frequency hopping technique, was proposed by [52]. This hybrid allocation solution allocates

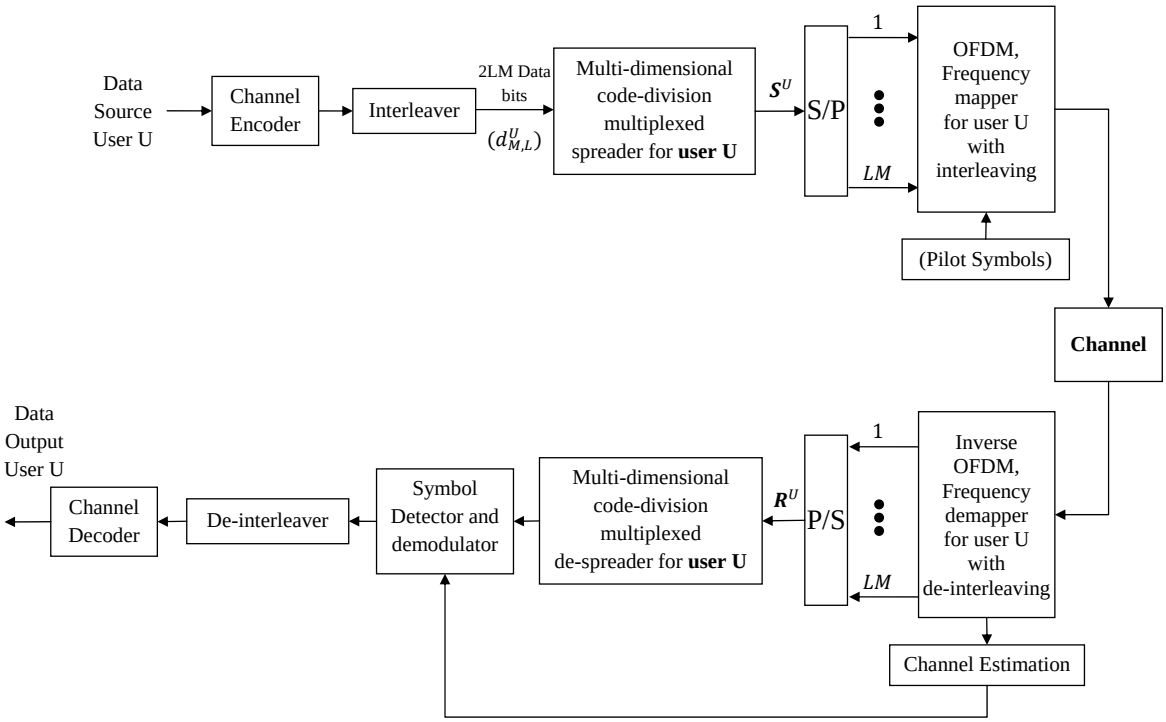

Figure 4.10: *Transmitter and receiver of proposed multi-dimensional code-division-multiplexed OFDMA system for one user U.*

sub-carriers to different users in each OFDM symbol by using a frequency hopping pattern. This results in uncorrelated channel distortions between successive OFDM symbols, due to the frequency diversity achieved by hopping the user's sub-carriers across the bandwidth [52]. However, channel coding is necessary to take advantage of this frequency diversity, as the system can not exploit it during the de-spreading process [52]. This scheme prevents inter-cell interference, but has a higher channel estimation complexity and pilot overhead when compared to the adjacent sub-carrier allocation scheme. It can be seen that these various allocation schemes all have their tradeoffs and the system should be implemented with the optimal scheme by regarding the channel conditions in which it would operate.

4.4.2 Receiver design

In Figure 4.10, an entire system with a transmitter and receiver for one user U is illustrated. The transmitter of the proposed system performs a user-specific frequency mapping of the user's spread signal $\mathbf{S}^U$, in which the chips are interleaved over the whole transmission bandwidth. To perform coherent data detection at the receiver, pilot symbols can be multiplexed

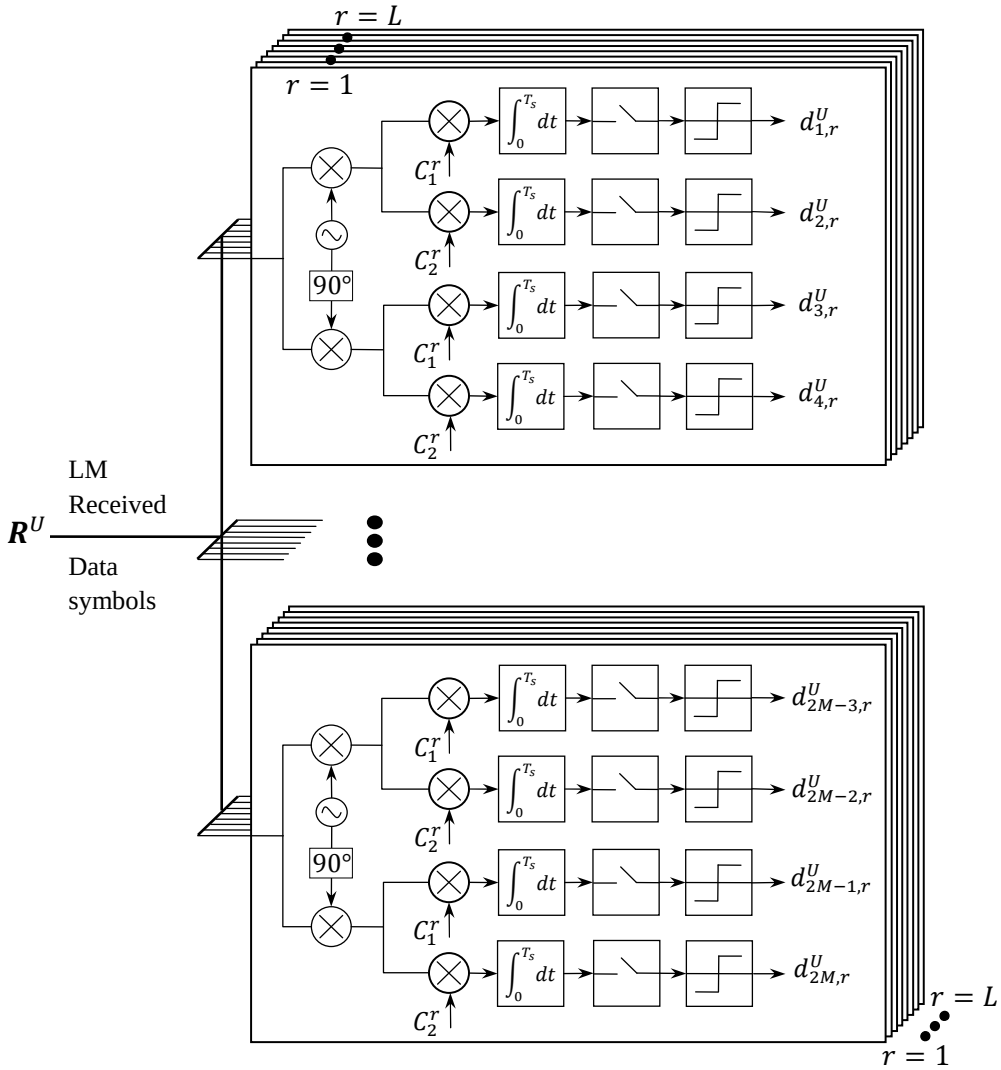

Figure 4.11: *Simple multi-dimensional correlation type receiver design requiring every rotated spreading code.*

into the transmitted data, which aids in frequency and time synchronisation.

After the transmitted signal is passed through the channel, the inverse OFDM with user-specific frequency de-mapping is performed. Additionally, the pilot symbols of the user are extracted and can be used for channel estimation, as they would describe the fading and noise on the sub-carriers of user U. A variety of single-user or multi-user detection techniques can be implemented for the detection of the data. The detection can be done on the sub-carriers belonging to a single user, therefore requiring less complex detection techniques. Furthermore, the estimation of LM data symbols belonging to one user can be

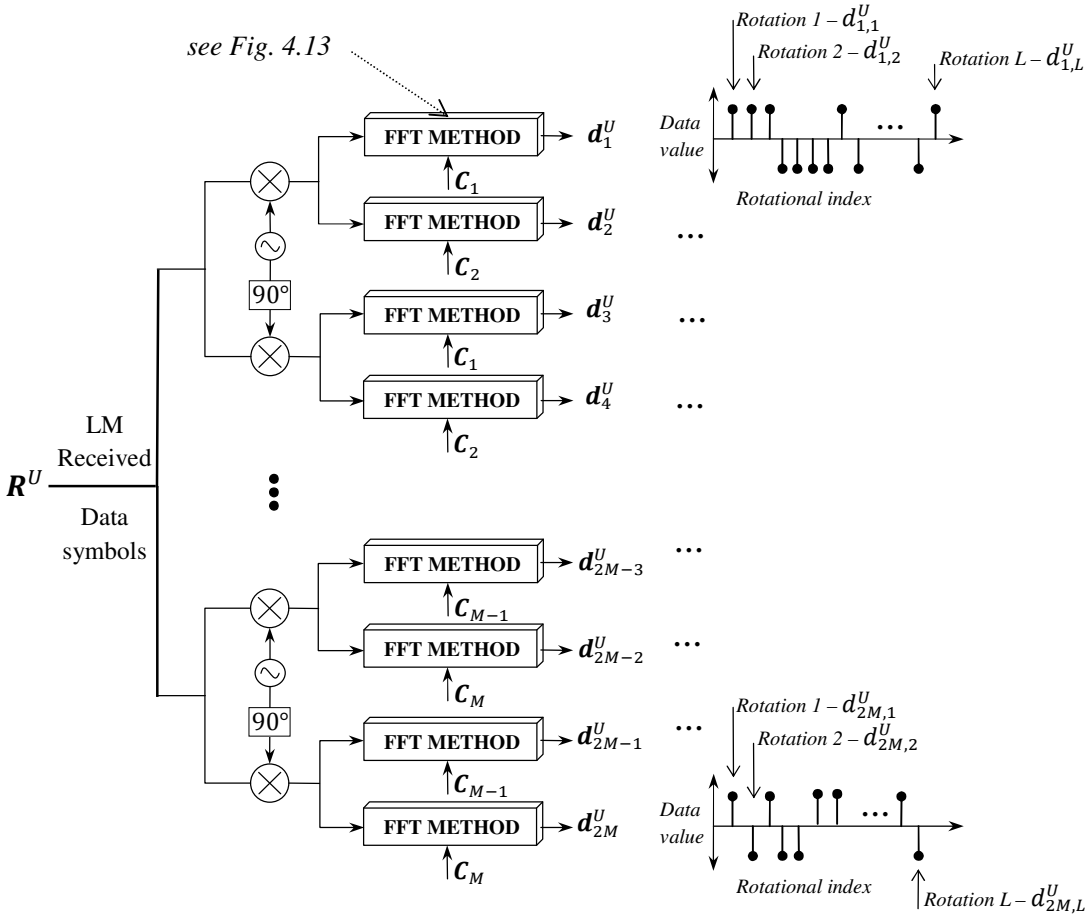

Figure 4.12: *Proposed despreading receiver using fast Fourier transform method.*

done simultaneously.

It should be noted that the transmitter and receiver structure contains similarities to an OFDM/OFDMA system. Components such as the FFT, channel estimation, equalisation and channel decoding can be used for both systems. The additional multi-dimensional code-division-multiplexed system is simply integrated into the OFDM scheme. In the following section some typical detection techniques are presented that can alternatively be used to improve the performance of the system at the expense of higher receiver complexity.

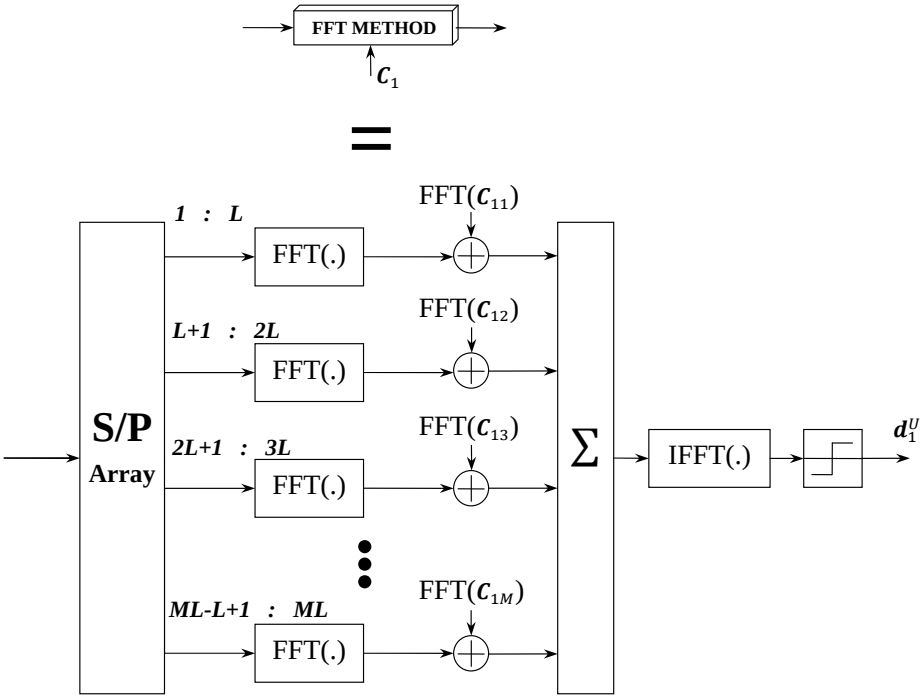

Figure 4.13: *Fast Fourier transform method for building block depicted in Figure 4.12.*

4.4.2.1 Multi-dimensional receivers for rotated codes

A receiver using a typical correlation type design can be seen in Figure 4.11. Each de-spreading branch has to make use of the specific rotated spreading sequence used at the transmitter to correctly de-correlate the received signal. An alternative, less complex and faster performing receiver algorithm using the FFT method is depicted in Figure 4.12 and 4.13. As explained in previous sections, the de-correlation of the rotated codes can be done in a more efficient way using the periodic properties of the code in the frequency domain. The de-correlation procedure for one branch has been explained in Section 4.1.2.1.

With the use of cyclic rotated complete complementary codes, the presented de-correlation algorithm, making use of fast Fourier transforms, provides an optimised way to de-spread the received signal. The mathematical description of the de-spreading process using the FFT method was given in (4.12) and an example of a resulting received vector is given in Figure 4.4.

4.4.3 Detection techniques

A general classification of detection techniques distinguishes between single-user detection and multi-user detection. In single-user detection, no information about MAI is taken into consideration when detecting a user's signal. Single-user detection can be realised by one tap equalisation to compensate for the distortion in the channel resulting from flat fading on each sub-carrier, followed by user specific de-spreading. Single-user detection is a sub-optimum approach, since the MAI is seen as noise. Some of the single-user detection techniques can make use of maximum ratio combining (MRC), equal gain combining (EGC), and zero forcing (ZF) [9].

On the other hand, multi-user detection makes use of a priori knowledge of the spreading codes of the interfering users and exploits it in the detection process. This performance improvement is achieved with complex receiver designs. Multi-user detection techniques can again be classified as either linear or non-linear.

4.4.3.1 Linear multi-user detectors

A linear de-correlation receiver is the simplest multi-user detection strategy. It is similar to a zero-forcing equaliser in which the estimates of the symbols are obtained by filtering the signal with the inverse correlation matrix. Its simplistic design and the fact that the detector does not require knowledge of the received amplitudes or users' powers adds to its benefits, however the drawback lies in its noise enhancement [53].

Again, similar to a minimum mean square error (MMSE) equaliser, a MMSE multi-user detector finds a tradeoff between interference suppression and noise enhancement. The MMSE does not completely remove the interference, but the signal distortions are still smaller than that of the de-correlation receiver.

4.4.3.2 Non-linear multi-user detectors

Non-linear detectors exploit the fact that the transmitted signal can only consist of members of a finite transmit alphabet, whereas linear detectors ignore this fact and allow the estimated received signal to attain any continuous value. Some of the commonly used non-linear multi-user detection schemes are parallel interference cancellation (PIC) detectors, serial

interference cancellation (SIC) detectors, decision-feedback detectors, and the multi-user maximum-likelihood sequence estimation (MLSE) detectors [11], [53].

The MLSE is seen as the optimum detector which exploits the maximum a posteriori (MAP) criterion, but is generally seen as too complex to implement for practical purposes, since the complexity grows exponentially with the number of users. It makes use of a trellis and Viterbi detector and is more often used to gain insight into the performance limits of multi-user detection [53]. Other less complex joint detection techniques make use of linear block equalisation techniques, such as the previously mentioned MMSE technique, and joint detection applying a zero forcing block linear equaliser scheme.

The principle of interference cancellation is to detect and reconstruct the interference contribution in a signal with single-user detection and then to subtract it from the received signal before detecting the information of the user or signal of interest.

As already mentioned previously, the perfect correlation properties of the spreading codes which are implemented in the proposed system, make it unnecessary to use complex multi-user detection techniques due to the fact that the different users can simply and efficiently be de-correlated because of the unique MAI-free properties of the codes. Self-interference in each user in multi-path scenarios can be reduced by some of the above mentioned techniques. The orthogonality of the codes prevents the signals from interfering with each other and a simple correlator can de-correlate the orthogonal complete complementary codes. A typical correlation type multi-dimensional receiver can be seen in Figure 4.11, and the FFT receiver which was mentioned in Section 4.1.2.1, is illustrated in Figure 4.12.

CHAPTER 5

PERFORMANCE ANALYSIS

The characteristics of a mobile radio channel and the imperfections it introduces in a communication system is briefly described in the first part of this chapter. The statistical behaviour of a mobile communication channel is vital in the evaluation and analysis of a wireless communication system and important effects like multipath fading, Doppler shift, interference and shadowing need to be considered. Therefore, some useful statistical models of real world phenomena in wireless communication channels are presented, and will be used in the latter part of the chapter, which will focus on the results, performance analysis, and advantages/disadvantages of the proposed multi-dimensional spread spectrum multi-carrier system.

5.1 THE CHANNEL

The transmitted signal in a mobile radio channel undergoes different propagation effects. These can be mainly characterised as follows:

Multipath propagation occurs when the radio waves are affected by three different types of physical phenomena, namely reflection, diffraction, and scattering. This results in the system receiving numerous signals arriving from different directions with different delays, phases, and attenuations. Hence, the combined received signal has amplitude and phase variations.

Doppler spread leads to changes in the phase and amplitude of the arriving signals, resulting in time-variant multipath propagation which is caused by objects moving in the mobile radio channel. The variations in signal strength due to time-variant multi-path propagation is referred to as fast fading [9].

Shadowing refers to the attenuation of the signal strength, caused by the obstruction of the

transmitted signal. This is called slow fading, because the signal varies only with large changes in the distance or position of the receiver and transmitter, whereas with fast fading, small movements in the order of a wavelength is enough to significantly alter the signal composition [54].

Path loss defines the loss in mean signal power with the increase in distance between receiver and transmitter.

5.1.1 The multipath channel model

The mobile channel with respect to its fast fading characteristic can be defined by the time-variant channel impulse response $h(\tau,t)$, or by the channel transfer function $H(f,t)$. It is assumed that the channel has fading statistics that remain constant over short periods of time or small distance (wide-sense stationary random process) [9]. If a number of different impulses over N_p different paths are received due to multipath propagation, the composite impulse response is given by:

$$h(\tau,t) = \sum_{p=0}^{N_p-1} a_p e^{j(2\pi f_{D,p} t + \varphi_p)} \delta(\tau - \tau_p), \tag{5.1}$$

where

$$\delta(\tau - \tau_p) = \begin{cases} 1 & \text{if } \tau = \tau_p \\ 0 & \text{otherwise} \end{cases} \tag{5.2}$$

and a_p is the amplitude, $f_{D,p}$ is the Doppler frequency, φ_p is the phase, and τ_p is the propagation delay associated with path p, for $p = 0,...,N_p - 1$ [9]. The channel transfer function, $H(f,t)$, which is the Fourier transform of $h(\tau,t)$, is given by

$$H(f,t) = \sum_{p=0}^{N_p-1} a_p e^{j\left(2\pi\left(f_{D,p} t - f\tau_p\right) + \varphi_p\right)}. \tag{5.3}$$

The Doppler frequency $f_{D,p}$ depends on the velocity v of the base station, the carrier frequency f_c, the angle of incidence α_p of the wave from path p, and the speed of light c,

according to:

$$f_{D,p} = \frac{v f_c \cos(\alpha_p)}{c}. \tag{5.4}$$

5.1.2 Parameters of small scale fading

The average output power of the channel as a function of the delay τ is given by the power density spectrum $p(\tau)$, which characterises the frequency selectivity of the channel [9]. The mean excess delay $\overline{\tau}$ and the root mean square (RMS) delay spread σ_τ are important channel parameters that provide a benchmark amongst different multipath fading channels [54]. Additionally, the delay power density spectrum makes use of these parameters.

The mean excess delay $\overline{\tau}$ of the first moment of the power delay profile is given by

$$\overline{\tau} = \frac{\sum_{p=0}^{N_p-1} \tau_p |a_p|^2}{\sum_{p=0}^{N_p-1} |a_p|^2}, \tag{5.5}$$

where $|a_p|^2$ is the power of path p. The RMS delay spread σ_τ is defined as

$$\sigma_\tau = \sqrt{\overline{\tau^2} - (\overline{\tau})^2} \tag{5.6}$$

$$= \sqrt{\frac{\sum_{p=0}^{N_p-1} \tau_p^2 |a_p|^2}{\sum_{p=0}^{N_p-1} |a_p|^2} - \overline{\tau}^2}. \tag{5.7}$$

The coherence bandwidth, denoted by $(\Delta f)_c$, is generally defined as inversely-proportional to the delay spread (5.6) and defines the bandwidth over which the signal propagation characteristics are correlated. The coherence bandwidth is approximated by

$$(\Delta f)_c \approx \frac{1}{\sigma_\tau}, \tag{5.8}$$

where the relationship in (5.8) can vary depending on the precise definition. For example, the coherence bandwidth can yield values between $(\Delta f)_c \approx \frac{1}{50\sigma_\tau}$ and $(\Delta f)_c \approx \frac{1}{5\sigma_\tau}$, when the correlation of the bandwidth or the frequency correlation function lies above 0.9 or 0.5, respectively [54].

5.1.3 Frequency and time dispersive fading

Wireless channels can undergo two major channel effects, multipath delay spread and Doppler spread, which causes time and frequency dispersion, respectively. Fading over a frequency domain due to time dispersion can generally be called frequency-selective or frequency-non-selective fading, depending on the relation between the signal bandwidth B_s and the coherence bandwidth $(\Delta f)_c$.

5.1.3.1 Time dispersion

The channel is said to be frequency-non-selective or flat if the signal bandwidth is smaller than the coherence bandwidth and the symbol period T_s is greater than the delay spread τ of the multipath channel $h(\tau,t)$. Thus, as long as the symbol period is greater than τ, ISI is not significant. This type of fading channel is often referred to as a narrowband channel or a channel undergoing flat fading. Therefore, while the amplitude and linear phase response within a passband is constant and the bandwidth of the channel is wider than that of the signal, the received signal undergoes frequency-non-selective fading as given by the conditions in (5.9)

$$B_s \ll (\Delta f)_c \quad \text{and} \quad T_s \gg \sigma_\tau. \tag{5.9}$$

On the other hand, when the channel has a constant amplitude and linear phase response only within a channel bandwidth narrower than the signal bandwidth, then the signal is said to be subject to frequency-selective fading [54]. The ISI is more prominent due to the short symbol duration compared to the channel delay spread. Here the frequency response is not flat and the received signal has different amplitudes in the frequency response and will undergo frequency-selective fading. A frequency-selective channel is also referred to as a wideband channel, as the signal bandwidth is greater than the channel's coherence bandwidth [11], [54]. Hence, frequency-selective fading occurs when

$$B_s > (\Delta f)_c \quad \text{and} \quad T_s > \sigma_\tau. \tag{5.10}$$

5.1.3.2 Frequency dispersion

The received signal experiences fast or slow fading depending on the severity of the Doppler spread. If the coherence time is smaller than the symbol period, resulting in a quickly varying impulse response in the symbol period, the channel is considered to be fast fading. A Doppler shift or spread in the frequency domain is a result of variations in the time domain due to movements of the receiver and transmitter. The frequency dispersion in a channel is commonly quantified by the maximum occurring Doppler frequency f_{Dmax} and the Doppler spread B_d, which is the bandwidth of the Doppler power density spectrum. The Doppler spread or bandwidth is generally twice that of the maximum Doppler shift, i.e. $B_d = 2f_{Dmax}$ [9]. By defining the coherence time $(\Delta t)_c$ as inversely proportional to the Doppler spread, as

$$(\Delta t)_c \approx \frac{1}{B_d} \approx \frac{1}{2f_{Dmax}} \tag{5.11}$$

together with the following conditions

$$B_d > B_s \quad \text{and} \quad T_s > (\Delta t)_c, \tag{5.12}$$

then the transmitted signal is subject to fast fading [54].

Also, when the impulse response slowly varies compared to the transmitted signal, the channel does not change over the duration of a symbol and is referred to as a static channel. Therefore, the Doppler spread is much smaller than the bandwidth of the baseband transmitted signal, resulting in the channel undergoing slow fading, given the conditions in (5.13):

$$B_d \ll B_s \quad \text{and} \quad T_s \ll (\Delta t)_c. \tag{5.13}$$

The coherence time $(\Delta t)_c$ is the duration in which the channel is considered time-invariant, and by defining it as the time over which the time correlation equals 0.5 and above, it can be approximated by $(\Delta t)_c \approx \frac{9}{16\pi f_{Dmax}}$ [54], [9]. Under the assumption that a Rayleigh-faded signal varies slowly as given by equation (5.11), and $(\Delta t)_c \approx \frac{9}{16\pi f_{Dmax}}$ is derived under the assumption that a signal varies very quickly, a more general definition of both can be given by taking the geometric mean [54],

$$(\Delta t)_c = \sqrt{\frac{9}{16\pi f_{Dmax}^2}} = \frac{0.4231}{f_{Dmax}}. \tag{5.14}$$

The coherence bandwidth is important when analysing the performance of spreading and frequency interleaving techniques, exploiting the frequency diversity of the channel. Frequency diversity is exploited when the separation of sub-carriers that transmit the same information, exceeds the coherence bandwidth. Likewise, the coherence time of a channel is of importance when evaluating coding and interleaving schemes. Thus, time diversity is exploited if the coherence time is smaller than the separation of time slots carrying the same information [9]. A system exploiting the frequency and time diversity can achieve an overall diversity of

$$D_O = D_f D_t, \tag{5.15}$$

where

$$D_f = \frac{B_s}{(\Delta f)_c}, \tag{5.16}$$

$$D_t = \frac{T_{frame}}{(\Delta t)_c}. \tag{5.17}$$

A number of time slots create a time frame duration denoted as T_{frame}, from which the maximum achievable time diversity D_t in one time frame can be computed. Similarly, the maximum frequency diversity is given by D_f, where B_s is the signal bandwidth [9].

5.1.4 Statistical characterisation of a fading channel

The statistical characteristics of the fading process can be modelled by several probability distributions. When assuming a large number of scatterers in the channel that contribute to the signal at the receiver, the central limit theorem can be applied to lead to a Gaussian process model for the channel impulse response [11]. The process is zero-mean and has a variance of σ^2 when there is no dominant line-of-sight (LOS) propagation path or component and the magnitude of the corresponding channel transfer function

$$r = r(f,t) = |H(f,t)| \tag{5.18}$$

is a random variable r with a Rayleigh amplitude probability distribution, given by

$$p(r) = \frac{2r}{\Omega} e^{-r^2/\Omega}, \qquad r \geq 0, \tag{5.19}$$

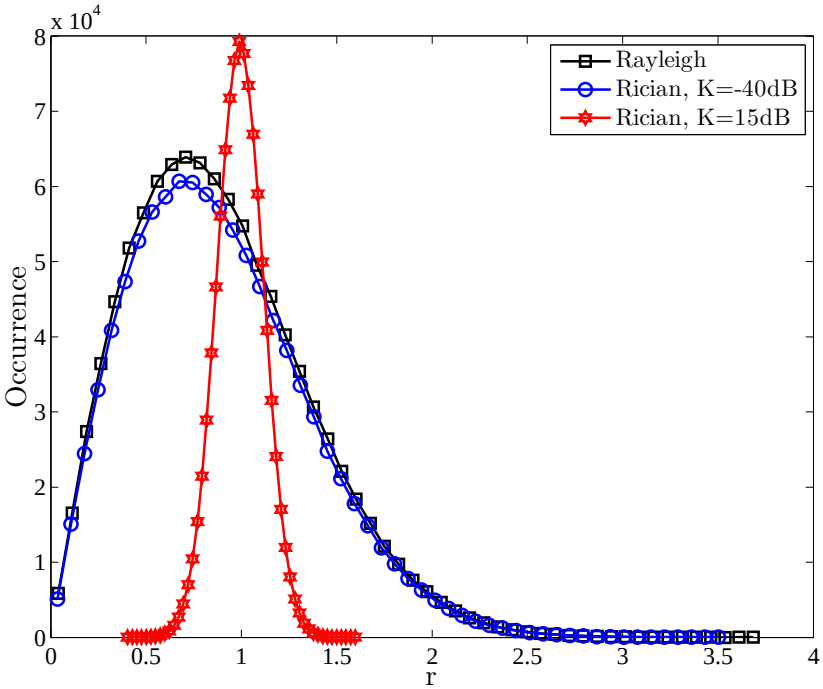

Figure 5.1: *Example of Rayleigh and Rician fading channel distributions for $K_r = -40$ dB and $K_r = 15$ dB from* 1000000 *realisations.*

where the average power is

$$\Omega = E\{|H(f,t)|^2\} = E\{r^2\} = 2\sigma^2 \tag{5.20}$$

and the phase is uniformly distributed in the interval $(0, 2\pi)$. However, if the multipath channel contains a LOS or dominant component together with randomly moving scatterers, the channel is no longer zero-mean and the magnitude of the channel transfer function r follows the Rician distribution given by

$$p(r) = \frac{2r}{\Omega} e^{-(r^2/\Omega + K_r)} I_0\left(2r\sqrt{\frac{K_r}{\Omega}}\right), \qquad 0 \leq r < \infty. \tag{5.21}$$

The Rician K-factor K_r is determined by the ratio of power of the dominant path to the scattered paths and $I_0(.)$ is the modified zeroth-order Bessel function of the first kind [11], [9]. In the case that $K_r = 0$, the Rician distribution (5.21) reverts back to a Rayleigh distribution (5.19). Hence, the Rayleigh fading channel can be considered a Rician fading channel when there is no dominant propagation path. It is generally assumed that $K_r \sim -40$ dB for the Rayleigh fading channel and $K_r > 15$ dB for the Gaussian channel as seen in Figure 5.1 [54].

Table 5.1: *Power delay profiles of COST 207 channel models [55].*

	Typical Urban (TU)		Bad Urban (BU)		Rural Area (RA)		Hilly Terrain (HT)	
Tap	Delay (μs)	Power (dB)	Delay (μs)	Power (dB)	Delay (μs)	Power (dB)	Delay (μs)	Power (dB)
1	0	-3	0	-2.5	0	0	0	0
2	0.2	0	0.3	0	0.1	-4	0.1	-1.5
3	0.5	-2	1.0	-3	0.2	-8	0.3	-4.5
4	1.6	-6	1.6	-5	0.3	-12	0.5	-7.5
5	2.3	-8	5.0	-2	0.4	-16	15.0	-8.0
6	5.0	-10	6.6	-4	0.5	-20	17.2	-17.7

Generally this means that for $K_r \to 0$ the Rician distribution becomes a Rayleigh distribution and when $K_r \to \infty$ it approximates a Gaussian distribution [53].

5.1.5 Frequency-selective fading channel models

The characteristics of a multipath fading channel can be specified by its power delay profile (PDP). The PDP provides the relative delays and average powers of different multiple signal paths. The COST 207 and ITU-R are only some of the many standardised channel models available which define the statistics of the discrete propagation paths [55]. Frequency-selective fading channels, for example, are easily described by a PDP and the simple Tapped Delay Line model can be used for implementing the multipath channel. Examples of COST 207 channel models with 6 taps are listed in Table 5.1. Different propagation environments and their respective power profiles and path delays are provided. Different Doppler spectra

Table 5.2: *Power delay profiles of ITU-R channel models [56]*

	ITU Pedestrian B		ITU Vehicular A		ITU Vehicular B	
Tap	Delay (ns)	Power (dB)	Delay (ns)	Power (dB)	Delay (ns)	Power (dB)
1	0	0.0	0	0.0	0	-2.5
2	200	-0.9	310	-1.0	300	0.0
3	800	-4.9	710	-9.0	8900	-12.8
4	1200	-8.0	1090	-10.0	12900	-10.0
5	2300	-7.8	1730	-15.0	17100	-25.2
6	3700	-23.9	2510	-20.0	20000	-16.0

Table 5.3: *Comparison of different channel models (COST 207) with respect to their mean excess delay, delay spread, and coherence bandwidth.*

Environment	$\bar{\tau}$ (μs)	σ_τ (μs)	$(\Delta f)_c$ (kHz)
Hilly Terrain (HT)	4.36	6.90	29.0
Bad Urban (BU)	2.62	2.52	79.4
Typical Urban (TU)	0.99	0.98	204.1
Rural Area (RA)	0.11	0.11	1818.2

are defined for the different taps in [55], though for simplicity the classical Doppler spectrum could be used. Similarly, Table 5.2 presents the PDPs for some of the ITU-R channel models.

A comparison of channel models in different environments with respect to their mean excess delay, rms delay spread, and coherence bandwidth is presented in Table 5.3. The mean excess delay and rms delay spread can be found according to (5.5) and (5.6), respectively. The coherence bandwidth of the different scenarios is obtained according to $(\Delta f)_c \approx \frac{1}{5\sigma_\tau}$.

The time variance of the channel also depends on the velocity v of the mobile station. An overview on multiple velocities and their respective Doppler frequencies occurring at a carrier frequency of 2.5 GHz are presented in Table 5.4. Additionally, the respective coherence time according to (5.14) is given for the different velocities and Doppler frequency examples.

Table 5.4: *Velocity of a mobile station and the resulting Doppler frequency and coherence time at a carrier frequency of $f_c = 2.5$ GHz.*

Velocity v (km/h)	f_{Dmax} (Hz)	$(\Delta t)_c$ (ms)
3	7	60.45
43	100	4.23
108	250	1.69
216	500	0.84
302	700	0.60

5.1.5.1 *Tapped delay line (TDL) model*

There are many different flat fading generators and different methods or models to simulate multipath channels, some of the models include the Clarke's reference model, Jake's model, filtered white Gaussian noise (FWGN) model, and many others. The tapped delay line model is realised by employing multiple frequency-non-selective fading generators. These flat fading generators are independent of each other and each have an average power of one, as seen in Figure 5.2. The output of the multiple independent flat fading generators is multiplied by the tap powers. The TDL method can be seen as a finite impulse response (FIR) filter with outputs given by

$$y(n) = \sum_{d=0}^{L_D-1} h_d(n)x(n-d), \tag{5.22}$$

where L_D is the number of taps in the FIR filter [54]. If the tapped delays are not integer multiples of the sampling period, methods such as tap interpolation, rounding, or tap re-sampling can be used to adjust the taps to coincide with the sampling period [54].

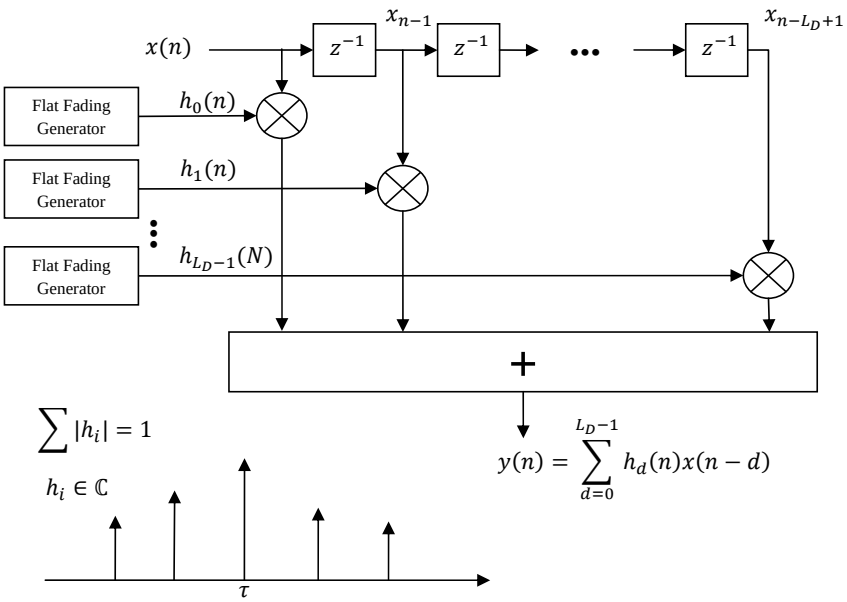

Figure 5.2: *Frequency-selective fading channel model using the TDL model.*

5.1.6 Multi-carrier fading channel statistics

Simulations of discrete multipath scenarios in numerous channel models are computationally inefficient, since each data symbol and its numerous path contributions needs to be calculated in the time domain. A more efficient and simplified approach is simulating a multi-carrier system in the frequency domain [9]. However, this is only possible when sub-carriers are assumed to undergo frequency non-selective fading and the system is time-invariant during one OFDM symbol. Generally this is applicable to well designed systems that can fulfill these conditions. The discrete channel transfer function can be adapted to multi-carrier signals, resulting in complex-valued channel fading coefficients which can then be independently generated for each sub-carrier and OFDM symbol given by

$$\begin{aligned} H_{n,i} &= H(n\Delta f, iT_s') \\ &= \sum_{p=0}^{N_p-1} a_p e^{j\left(2\pi(f_{d,p} iT_s' - n\Delta f \tau_p) + \varphi_p\right)} \\ &= a_{n,i} e^{j\varphi_{n,i}}. \end{aligned} \tag{5.23}$$

The continuous channel transfer function $H(f,t)$ is sampled at the OFDM symbol rate $1/T_s'$ in the time domain and in frequency at the carrier spacing of Δf. The duration of T_s' equals the total OFDM symbol duration including the guard interval. Therefore, in (5.23), a symbol transmitted on the nth sub-carrier of an OFDM symbol i is multiplied by the resulting fading amplitude $a_{n,i}$ chosen from any above mentioned distribution $p(r)$ (Rician/Rayleigh) and is rotated by a phase $\varphi_{n,i}$, uniformly distributed over the interval $(0, 2\pi)$ [9]. Discrete multi-path channel models can be directly applied to (5.23), resulting in one complex-valued multiplication per sub-carrier in the frequency domain, avoiding unnecessary FFT operations.

5.1.6.1 Uncorrelated fading channel models

A simplification of the channel model for multi-carrier systems, as mentioned above, is based on the assumption that the fading on adjacent data symbols after inverse OFDM and de-interleaving can be considered uncorrelated [9], [57]. This holds, for example, when the system is provided with a frequency interleaver which ensures that neighbouring symbols fade independently and the interleaving depth exceeds the coherence bandwidth. Additionally, appropriate time interleaving is applied to ensure that fading in adjacent OFDM symbols

is independent and frequency non-selective fading per sub-carrier and time-invariance during one OFDM symbol is guaranteed [57].

Uncorrelated fading channel models for multi-carrier systems are simple to implement in the frequency domain; more computationally efficient, and simulation results can easily be reproduced. Depending on the situation, the evaluation of a given system using an uncorrelated Rayleigh fading channel model is sufficient in presenting reference curves for further analysis. Standardised channel models producing correlated fading in time and frequency can be used when performing more complex performance degradation investigations of subsystems, such as interleavers and channel estimators.

5.1.7 The Gaussian noise channel

If the only impairment to a communication system is a linear addition of white or wideband noise with a constant spectral density, the channel can be modelled as an additive white Gaussian noise (AWGN) channel with a Gaussian amplitude distribution. The AWGN model only takes wideband Gaussian noise into account and neglects previously mentioned channel effects such as fading, frequency selectivity, dispersion or interference. The degradation of a communication system in a noisy channel can be attributed to many additions of natural noise sources (for example thermal noise), which can be statistically characterised by the Gaussian amplitude distribution, described by the probability density function (PDF)

$$p(\eta|\mu,\sigma^2) = \frac{1}{\sqrt{2\pi\sigma^2}} e^{-\frac{(\eta-\mu)^2}{2\sigma^2}}, \tag{5.24}$$

where μ is the expected value and σ^2 is the variance or power of the random noise variable η [58]. The channel is said to be discrete in time but has a continuous input and output [59].

5.1.7.1 Noise scaling

To compare the bit error rates of various modulation schemes used in a digital communication system, the ratio E_b/N_0 is very useful, as it is independent of the equivalent noise bandwidth and normalises the curves to the amount of energy needed to transmit one bit. The standard deviation of any noise source to test the BER of a communication system can be obtained by calculating a power factor with which the output Gaussian distributed noise source can be scaled with to achieve a given E_b/N_0 value [58].

The output signal-to-noise ratio (SNR) is altered by scaling the variance η of the applied noise by the amplitude noise scaling factor k_η, defined by [58]

$$k_\eta^2 = \frac{\sigma_{in}^2 f_{samp}}{10^{\left(\frac{E_b/N_0}{10}\right)} 2 f_{bit}}, \tag{5.25}$$

where σ_{in}^2 is the variance of the input signal, f_{bit} is the uncoded bit rate, f_{samp} is the sampling frequency, E_b is the energy per uncoded bit, and N_0 is the single-sided noise PSD of AWGN. The ratio $\frac{E_b}{N_0}$ is the normalised SNR per source bit in Decibel. Scaled noise samples with variance $k_\eta^2 \sigma_\eta^2$ are created with the power scaling factor, or squared value k_η^2, where σ_η^2 is the variance of the noise process η.

When assuming the system is in baseband and the input signal has unit variance, (5.25) can be re-written as

$$k_\eta^2 = \frac{n_{samp}}{10^{\left(\frac{E_b/N_0}{10}\right)} 2 R_c}, \tag{5.26}$$

where n_{samp} is the constant defining the number of samples used to represent a single input bit, and R_c is the code rate if channel coding is employed [26]. Thus, noise samples can be amplitude scaled by k_η to produce Gaussian noise samples with a required noise variance as dictated by E_b/N_0.

5.1.8 Theoretical performance

5.1.8.1 Error probability in AWGN

The analytical BER expressions in AWGN for a BPSK system are given as

$$P_b = Q\left(\sqrt{\frac{2E_b}{N_0}}\right) \quad or \quad P_b = \frac{1}{2}\operatorname{erfc}\left(\sqrt{\frac{E_b}{N_0}}\right), \tag{5.27}$$

where Q is the Gauss tail probability given in (2.31), and the Gauss error function erfc(.) is defined by $\operatorname{erfc}(x) = \frac{2}{2\pi}\int_x^\infty e^{-t^2} dt$. Note that since there is only one bit per symbol, this is also the symbol error rate. Additionally, the probability of bit-error for a QPSK system is the same as for BPSK. For the case when M is large and QPSK is not implied, the approximation

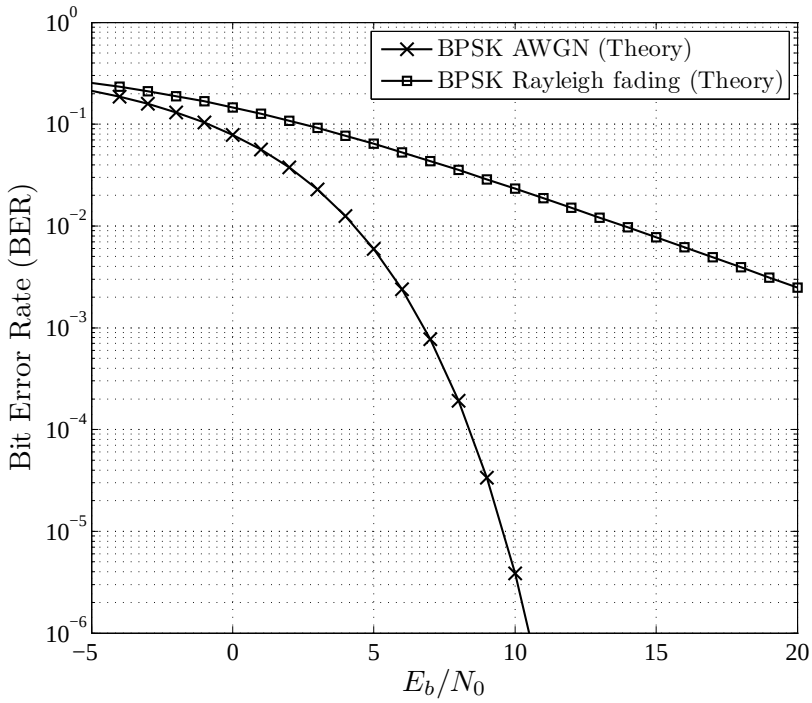

Figure 5.3: *Theoretical performance curves for a BPSK/QPSK system in an AWGN and Rayleigh fading channel.*

of $\sin\frac{\pi}{M} \approx \frac{\pi}{M}$ can be used to find another approximation to the symbol error probability as

$$P_e \approx 2Q\left(\sqrt{\frac{2\pi^2 \log_2 M}{M^2}\frac{E_b}{N_0}}\right) \quad \text{for large } M. \tag{5.28}$$

Since most probable errors due to noise result in the erroneous selection of an adjacent phase to the correct phase, most k-bit symbol errors contain only a single bit-error if Gray coding is employed [11]. Hence, the equivalent bit error probability for M-ary PSK is well approximated as $P_b \approx \frac{1}{k}P_e$. In Figure 5.3, the theoretical BER graph for a BPSK/QPSK modulation scheme is presented, and serves as a benchmark in the evaluation of the proposed system in subsequent simulation tests.

5.1.8.2 Error probability in fading channels

The error rate performance of binary PSK when transmitting over a frequency-nonselective, slowly fading channel can be found by noting that the error rate of binary PSK, as mentioned above, is

$$P_b(\gamma_b) = Q\left(\sqrt{2\gamma_b}\right) \tag{5.29}$$

where $\gamma_b = \frac{\alpha^2 E_b}{N_0}$. Equation (5.29) can be seen as a conditional error probability, where the condition is that α is fixed [11]. In Rayleigh fading, when α is Rayleigh-distributed, α^2 has a chi-square probability distribution with two degrees of freedom. Consequently γ_b is also a chi-square distribution and it can be shown that

$$p(\gamma_b) = \frac{1}{\bar{\gamma}_b} e^{-\gamma_b/\bar{\gamma}_b}, \qquad \gamma_b \geq 0 \tag{5.30}$$

where $\bar{\gamma}_b$ is the average signal-to-noise-ratio, defined as $\bar{\gamma}_b = \frac{E_b}{N_0} E\left(\alpha^2\right)$ and the term $E(\alpha^2)$ is simply the average value of α^2 [11]. Then to obtain the error probability when α is random, as in Rayleigh fading, the average of $P_b(\gamma_b)$ over the probability density function of γ_b needs to be taken as in (5.31):

$$P_b = \int_0^\infty P_b(\gamma_b) p(\gamma_b)\, d\gamma_b. \tag{5.31}$$

When evaluating this integral with (5.29) and (5.30), the result is the probability of error for binary PSK given by

$$P_b = \frac{1}{2}\left(1 - \sqrt{\frac{\bar{\gamma}_b}{1+\bar{\gamma}_b}}\right). \tag{5.32}$$

For large SNR, i.e., $\bar{\gamma}_b \gg 1$, the performance of coherent PSK can be simplified to

$$P_b \approx \frac{1}{4}\bar{\gamma}_b. \tag{5.33}$$

However, with the use of redundancy and diversity techniques, the performance in fading channels can be improved. Hence, if the diversity order is increased and the number of

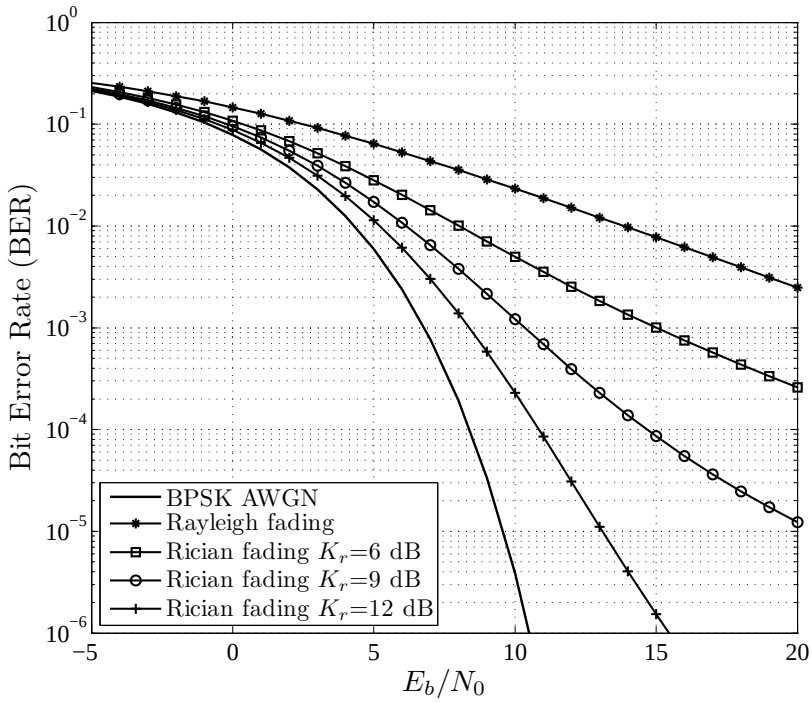

Figure 5.4: *Theoretical performance curves in a fading channel for a BPSK/QPSK system with different Rician K-factors (K_r).*

diversity branches $L > 1$, then the probability of error is given by [60], [61]

$$P_b = \frac{1}{2}\left[1 - \sqrt{\frac{\bar{\gamma}}{1+\bar{\gamma}}}\sum_{i=0}^{L-1}\binom{2i}{i}\left(\frac{1-\left(\frac{\bar{\gamma}}{1+\bar{\gamma}}\right)}{4}\right)^{i}\right]. \tag{5.34}$$

The theoretical performance of a BPSK system in a fading channel with different Rician K-factors is given in Figure 5.4.

5.2 DESCRIPTION OF SIMULATION PLATFORM

In this section the performance of the proposed multi-dimensional code-division OFDMA system in different channel conditions will be analysed. The uncoded simulation platform used for the evaluation is presented in Figure 5.5. The evaluation platform depicts the basic building blocks needed in the evaluation of the performance of the system in AWGN and in multipath fading.

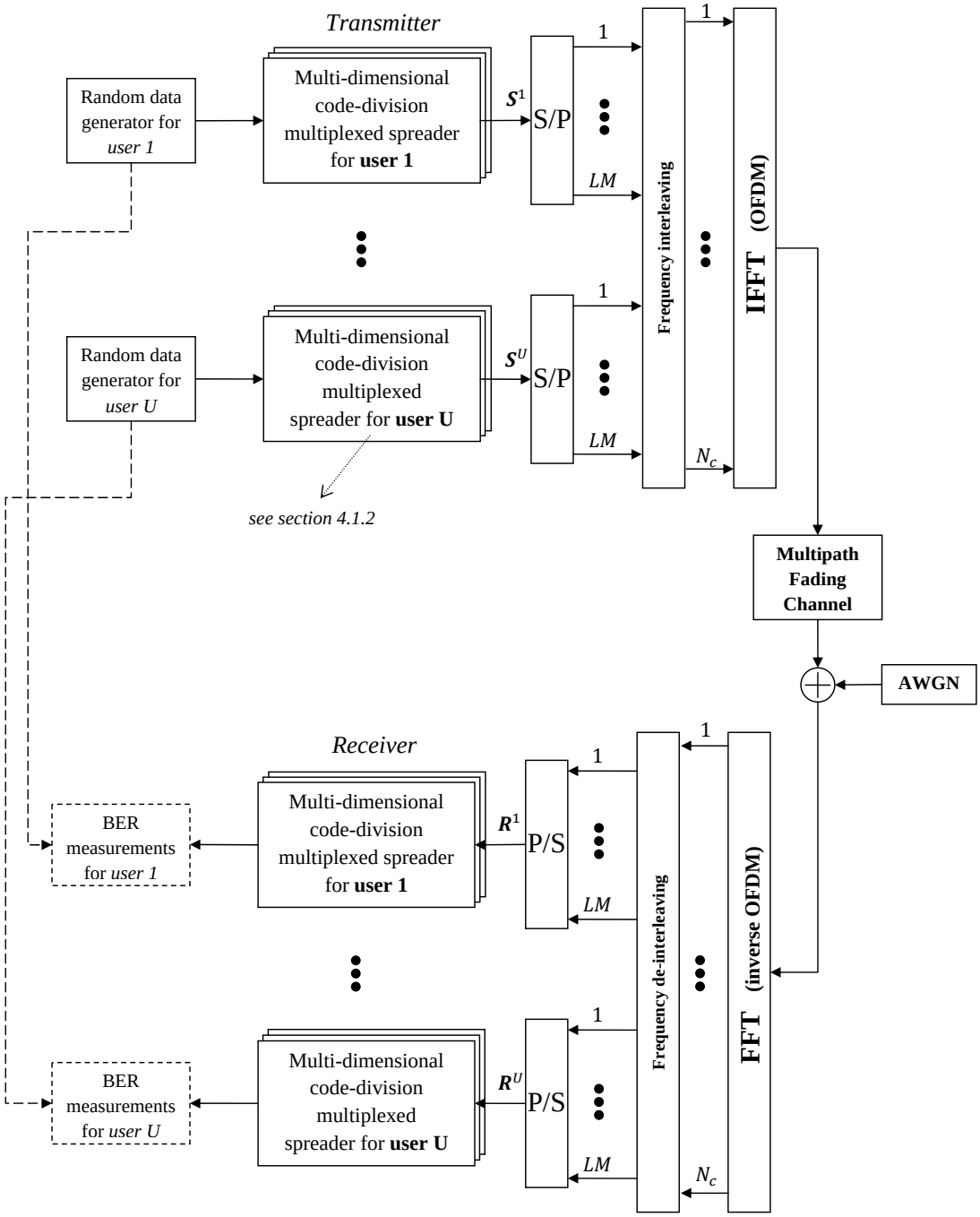

Figure 5.5: *Basic simulation platform of the multi-dimensional code-division OFDMA system using cyclically rotated orthogonal complete complementary spreading codes.*

The system is capable of supporting multiple users, restricted only by the number of available sub-carriers in the system. The spreading sequences and the multi-dimensional code-division-multiplexed spreading unit were discussed in Chapter 3 and Chapter 4, respectively.

The simulation platform generates uniform random data for each user which is then spread across the specifically allocated sub-carrier exclusively assigned to each user. Hence, code-division is used for simultaneous transmission of each user's data on the same sub-carriers. These sub-carriers or OFDM frames are then transmitted over an AWGN or multipath fading channel. The received data is de-spread and compared to the original transmitted data to establish a specific bit error rate for that user (or the average of all users) for either an AWGN or multipath fading channel.

5.2.1 System parameters

The proposed system has many design alternatives and numerous parameters can be set depending on the specific system requirement. Thus, the design greatly depends on the channel conditions, performance, and throughput requirements.

In this study, only the basic system without any complex performance gaining receiver structures is illustrated. Additional subsystems to further improve the error performance will only introduce additional complexity and overhead, which is not the focus of this research. Only the bare un-coded communication system structure is evaluated, since additional improvement techniques can always be integrated if the need arises. This allows for a uniform evaluation and comparison of the system as different estimation and coding schemes provide different signal-to-noise ratio degradation effects. Hence, perfect carrier and symbol timing recovery is assumed in the evaluation of the system design and BER improvement techniques such as channel coding, equalisation and channel estimation techniques will not be evaluated in the scope of this dissertation, thus creating opportunity for further research.

5.2.1.1 Spreading codes

With regard to the spreading codes, a BPSK system can make use of a length 16 elementary code ($L = 16$) and a flock size of $M = 4$. This produces 2×4-dimensional modems that can make use of 16 rotations to produce 128 information bits that are transmitted in 64 bits, yielding a spectrum efficiency of $8 \times 16/64 = 2$ bits/s/Hz for that specific user. Some of the available complete complementary codes are listed in appendix A. A summary of the spreading code utilised in the performance analysis is given in Table 5.5.

Table 5.5: *Spreading code used for the simulations.*

Matrix dimension size	Element code length	Cyclic rotations	Spreading sequence length	Flock and set size	Processing gain
4	16	16	64	4	64

5.2.1.2 OFDM parameters

The multi-carrier system can employ multiple sub-carriers, depending on the available bandwidth and the number of users required. Each user is assigned to LM sub-carriers given the spreading codes listed above. Thus, the general amount of sub-carriers needed for U users is

$$N_c = LM \times U. \tag{5.35}$$

The multi-carrier system exploits the fact that the symbol duration of the transmitted symbol is larger than the maximum delay $T_d \gg \tau_{max}$, where the duration per symbol increases with the number of sub-carriers N_c. This in turn decreases the amount of ISI and the number of interfering symbols, given by $N_{ISI,mc} = \lceil \frac{\tau_{max}}{N_c T_d} \rceil$ [9]. The possible residual ISI can be completely avoided or eliminated with the use of a guard interval, which cyclically extends the OFDM symbol duration.

However, this is not strictly necessary in the proposed system and the extra bandwidth used for a guard interval can be preserved. The ISI caused by the multipath effect can be reduced by the code-division CDMA type structure of the system, which is one of its salient features. The spreading codes allow for this ISI-free operation and the results thereof will be shown and explained in the following sections.

If only N_{used} sub-carriers out of a total of N_c (FFT size) sub-carriers are used for carrying data, note that the time-domain SNR is given by $SNR_t = SNR_f + 10\log\frac{N_{used}}{N}$ in decibel [54].

In Table 5.6, the system parameters for subsequent simulations are tabulated. This is only a guideline and parameters such as the number of pilot sub-carriers for example, would need to be altered when considering channel estimation or equalisation.

To achieve time-invariant fading per sub-carrier and OFDM symbol, the coherence band-

width $(\Delta f)_c$ of the channel needs to be greater than Δf and the coherence time $(\Delta t)_c$ of the channel needs to be greater than the symbol duration T_s'. These conditions can be satisfied by choosing the correct parameters in the system design.

Table 5.6: *Numerical values of the parameters that characterises the system.*

Parameters	Values
Number of users	$U = 32$
Spectral efficiency (one user)	$\eta_f = 2$ bits/s/Hz
Cyclic rotations/Elementary code length	$L = 16$
Spreading sequence length	$L \times M = 64$
Channel bandwidth	$B_s = 20$ MHz
Number of sub-carriers	$N_c = 2048$
Number of pilot sub-carriers	N_p = optional
Number of null sub-carriers	N_z = optional
Sub-carrier spacing	$\Delta f = 9.76$ kHz
Symbol duration (useful)	$T_s = 102.4\ \mu s$
Cyclic prefix or guard band (1/4, 1/8, etc.)	$T_s/8 = 12.8\ \mu s$
Total symbol duration	$T_s' = 115.2\ \mu s$
Carrier frequency	$f_c = 2.5$ GHz
Maximum throughput BPSK (no overhead, 1 user)	$f_{bmax} = \eta_f \times B_s = 40$ Mb/s

5.3 SIMULATION RESULTS

5.3.1 System waveforms and signal spectrum

The transmitted time response signal of the cyclically rotated spread spectrum signal after the IFFT is shown in Figure 5.6. Thereafter, the signal can be converted to a passband continuous time signal by applying a transmit filter. This is then followed by modulating the signal to a specific carrier frequency before transmission. An example of the time response of the transmitted signal is depicted in Figure 5.8. The frequency responses or power spectral density (PSD) of the entire signal is given in Figure 5.9.

The signal levels of the sum of all spread and rotated signals of one fully loaded user is depicted in a two-dimensional histogram in Figure 5.7. The histogram shows the total number of occurrences for each imaginary and real value the signal can attain, taken from 10000 random input samples. It can be seen that the signal levels have a Gaussian-like distribution

and can be compared to a QAM output signal. The level distribution and symbol energy depends on the element code length and the number of codes that are being stacked or summed together.

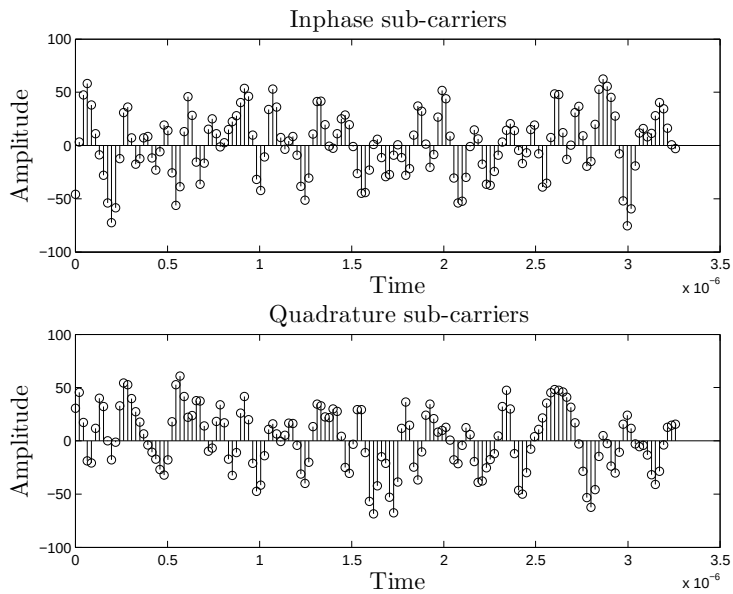

Figure 5.6: *Discrete time signal of transmitted signal with all rotations.*

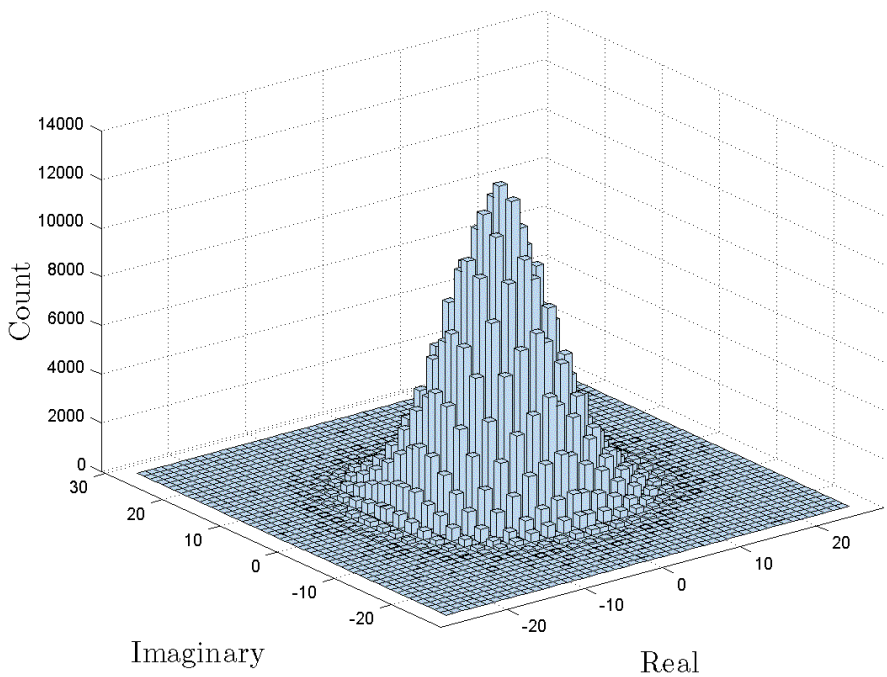

Figure 5.7: *Histogram of the symbol level distribution of fully loaded user with 10000 random input bits ($PG = 64$, $M = 4$ and $L = 16$).*

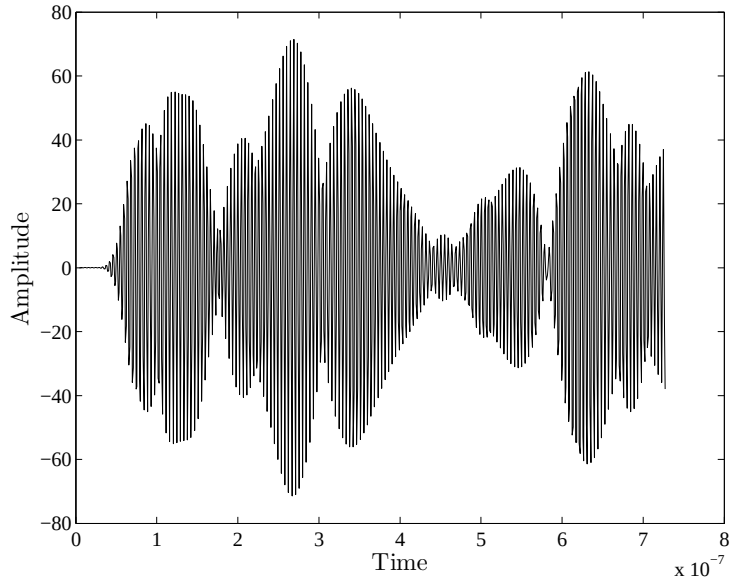

Figure 5.8: *Time response of transmitted passband signal.*

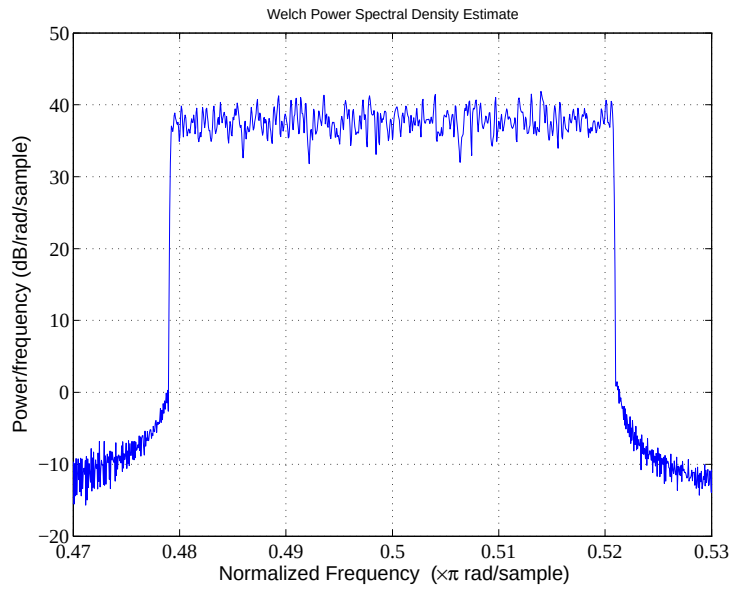

Figure 5.9: *Power spectral density estimate of transmitted signal.*

5.3.2 Performance results in an AWGN channel

This section introduces the BER performance in AWGN. The following curves are given in terms of bit energy to noise ratio (E_b/N_0). The simulated uncoded bit error rate performance in AWGN for the multi-dimensional system supporting $U = 32$ users is given in Figure 5.10. It confirms that the system yields a BPSK/QPSK performance, but with a much greater

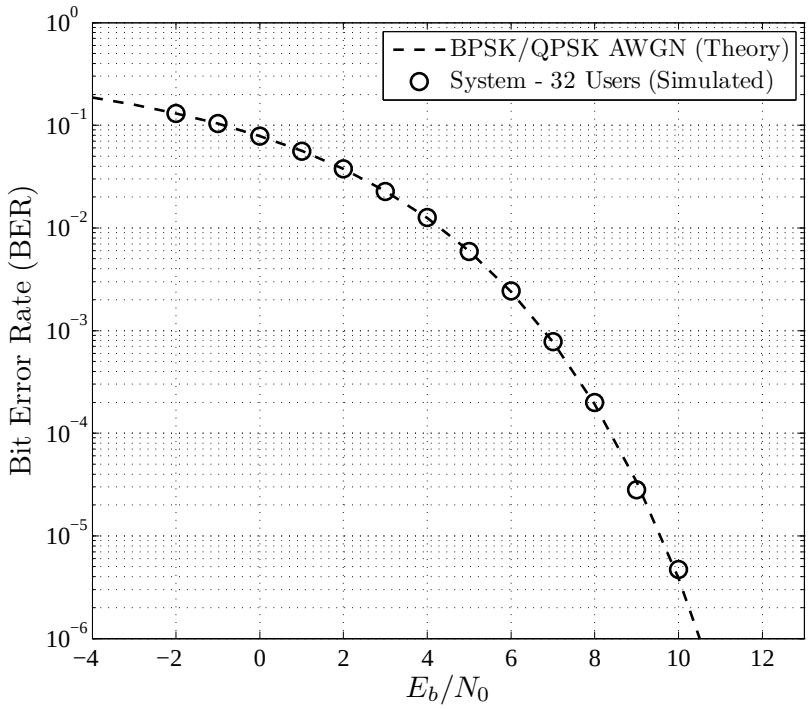

Figure 5.10: *Simulated uncoded performance curves in an AWGN channel for 32 users.*

throughput rate and spectral efficiency than a theoretical BPSK/QPSK CDMA or OFDMA type system. The basic system without any complex receiver structures is simulated. The system is capable of supporting multiple users by making use of OFDMA subchannelisation techniques. The different users all experience the same noise effects in AWGN. Thus, the system performance does not degrade with an increase in the number of users, because users are separated by different orthogonal frequencies. Each user can effectively receive all spread and cyclically rotated data due to the perfect despreading resulting from the ideal correlation properties of the orthogonal codes selected.

When considering BPSK modulation and the multi-dimensionality of the novel transmission scheme, a spectral efficiency of 2 bits/s/Hz can be achieved for one user. This shows that an increased throughput can be achieved double that of a theoretical BPSK system. This is achieved by the multi-dimensional building block which allows the system to re-use the spreading codes in other dimensions.

5.3.3 Performance results in a multipath fading channel

This section provides the BER performance in multipath fading channels using BPSK modulated data, where the presented BER results are averaged over 32 users split by frequencies. As explained above, the number of users depends only on the FFT size and bandwidth constraints, thus similar performance is expected for an increase in number of users. The presented performance is therefore valid for a fully loaded system due to the MAI-free operation. The MAI-free operation allows the system to be upper-bounded by the single user theoretical performance curve even with an increasing number of users, whereas MC-CDMA and other CDMA type schemes greatly decrease in performance with each additional user because of the present MUI/MAI.

The number of sub-carriers is chosen according to the given bandwidth to incur flat fading per sub-carrier, as done in OFDM systems. Figure 5.12 shows the average uncoded BER versus the SNR per bit for the system in a Rician fading channel. The multi-user system perfectly follows the theoretical single-user performance curves in a multipath channel. This demonstrates that the system is capable of achieving multiple access whilst maintain the BER performance of a single-user system, without the usual degradation effects found with an increase in number of users.

The channel used in the simulation is implemented as an uncorrelated Rayleigh fading channel as described in detail in Section 5.1.6. It can be seen that the performance of the uncoded system is not optimal, since the frequency-non-selectivity in each sub-carrier causes performance degradation if a sub-carrier undergoes a deep fade. The diversity achieved with the uncoded system is one, thus the addition of channel coding would fully exploit the frequency diversity.

The system can tolerate a certain amount of asynchronism between users, which is helpful in the uplink. There are various methods for a system to synchronise itself, reducing the amount of ISI and ICI. Synchronisation can be applied with less complexity to the system, as the data symbols of one user are transmitted exclusively on a set of sub-carriers. A guard time can be used in addition to combat extra ISI and ICI, however as seen in Figure 5.13, the guard time in a non-spread system is far more vital in the reduction of the effects of ISI as in the proposed spread code-division OFDMA type system.

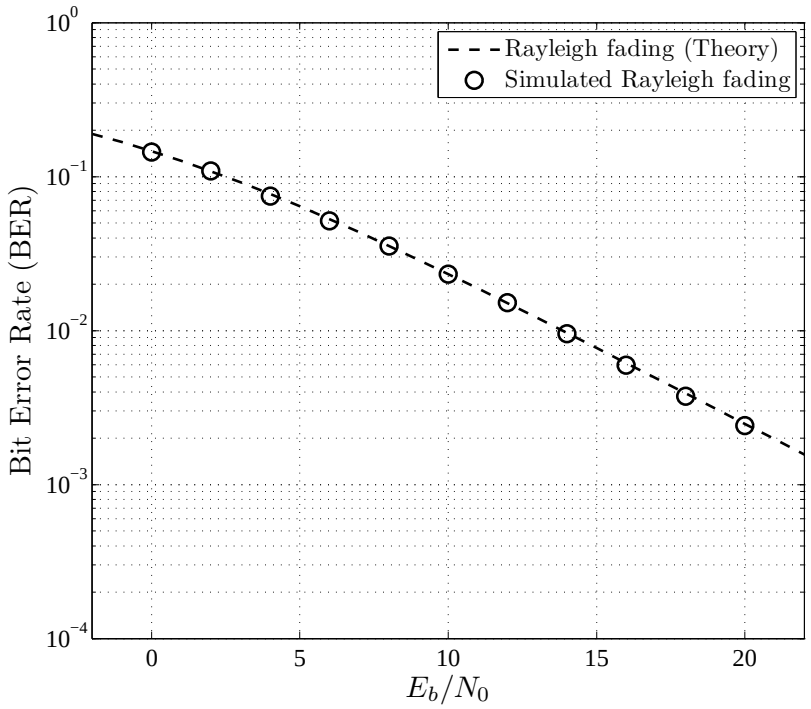

Figure 5.11: *Simulated uncoded performance curve in a fading Rayleigh channel.*

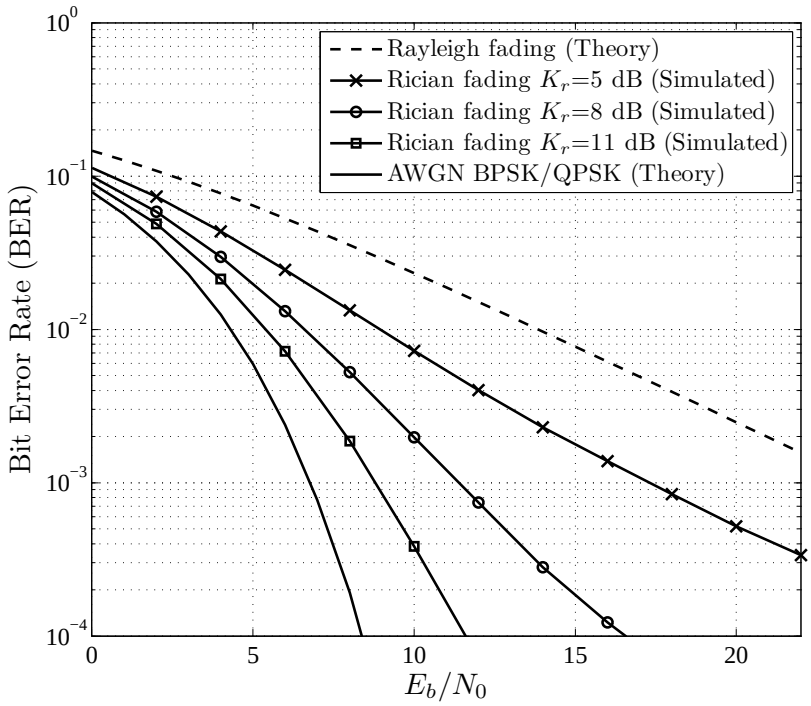

Figure 5.12: *Simulated BER curves in a fading Rician channel for a BPSK/QPSK system with different Rician K-factors.*

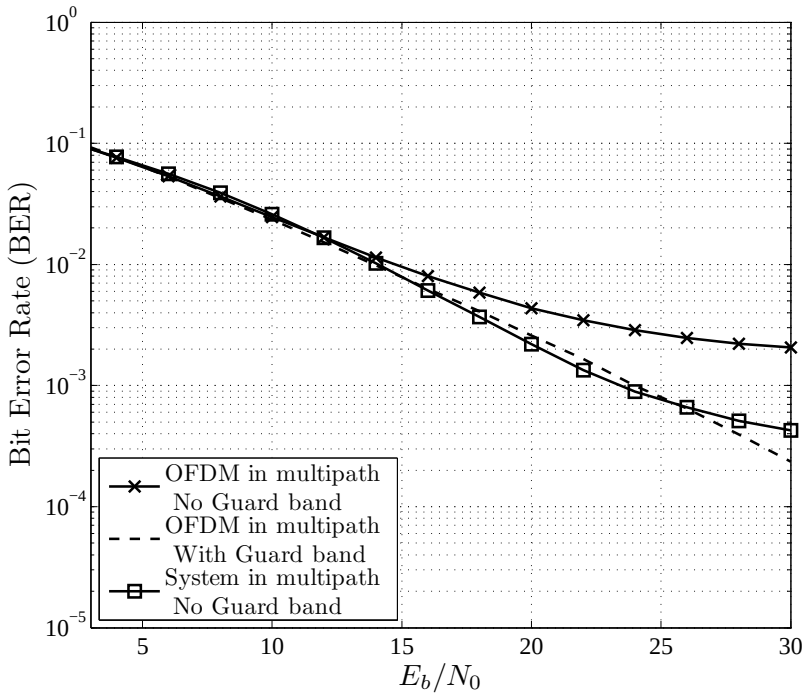

Figure 5.13: *Simulated BER curves showing ISI effects on the performance of the system with guard bands and without. Both systems have identical parameters and are subject to flat fading as long as the guard band is large enough.*

Figure 5.13 illustrates the BER performance of an ordinary BPSK OFDM system with a N_c point FFT with and without a guard interval in a 6 tap Rayleigh fading channel with a maximum delay less than the channel impulse response to incur flat fading if a guard band is to be applied. It can be seen that the performance without any guard band for the OFDM system is not consistent with that of the analytic result in a Rayleigh fading channel and the effect of ISI becomes more pronounced as the SNR increases. However, in the proposed system, the effect of ISI and the performance degradation is far less, considering the same system parameters. This implies that the system is subject to flat fading and shows that the spreading codes can cope with some of the ISI and a smaller guard band is required to reduce the error floor at higher signal-to-noise ratios. A reduction in the guard band improves the bandwidth efficiency. If the system on the other hand employs a large guard band, the BER performance of the system decreases below the analytical performance curve of an ordinary OFDM system. This shows that the system is more robust and the spreading codes enable the system to perform well with a smaller guard band. The performance of the system with a guard band is far better than an un-spread OFDM system with the same guard band length as can be seen in Figure 5.14, in which a guard band is used to additionally improve the system

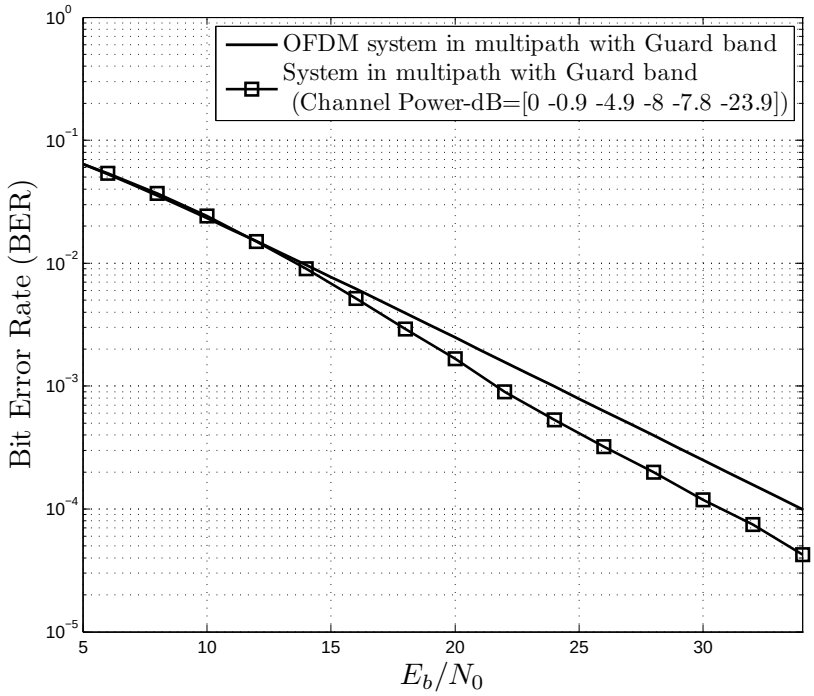

Figure 5.14: *Comparison of simulated uncoded performance curves of OFDM and the presented system in a multipath fading channel making use of a guard band.*

performance.

In any multi-carrier system, the sub-carrier spacing Δf is relatively small and Doppler effects can cause significant ICI. If all sub-carriers are affected by the same Doppler shift, ICI can be avoided by compensating for the Doppler shift in the receiver [9]. However, if the Doppler spread approaches the carrier spacing, ICI greatly degrades the system performance. The sub-carrier spacing should therefore be chosen such that the Doppler spread and ICI can be neglected by choosing $\Delta f \gg f_{Dmax}$. This is generally standard practice when designing an OFDM type wireless system and thus complex ICI mitigation techniques can be avoided. However, various ICI mitigation techniques, such as frequency domain Rake receivers, can be implemented to resolve the different Doppler frequencies, if the Doppler spread is higher or in the order of the carrier spacing [9].

Another simulation result which shows the typical flat fading behaviour of the system can be seen in Figure 5.15. For this simulation, the channel is chosen to be frequency-selective and time-variant, in correspondence with the channel models given by the COST 207 standard [55]. Table 5.1 lists some of the power delay profiles of the COST 207 models, required to

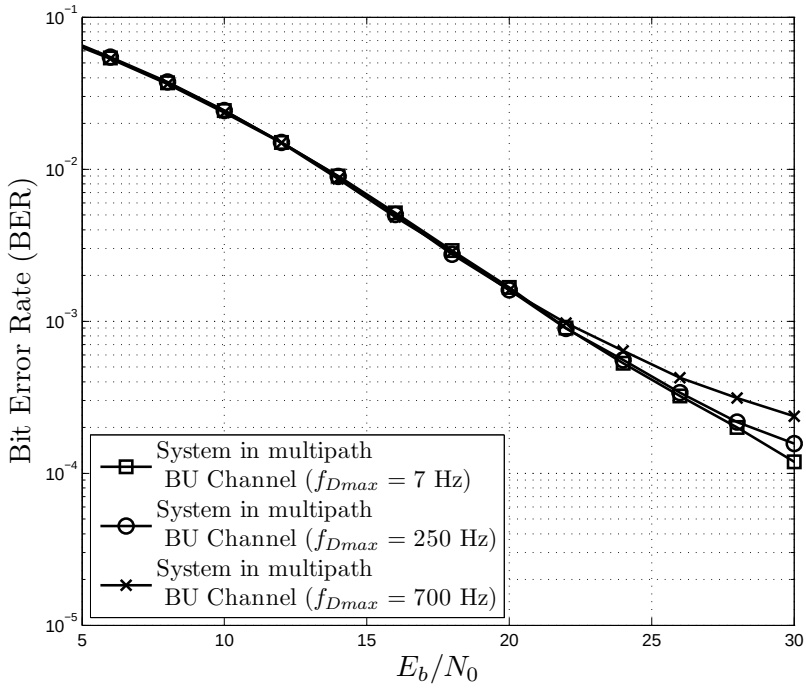

Figure 5.15: *Simulated BER curve for mobile radio channel with different Doppler frequencies f_{Dmax}.*

Table 5.7: *Channel model used for the simulation of Figure 5.15.*

Tap	Delay (μs)	Power (dB)
1	0	-2.5
2	0.3	0
3	1.0	-3
4	1.6	-5
5	5.0	-2
6	6.6	-4

model frequency-selective fading channels. As seen in the results, the effects of the time-variant channel only become evident for large signal-to-noise ratios. The interference and phase shifts between sub-carriers and the loss in orthogonality leads to an increased error floor when increasing the Doppler frequency. The bad urban (BU) fading channel of the COST 207 standard was used in the simulation, of which the PDP is given in Table 5.7.

5.4 PROPERTIES AND PERFORMANCE OF SYSTEM

In a multi-carrier-CDMA system, each user is associated with its own channel in the uplink, and the transmitted symbols undergo their own channel distortions requiring complex multi-user detection schemes to restore the orthogonality amongst users. The proposed system however, improves the performance and reduces the complexity of detection, as the transmitted symbols that generate interference are affected by the same channel distortion, since the data symbols of the same user are transmitted on a given set of sub-carriers.

MC-CDMA systems generally have to cope with multiple access interference, whereas the simulated system only has to cope with self-interference which is caused by the contribution of signals from the same user [9]. Thus, MAI is not present in the system. Additionally, only a single-user low complexity detection strategy is required at the receiver to achieve good performance, since the detection only needs to be applied to the sub-carriers assigned to one user. Reduced channel estimation complexity is also expected, seeing that each sub-carrier is exclusively used by one user. Since there is no MAI present, the same interface can be used for the uplink as well as for the downlink of the system. MC-CDMA systems can achieve their high bandwidth efficiency only in the downlink, whereas the presented system is more suitable for the uplink.

In multi-user systems such as MC-CDMA schemes, the near-far problem places a fundamental limit on the performance of the system, and this issue is generally not considered in many multi-carrier and multi-user system designs and evaluations. However, the presented system is resistant to the near-far problem due to the absence of MAI and the fact that each user is de-correlated independently. Hence, very costly and complex near-far mitigation mechanisms such as power control algorithms are unnecessary.

An MC-CDMA system spreads n data symbols over $n.L$ sub-carriers and is capable of exploiting more frequency diversity; however, this makes the channel estimation and reception more difficult. On the other hand, the presented system spreads $2ML$ data symbols over ML sub-carriers and loses some of the diversity, but facilitates simpler channel estimation. However, this frequency diversity loss, which cannot be exploited at the de-spreading process, can be made up for by employing channel coding. Channel coding can be assigned independently to each user, allowing for more robustness and added redundancy for that specific user. Inter-cell interference and resulting errors can thus be reduced by adding fewer spread-

ing codes to a user's signal, by making use of fewer carriers or by well known forward error correcting (FEC) codes.

The system, making use of the OFDMA features, can dynamically assign users to different sub-carriers and control the amount of sub-carriers available to each user. Thus, the throughput for a specific user could be increased or decreased depending on the channel conditions and required throughput or quality of service needed by a user. The system can also make use of a limited number of sub-carriers which can bring about a reduction in the peak-to-average power ratio (PAPR) of the transmitted signal. This in turn would allow for a decrease in amplifier back-off, reducing the mobile terminal power consumption [62].

Additionally, the code-division or spreading of the data in the system allows for variable data rate transmission for each user. Thus, a wide range of multi-rate services with different data rates (video, audio, image, speech, etc.) can be supported. The system would only need to alter the amount of multiplexed spreading codes at the transmitter to change the transmission rate, without the need for implementing adaptive coding and modulation schemes in both the transmitter and receiver.

The BER performance of the system compares to conventional OFDM if the Rayleigh fading over all chips of the spreading code is flat. If either one or two-dimensional spreading is applied with interleaving of the chips in the frequency and/or time domain, the diversity performance curves are lower-bounded by the theoretical BER diversity performance curves of a Rayleigh fading channel, where the spreading code length corresponds to the diversity order. The performance of spreading in multiple domains achieves a higher processing gain and the ability to use three different dimensions adds to the flexibility of the system, as resources can be allocated in the frequency, time, and code space. Further diversity schemes like space, angle or polarisation diversity, which are not within the scope of this study, can additionally increase the overall diversity and performance of the system.

CHAPTER 6

CONCLUSION

The primary objectives of next-generation wireless networks for mobile and broadband services is to make use of the limited radio spectrum in order to achieve higher data rates and throughput with higher bandwidth efficiency and user-capacity. By combining OFDMA and a modified spread spectrum multi-dimensional modulation method in a novel manner with the use of complete complementary codes and a cyclic rotation scheme, a unique flexible digital broadcasting technique, which supports high data rates and capacities over hostile radio channels, was developed. The generic architecture of the analysed system integrates existing techniques into a design that is adaptable and reconfigurable to different standards and technologies. This provides for scalability, easy integration into existing platforms and also provides opportunities for new research and development.

The system possesses several advantages over currently available 2G and 3G mobile cellular systems. It can, firstly, achieve a much higher bandwidth efficiency than conventional CDMA systems by yielding an efficiency per user equal to the un-spread theoretical spectral efficiency of the modulation method used, except for BPSK modulation, in which case the system can achieve 2 bits/s/Hz (double the theoretical). Secondly, the system offers MAI-free operation. This attributes to co-channel interference reduction, capacity increase, resilience against the near-far problem and in addition, the system has an improved throughput. Thirdly, due to its spectral efficiency, the system can make use of the additionally available resources when not fully loaded, enabling it to achieve a more reliable transmission and improve the BER performance. Finally, the system achieves multiple access with the use of OFDMA techniques and is greatly flexible in the way in which it spreads the data, resulting in various design alternatives with diversity improvements. The code-division or spreading of the data can offer numerous advantages such as possible data rate adaption, less complex channel estimation and diversity gains.

The integration of a multi-dimensional modem with the multi-carrier functionality of

OFDMA produced a novel system that is not only applicable to cellular technology and wireless broadband solutions, but also in wired digital data communications technologies such as in digital subscriber lines (DSL). By making use of a novel method of cyclically rotating complete complementary code families with a multi-layered modulation technique, a method has been devised which greatly improves throughput and spectrum efficiency of the basic transmission scheme.

The proposed communications system shows improvements to the fundamental modulation technique without the aid of complex forward error correcting (FEC) codes. The system lays a powerful foundation which can outperform previous designs where the basis lacks in efficiency, performance and throughput. Therefore, the proposed system would show greater improvements and would reach the Shannon bound more easily with the addition of channel coding, interleaving and equalisation, compared to previously designed systems implementing the same improvement techniques.

The research conducted in this study has shown that by combining the benefits of both OFDM and a multi-dimensional CDMA type modulation scheme using cyclically rotated mutually orthogonal complete complementary spreading codes, a multiple-access, spectrally efficient, and high throughput system can be created. Thus, well established multi-carrier systems using OFDMA can be improved by incorporating spread spectrum techniques as described in this research, to add processing gain and diversity without any loss in bandwidth efficiency. The performance, diversity and throughput of the system can be altered by applying different spreading techniques while still retaining the advantages of an OFDMA scheme. The system is more flexible in user assignment and shows higher data throughput rates due to code-division duplexing and the multi-dimensionality of the modem, whilst still maintaining the BER performance equivalent to that of single-layered modulation. Various benefits such as low complexity channel estimation and synchronisation, rate adaption, and resistance to the near-far problem can be attributed to the system. This novel flexible combination forms an attractive modulation technique for next-generation communication systems that require high data rates, high spectral efficiency, diversity, and robustness in harsh channel conditions.

6.1 RECOMMENDATIONS AND FUTURE RESEARCH

This research is devoted to demonstrate and highlight the importance of combining multi-carrier and spread spectrum technology for future wireless communication systems. The main concept, design, functionality and performance of the system was introduced in this study. The research has additionally raised a number of interesting questions and creates many possible future research opportunities in this field and specifically on this type of system.

There is a possibility for further research by introducing coding to this system. The system has an innate structure which can be used for the implementation of a coding scheme. Specifically, the cyclic rotation of the spreading code can be exploited by a coding scheme to greatly improve the system performance in an efficient way by using the existing rotations of the spreading codes. A tradeoff between spectral efficiency and an increase in BER performance would have to be considered.

A further study to investigate the performance improvements when applying multiple input multiple output (MIMO) techniques is needed. A MIMO implementation would gain in space diversity and aid in the mitigation of fading effects. The system can then make use of space-time block codes (STBC) to improve the frequency diversity and add spatial diversity gains. STBC schemes are known for their efficiency in channels which lack in frequency and time diversity. This combination with STBC and the performance over realistic MIMO channels with various receiver designs would provide some interesting results and warrants further investigation.

Research on a combined method of spreading of the system in three dimensions simultaneously, is another field that shows particular potential, as traditional OFDMA schemes do not provide any processing gain. The data spreading in the particular system can be performed in the time, frequency, and in the code space. Since the system incorporates spread spectrum in an OFDMA system, the data can be spread across the different dimensions, thereby greatly increasing the diversity. This would result in a full-diversity system, when coding is also considered. The bandwidth efficiency and bit error rate over multipath fading channels when spreading in all dimensions, even including the spatial dimension, could be investigated.

Perfect synchronisation and knowledge of the channel was assumed during the simulations. Future research could investigate the effects of asynchronism in user signals in the system, the resulting bandwidth loss due to guard intervals and the BER performance. A variety of channel estimation and equalisation schemes could be incorporated into the system to allow for an easier comparison and more realistic performance analysis. The comparison of the complexity, performance and spectral efficiency of such techniques would be another area of interest.

One key weakness of multi-carrier signals is the high peak-to-average power ratio. Further research on the PAPR performance of the system needs to be done, considering that the complementary codes are known to have good properties to serve as peak-to-average power reduction codes. The inherent PAPR of the spreading sequence can be estimated in the frequency domain by the sidelobes of the autocorrelation function. Since the sequences have no sidelobes, as was shown in this study, the PAPR of the sequence is known to be low. The inherent structure of the system and code implementation could provide some interesting results with respect to the PAPR. The signal envelope variations and the total system degradation with various input power backoff ratios could form part of the research to be conducted on the power efficiency of the system.

Many areas of this novel technology remain underexplored and this research has created a starting point or basis for further investigation. Additionally, many questions were uncovered and a variety of problems that require further study and experimentation were highlighted. This research has provided an in-depth insight into the high potential of this novel integration of the proven technologies namely multi-dimensional, spread spectrum and multi-carrier techniques.

BIBLIOGRAPHY

[1] M. L. Roberts, M. A. Temple, R. F. Mills, and R. A. Raines, "Evolution of the air interface of cellular communications systems toward 4G realization," *IEEE Commun. Surveys & Tutorials*, vol. 8, no. 1, pp. 2–23, 2006.

[2] E. Dahlman, Y. Jading, S. Parkvall, and H. Murai, "3G Radio Access Evolution – HSPA and LTE for Mobile Broadband," *IEICE Trans. on Commun.*, vol. E92-B, no. 5, pp. 1432–1440, May 2009.

[3] Radiocommunication Sector (ITU-R), "ITU global standard for international mobile telecommunications "IMT-Advanced"," 2010. [Online]. Available: http://www.itu.int/ITU-R/index.asp?category=information&rlink=imt-advanced&lang=en

[4] ITU's Radiocommunication Sector (ITU-R), "ITU paves way for next-generation 4G mobile technologies," 2010. [Online]. Available: http://www.itu.int/net/pressoffice/press_releases/2010/48.aspx

[5] Tellabs, "4G: The What, Why and When," *White Paper, Tellabs*. [Online]. Available: http://www.tellabs.com/resources/papers/tlab_4g-whatwhywhen.pdf

[6] "IEEE Standard for Information technology Telecommunications and information exchange between systems–Local and metropolitan area networks–Specific requirements Part 11: Wireless LAN Medium Access Control (MAC) and Physical Layer (PHY) Specifications," *IEEE Std 802.11n-2009 (Amendment to IEEE Std 802.11-2007)*, 2009.

[7] "IEEE Standard for Local and metropolitan area networks Part 16: Air Interface for Broadband Wireless Access Systems Amendment 3: Advanced Air Interface," *IEEE Std 802.16m-2011 IMT-Advanced radio interface*, 2011.

[8] J. Korhonen, *Introduction to 3G mobile communications*, 2nd ed. Artech House Publishers, Nov. 2003.

[9] K. Fazel and S. Kaiser, *Multi-carrier and spread spectrum systems: from OFDM and MC-CDMA to LTE and WiMAX*, 2nd ed. John Wiley & Sons Inc., 2008.

[10] E. Haas, "Institut für Kommunikation und Navigation," *Communications Systems*, 2004. [Online]. Available: http://www.kn-s.dlr.de/people/haas/

[11] J. G. Proakis and M. Salehi, *Digital Communications*, 5th ed. New York: McGraw-Hill, 2008.

[12] S. Kaiser and K. Fazel, "A flexible spread-spectrum multi-carrier multiple-access system for multi-media applications," in *8th IEEE Int. Symp. on Personal, Indoor and Mobile Radio Commun. (PIMRC'97)*, vol. 1, 1997, pp. 100–104.

[13] S. Kaiser, "MC-FDMA and MC-TDMA versus MC-CDMA and SS-MC-MA: performance evaluation for fading channels," in *5th IEEE Int. Symp. on Spread Spectrum Tech. and Appl. (ISSSTA'98)*, Sep. 1998, pp. 200–204.

[14] S. Kaiser and W. A. Krzymien, "Performance Effects of the Uplink Asynchronism in a Spread Spectrum Multi-Carrier Multiple Access System," *Eur. Trans. Telecomms.*, vol. 10, no. 4, pp. 399–406, Jul. 1999.

[15] K. Zheng, G. Zeng, and W. Wang, "Performance Analysis for OFDM-CDMA With Joint Frequency-Time Spreading," *IEEE Trans. Broadcast.*, vol. 51, no. 1, pp. 144–148, Mar. 2005.

[16] L.-L. Yang and L. Hanzo, "Multicarrier DS-CDMA: A Multiple Access Scheme for Ubiquitous Broadband Wireless Communications," *IEEE Commun. Mag.*, vol. 41, no. 10, pp. 116–124, Oct. 2003.

[17] H.-H. Chen, J.-F. Yeh, and N. Suehiro, "A Multicarrier CDMA architecture based on orthogonal complementary codes for new generations of wideband wireless communications," *IEEE Commun. Mag.*, vol. 39, no. 10, pp. 126–135, Oct. 2001.

[18] C. Han, N. Suehiro, and T. Hashimoto, "N-Shift Cross-Orthogonal Sequences and Complete Complementary Codes," in *IEEE Int. Symp. on Inf. Theory (ISIT'07)*, Jun. 2007, pp. 2611–2615.

[19] H.-H. Chen, D. Hank, M. E. Magaña, and M. Guizani, "Design of next-generation CDMA using orthogonal complementary codes and offset stacked spreading," *IEEE Wireless Commun.*, vol. 14, no. 3, pp. 61–69, Jun. 2007.

[20] H.-H. Chen, S.-W. Chu, N. Kuroyanagi, and A. J. Han Vinck, "An algebraic approach to generate super-set of perfect complementary codes for interference-free CDMA," *Wirel. Commun. Mob. Comput.*, vol. 7, no. 5, pp. 605–622, Jun. 2007.

[21] M. E. Magaña, T. Rajatasereekul, D. Hank, and H.-H. Chen, "Design of an MC-CDMA System That Uses Complete Complementary Orthogonal Spreading Codes," *IEEE Trans. Veh. Technol.*, vol. 56, no. 5, pp. 2976–2989, Sep. 2007.

[22] L. P. Linde and J. D. Vlok, "A Multi-dimensional super-orthogonal modulation alternative to M-QAM WCDMA for next generation wireless applications," in *IEEE Proc. AFRICON'07*, 2007.

[23] L. P. Linde, L. Staphorst, and J. D. Vlok, "Performance of a quasi-synchronous four-dimensional super-orthogonal WCDMA modulator for next generation wireless applications," *South African J. of Sci.*, vol. 103, no. 11-12, pp. 459–464, Dec. 2007.

[24] F. E. Marx and L. P. Linde, "Four dimensional modem employing complex spreading sequences," in *IEEE Proc. AFRICON'99*, vol. 1, no. 7, 1999, pp. 221–226.

[25] L. P. Linde and J. D. Vlok, "Power and spectrally efficient four-dimensional super-orthogonal WCDMA building block for next generation wireless applications," *IEEE Commun. Lett.*, vol. 10, no. 7, pp. 519–521, 2006.

[26] J. D. Vlok, "Sparse Graph Codes on a Multi-dimensional WCDMA Platform," M.Eng. thesis, Univ. of Pretoria, 2007.

[27] D. J. Basilio, L. P. Linde, and B. T. Maharaj, "Power and spectrally efficient multi-dimensional WCDMA modem employing CPM," in *IEEE Proc. AFRICON'07*, Sep. 2007, pp. 1–7.

[28] L. P. Linde, W. R. Malan, and F. E. Marx, "Power and spectral efficiency of a family of constant-envelope root-of-unity filtered complex spreading sequences in WCDMA non-linear power amplification," in *IEEE Proc. AFRICON'02*, Oct. 2002, pp. 395–400.

[29] L. P. Linde, I. Pryra, and S. A. Swanepoel, "On a new family of complex spreading sequences with zero cross-correlation properties," *Trans. of the South African Inst. of Electr. Eng.*, vol. 94, no. 4, pp. 50–56, 2002.

[30] S. I. Park, S. R. Park, I. Song, and N. Suehiro, "Multiple-Access Interference Reduction for QS-CDMA Systems with a Novel Class of Polyphase Sequences," *IEEE Trans. Inf. Theory*, vol. 46, no. 4, pp. 1448–1458, Jul. 2000.

[31] M. P. Lötter and L. P. Linde, "Constant envelope filtering of complex spreading sequences," *IET Electron. Lett.*, vol. 31, no. 17, pp. 1406–1407, Aug. 1995.

[32] J. D. Vlok and L. P. Linde, "Performance of sparse graph codes on a four-dimensional CDMA system in AWGN and multipath fading," *IEEE Proc. AFRICON'07*, pp. 1–7, Sep. 2007.

[33] H.-H. Chen, *The next generation CDMA technologies*. Wiley Online Library, 2007.

[34] M. E. Magaña and T. Rajatasereekul, “Complete Complementary Orthogonal (CCO) Code-Based CDMA Using Natural Mapping QAM Constellations,” *Wireless Pers. Commun.*, vol. 38, no. 4, pp. 435–442, Jun. 2006.

[35] H.-H. Chen, “The REAL Approach to Generate Orthogonal Complementary Codes for Next Generation CDMA Systems,” *Interdisciplinary Inform. Sci.*, vol. 12, no. 2, pp. 147–161, 2006.

[36] H.-H. Chen, S.-W. Chu, and M. Guizani, “On Next Generation CDMA Technologies: The REAL Approach for Perfect Orthogonal Code Generation,” *IEEE Trans. Veh. Technol.*, vol. 57, no. 5, pp. 2822–2833, Sep. 2008.

[37] M. P. Lötter and L. P. Linde, “A comparison of three families of spreading sequences for CDMA applications,” in *Proc. IEEE South African Symp. on Commun. and Signal Process. COMSIG’94*, 1994, pp. 68–75.

[38] L. Lu and V. K. Dubey, “Performance of a Complete Complementary Code-Based Spread-Time CDMA System in a Fading Channel,” *IEEE Trans. Veh. Technol.*, vol. 57, no. 1, pp. 250–259, Jan. 2008.

[39] A. Schönhage and V. Strassen, “Schnelle Multiplikation Grosser Zahlen,” *Comput.*, vol. 7, no. 3, pp. 281–292, 1971.

[40] H.-H. Chen, H.-W. Chiu, and M. Guizani, “Orthogonal complementary codes for interference-free CDMA technologies,” *IEEE Wireless Commun.*, vol. 13, no. 1, pp. 68–79, Feb. 2006.

[41] Y. Wu and W. Y. Zou, “Orthogonal Frequency Division Multiplexing: A Multi-carrier Modulation Scheme,” *IEEE Trans. Consum. Electron.*, vol. 41, no. 3, pp. 392–399, Aug. 1995.

[42] W. Y. Zou and Y. Wu, “COFDM: An Overview,” *IEEE Trans. Broadcast.*, vol. 41, no. 1, pp. 1–8, Mar. 1995.

[43] T. Jiang, W. Xiang, H. H. Chen, and Q. Ni, “Multicast broadcast services support in OFDMA-based WiMAX systems [Advances in mobile multimedia],” *IEEE Commun. Mag.*, vol. 45, no. 8, pp. 78–86, Aug. 2007.

[44] M. Speth, S. A. Fechtel, G. Fock, and H. Meyr, “Optimum Receiver Design for Wireless Broad-Band Systems Using OFDM: Part I,” *IEEE Trans. Commun.*, vol. 47, no. 11, pp. 1668–1677, Nov. 1999.

[45] S. C. Thompson, "Constant Envelope OFDM Phase Modulation," PhD dissertation, Univ. of California, San Diego, 2005.

[46] Y. Shen and E. Martinez, *Channel Estimation in OFDM Systems*, Freescale Semiconductor Application Notes, Jan. 2006.

[47] S. Coleri, M. Ergen, A. Puri, and A. Bahai, "Channel Estimation Techniques Based on Pilot Arrangement in OFDM systems," *IEEE Trans. Broadcast.*, vol. 48, no. 3, pp. 223–229, Sep. 2002.

[48] "Air Interface for Fixed and Mobile Broadband Wireless Access Systems," *IEEE Std P802.16 (Amendment and Corrigendum to IEEE Std 802.16-2004)*, 2005.

[49] T. Kwon, H. Lee, S. Choi, J. Kim, D.-H. Cho, S. Cho, S. Yun, W.-H. Park, and K. Kim, "Design and implementation of a simulator based on a cross-layer protocol between MAC and PHY layers in a WiBro Compatible. IEEE 802.16e OFDMA system," *IEEE Commun. Mag.*, vol. 43, no. 12, pp. 136–146, Dec. 2005.

[50] B. Makarevitch, "Adaptive resource allocation for WiMAX," in *18th IEEE Int. Symp. on Pers., Indoor and Mobile Radio Commun. (PIMRC'07)*, Sep. 2007, pp. 1–6.

[51] A. Arkhipov and M. Schnell, "The influence of user frequency offset on the uplink performance of SS-MC-MA," in *Proc. of European Conf. on Wireless Technol. (ECWT'03)*, no. 2, Oct. 2003, pp. 451–454.

[52] L. Cariou and J.-F. Hélard, "MIMO frequency hopping spread spectrum multi-carrier multiple access: A novel uplink system for B3G cellular networks," *Telecommun. Syst.*, vol. 30, no. 1, pp. 193–214, Nov. 2005.

[53] A. F. Molisch, *Wireless Communications*. John Wiley & Sons Inc., 2006.

[54] Y. S. Cho, J. Kim, W. Y. Yang, and C. G. Kang, *MIMO-OFDM wireless communications with MATLAB*. John Wiley & Sons Inc., 2010.

[55] Commission of the European Communities, "Digital Land Mobile Radio Communications - COST 207," *Office for Official Publications of the European Communities, Luxembourg, 1989, Final Report*, Sep. 1988.

[56] Recommendation ITU-R M.1225, "Guidelines for Evaluation of Radio Transmission Technologies for IMT-2000," 1997.

[57] S. Kaiser, “Multi-carrier CDMA Mobile Radio Systems: Analysis and Optimization of Detection, Decoding, and Channel Estimation,” Ph.D. dissertation, VDI-Verlag, Fortschrittberichte VDI, series 10, no. 531, Jan. 1998.

[58] L. Staphorst, “Viterbi decoded linear block codes for narrowband and wideband wireless communication over mobile fading channels,” M.Eng. thesis, Univ. of Pretoria, 2005.

[59] D. J. C. MacKay, *Information theory, inference, and learning algorithms*. Cambridge University Press, Jun. 2003, vol. 22, no. 3.

[60] M. K. Simon, S. M. . Hinedi, and W. C. Lindsey, *Digital Communication Techniques: Signal Design and Detection*, 1st ed. Prentice Hall, 1995.

[61] M. K. Simon and M. S. Alouini, *Digital Communication over Fading Channels – A Unified Approach to Performance Analysis*, 1st ed. John Wiley & Sons Inc., 2000.

[62] S. Nobilet, J. F. Hélard, and D. Mottier, “Spreading Sequences for Uplink and Downlink MC-CDMA Systems: PAPR and MAI Minimization,” *Eur. Trans. Telecomms.*, vol. 13, no. 5, pp. 465–474, Sep. 2002.

APPENDIX A

LIST OF COMPLETE COMPLEMENTARY CODES

This appendix gives a list of some of the complete complementary codes used with different processing gains. The processing gain for a complete complementary code set is the product of its element code length N and its flock size M, where the set size is equal to the flock size $M = K$.

Some Complete Complementary Codes:

PG = 8, Length of element codes = 4, flock size = 2

$(+++-,+-++)(++-+,+---)$

PG = 16, Length of element codes = 8, flock size = 2

$(+++-++-+,+-+++---)(+++---+-,+-++-+++)$

PG = 32, Length of element codes = 16, flock size = 2

$(+++-++-++++---+-,+-+++---+-++-+++)(+++-++-+$
$---++++-+,+-+++----+--+---)$

PG = 64, Length of element codes = 32, flock size = 2

$(+++-++-++++---+-+++-++-+---++++-+,+-+++---$
$+-++-++++-+++----+--+--)(+++-++-++++---+-$
$---+--+-+++---+-,+-+++---+-++-+++-+---++++-$
$++-+++)$

PG = 64, Length of element codes = 16, flock size = 4

$(+++++-+-++--+--+,+-+-++++--+++--,++--+--+++$
$+++-+-,+--+++--+-+-++++)(++++-+-+++---++-,+-$
$+-----+--+--++,++---++-++++-+-+,+--+--+++-$
$+-----)(+++++-+---++-++-,+-+-++++-++---++,++$

−−+−−+−−−−−+−+,+−−+++−−−+−+−−−−)(++++−+−+−−
+++−−+,+−+−−−−−−++−++−−,++−−−++−−−−−+−+−,+−
−+−−++−+−+++++)

PG = 128, Length of element codes = 64, flock size = 2

(+++−++−++++−−−+−+++−++−+−−−+++−++++−++−+
+++−−−+−−−−+−−+−+++−−−+−,+−+++−−−+−++−++++−
+++−−−−+−−+−−−+−+++−−−+−++−+++−+−−−++++−++
−+++)(+++−++−++++−−−+−+++−++−+−−−+++−+−−−+
−−+−−−−+++−++++−++−+−−−+++−+,+−+++−−−+−++−+
+++−+++−−−−+−−+−−−−+−−−+++−+−−+−−−+−+++−−−
−+−−+−−−)

PG = 256, Length of element codes = 128, flock size = 2

(+++−++−++++−−−+−+++−++−+−−−+++−++++−++−+
+++−−−+−−−−+−−+−+++−−−+−+++−++−++++−−−+−++
+−++−+−−−+++−+−−−+−−+−−−−+++−++++−++−+−−−+
++−+,+−+++−−−+−++−++++−+++−−−−+−−+−−−+−+++−
−−+−++−+++−+−−−++++−++−++++−+++−−−+−++−+++
+−+++−−−−+−−+−−−−+−−−+++−+−−+−−−+−+++−−−−+
−−+−−−)(+++−++−++++−−−+−+++−++−+−−−+++−+++
+−++−++++−−−+−−−−+−−+−+++−−−+−−−−+−−+−−−−+
++−+−−−+−−+−+++−−−+−+++−++−++++−−−+−−−−+−−
+−+++−−−+−,+−+++−−−+−++−++++−+++−−−−+−−+−−−
+−+++−−−+−++−+++−+−−−++++−++−+++−+−−−+++−+
−−+−−−−+−−−++++−++−++++−+++−−−+−++−+++−+−−
−++++−++−+++)

Some Super Orthogonal Complementary Codes:

PG = 4, Length of element codes = 1, flock size = 4

(+,+,+,−)(+,−,+,+)(+,+,−,+)(+,−,−,−)

PG = 8, Length of element codes = 2, flock size = 4

(++,+−,++,−+)(+−,++,+−,−−)(++,+−,−−,+−)(+−,++,−+,++)

[PG = 16, Length of element codes = 4, flock size = 4

(+++−,++−+,+++−,−−+−)(+−++,+−−−,+−++,−+++)(+++−,++
−+,−−−+,++−+)(+−++,+−−−,−+−−,+−−−)

PG = 32, Length of element codes = 8, flock size = 4

(+++−++−+,+++−−−+−,+++−++−+,−−−++++−+)(+−+++−−−,+−++−+++,+−+++−−−,−+−−+−−−)(+++−++−+,+++−−−+−,−−−+−−+−,+++−−−+−)(+−+++−−−,+−++−+++,−+−−−+++,+−+++−+++)

PG = 32, Length of element codes = 4, flock size = 8

(+++−,+−++,++−+,+−−−,+++−,+−++,−−+−,−+++)(+++−,−+−−,++−+,−+++,+++−,−+−−,−−+−,+−−−)(+−++,+++−,+−−−,++−+,+−++,+++−,−+++,−−+−)(+−++,−−−+,+−−−,−−+−,+−++,−−−+,−+++,++−+)(+++−,+−++,++−+,+−−−,−−−+,−+−−,++−+,+−−−)(+++−,−+−−,++−+,−+++,−−−+,+−++,++−+,−+++)(+−++,+++−,+−−−,++−+,−+−−,−−−+,+−−−,++−+)(+−++,−−−+,+−−−,−−+−,−+−−,+++−,+−−−,−−+−)

PG = 64, Length of element codes = 16, flock size = 4

(+++−++−++++−−−+−,+++−++−+−−−+++−+,+++−++−+++−−−+−,−−−+−−+−+++−−−+−)(+−+++−−−+−++−+++,+−+++−−−−+−−+−−−,+−+++−−−+−++−+++,−+−−−++++−++−+++)(+++−++−++++−−−+−,+++−++−+−−−+++−+,−−−+−−+−−−−+++−+,+++−++−+−−−+++−+)(+−+++−−−+−++−+++,+−+++−−−−+−−+−−−,−+−−−+++−+−−+−−−,+−+++−−−−+−−+−−−)

PG = 64, Length of element codes = 8, flock size = 8

(+++−++−+,+−+++−−−,+++−−−+−,+−++−+++,+++−++−++−+++−−−,−−−++++−+,−+−−+−−−)(+++−++−+,−+−−−++++,+++−−−+−,−+−−+−−−,+++−++−+,−+−−−+++,−−−+++−+,+−++−+++)(+−+++−−−,+++−++−+,+−++−+++,+++−−−+−,+−+++−−−,+++−++−+,−+−−+−−−,−−−+++−+)(+−+++−−−,−−−+−−+−,+−++−+++,−−−+++−+,+−+++−−−,−−−+−−+−,−+−−+−−−,+++−−−+−)(+++−++−+,−+−−−+++,+++−−−+−,−+−−+−−−,−−−+−−+−,+−+++−−−,+++−−−+−,−+−−+−−−)(+−+++−−−,+++−++−+,+−++−+++,+++−−−+−,−+−−−+++,−−−+−−+−,+−++−+++,+++−−−+−)